Freiburg Lectures 2016

Graduiertenkolleg "Mass and Symmetries after the Discovery of the Higgs Particle at the LHC"

Tracking and Tracking Detectors

Norbert Wermes
University of Bonn

Outline

Lecture 1

Tracking

- momentum measurement
- vertex measurement
- influence of multiple scattering
- errors and what to do …

Lectures 2 & 3 & 4

Tracking Detectors

- the signal and the noise
- spatial resolution with structured electrodes
- gaseous detectors
- semiconductor detectors
- pixel detectors ... status and future

Freiburg Lectures 2016

Graduiertenkolleg "Mass and Symmetries after the Discovery of the Higgs Particle at the LHC"

Lecture 2

Tracking Detectors (Gas)

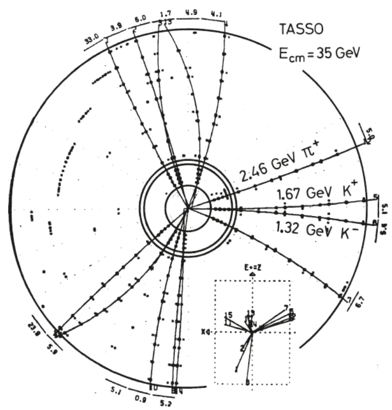

Norbert Wermes
University of Bonn

universitätbonn

SI LAB
Silizium Labor Bonn

Content Lecture 2

universitätbonn

- Main used trackers: gas-filled or Si
  - commonalities and differences
- How the signal develops
  - Shockley-Ramo theorem
  - **Weighting fields in**
    - parallel (w/o and w/ space charge)
    - cylindrical
    - patterned

    electrode configurations
- Gas amplification in gaseous detectors
- Diffusion and drift (short)
- Motion in E and B (short)
- **Space resolution** w/ patterned electrodes
  - binary
  - centroid
  - eta - method
- gas-filled detector types
  - operation modes
  - **avalanche – streamer – spark**
  - the magic of gases
  - ageing of gas filled wire chambers
  - cathode readout
  - stereo readout
- drift chambers
  - drift cells
  - stereo R/O
- Time Projection Chambers
- **New developments for LHC**
  - MPGDs
    - MSGC
    - GEM
    - Micromegas
  - RPCs

Break through advances in experimentation

Wire chambers
→ electronic recording
of particle tracks
→ electronic recording of tracks
→ σ = mm –> 50 µm,
0.05 channels / cm^2

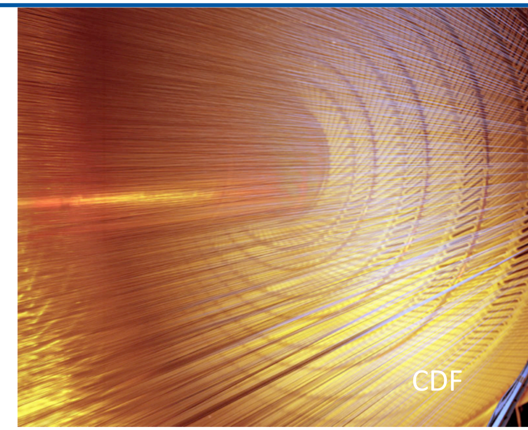

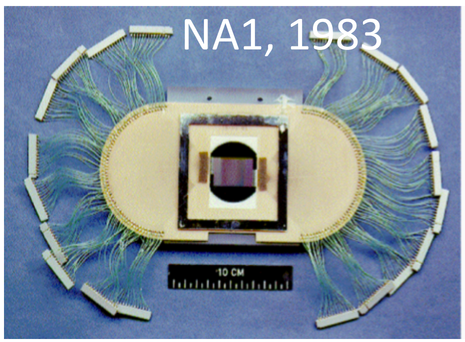

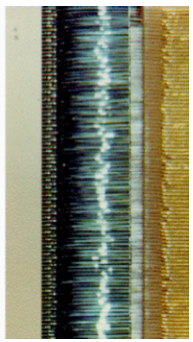

Silicon strip detectors
→ measurement of ps – lifetimes
and heavy quark "tagging"
→ σ < 5 µm, 50 channels / cm^2

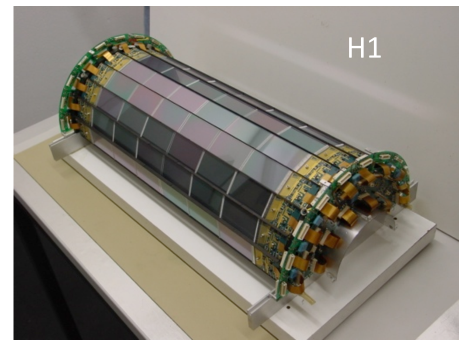

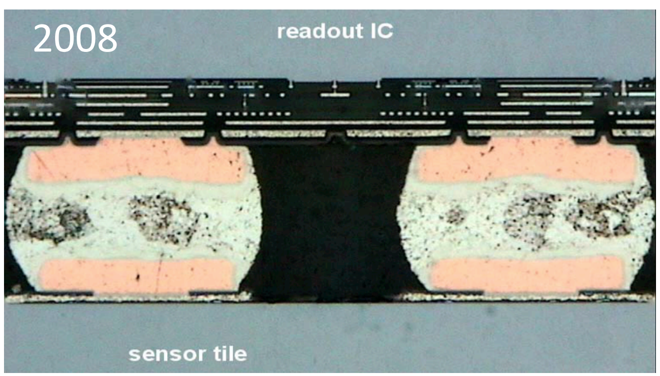

Pixel detectors
→ 3-dim point measurement
in high rate environments
like LHC
→ σ ~ 10 µm -> 2 µm,
→ 10 000 channels / cm^2

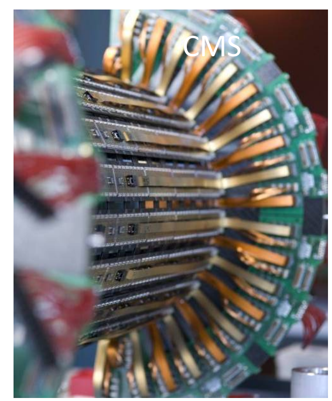

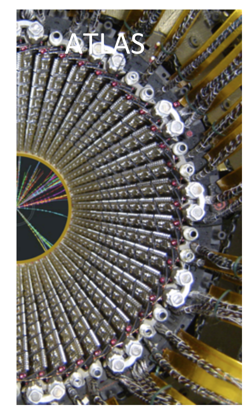

Tracking in pp collisions at 13 TeV (LHC)

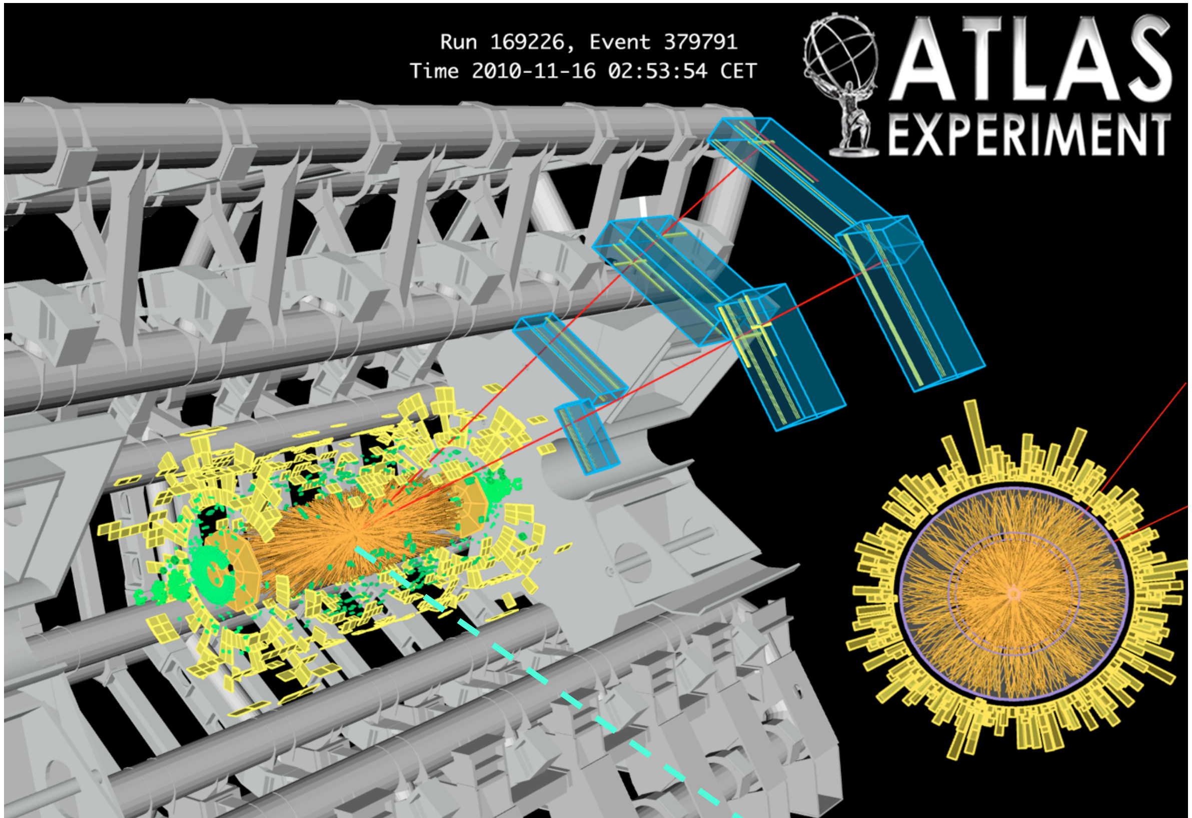

~1200 tracks every 25 ns
or ~ 10^{11} per second

⇒ high radiation dose

10^{15} n_{eq} / cm^2 / 10 yrs @ LHC

or

600 kGy (60 Mrad)
through ionisation of particles

position of
tracking detector (pixels, strips, straw tubes)

DEMANDS

LHC ≅ 10^6 x LEP in track rate !

Note: LHC Upgrade (2026): HL–LHC ≈ LHC x 10 !

Most tracking detectors are ionization detectors

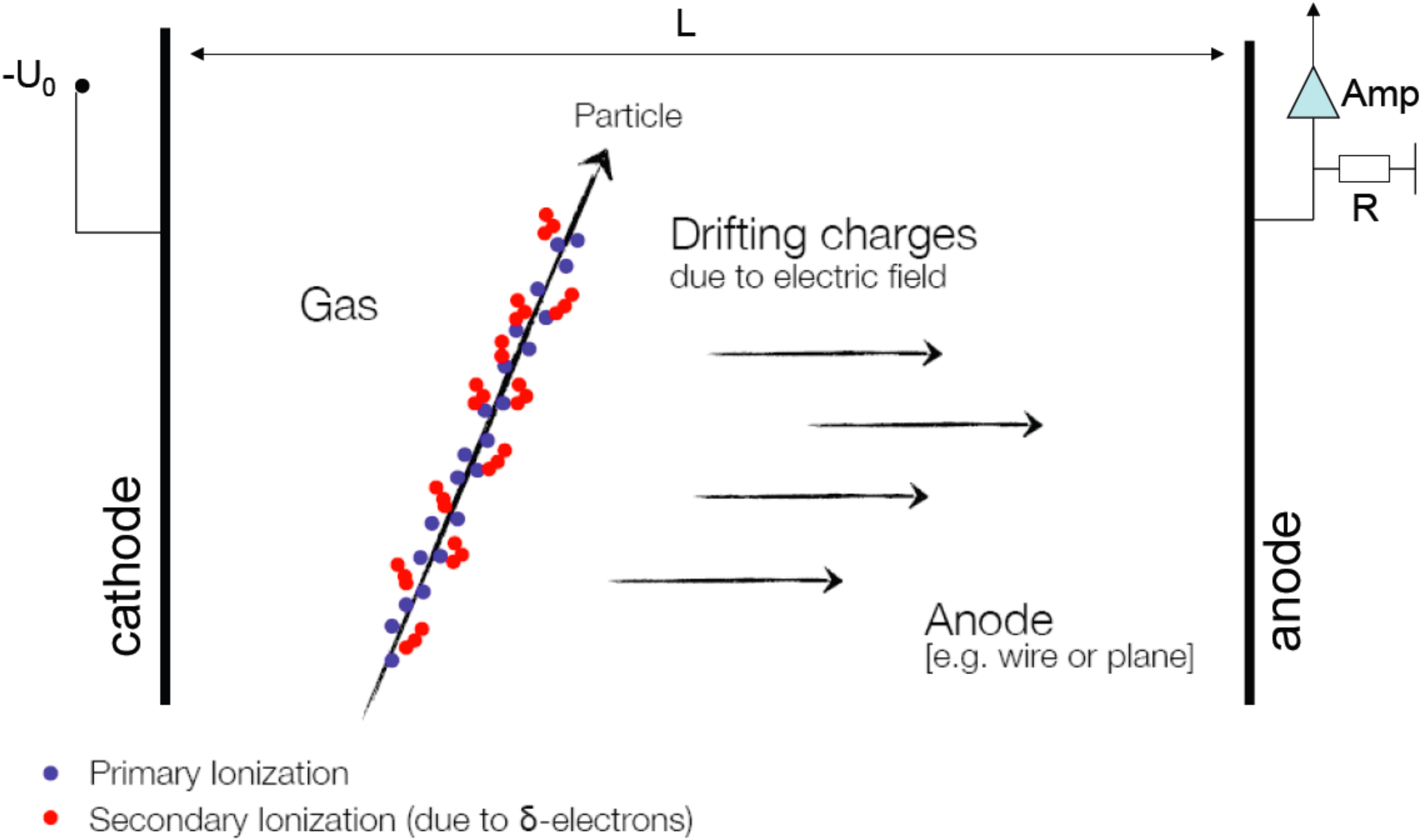

For trackers: gas-filled and semiconductor detectors

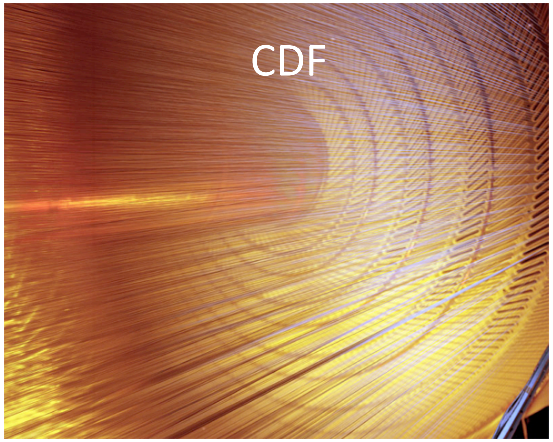

++	material	-
+	N_{meas}	--
low	cost	high
--	rate/speed	++
100 µm	resolution	10 µm

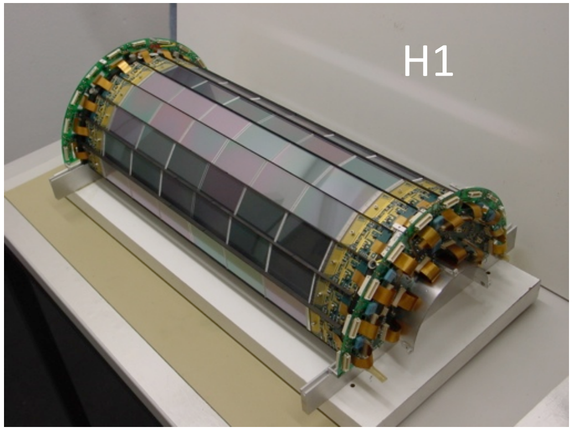

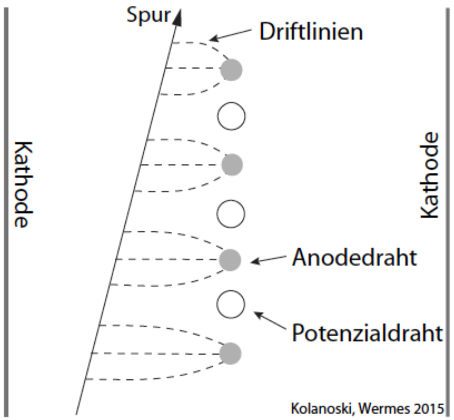

field near wire
E(r) ~ 1/r

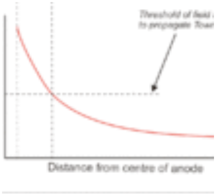

⇒ gas amplification

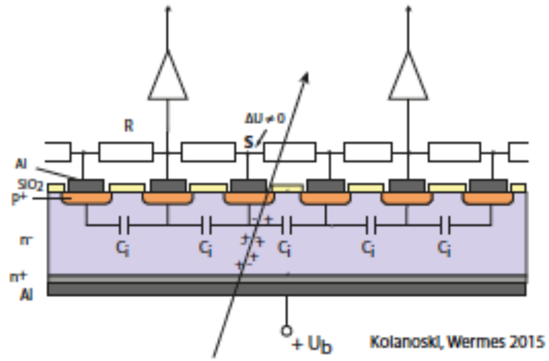

linear E

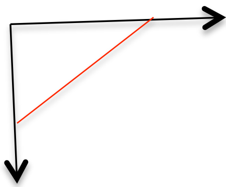

26 eV needed (Ar) per e/ion pair
94 e/ion pairs per cm
intrinsic amplification typ. 10^5
typ. noise: > 3000 e- (ENC)

3.65 eV (Si) needed per e/h pair
~10^6 e/h pairs per cm (20 000/250µm)
no intrinsic amplification
typ. noise: 100 e- (pix) to 1000 e- (strip)

How the signal develops

by “electrostatic induction” (influence electrique, elektrische Influenz)

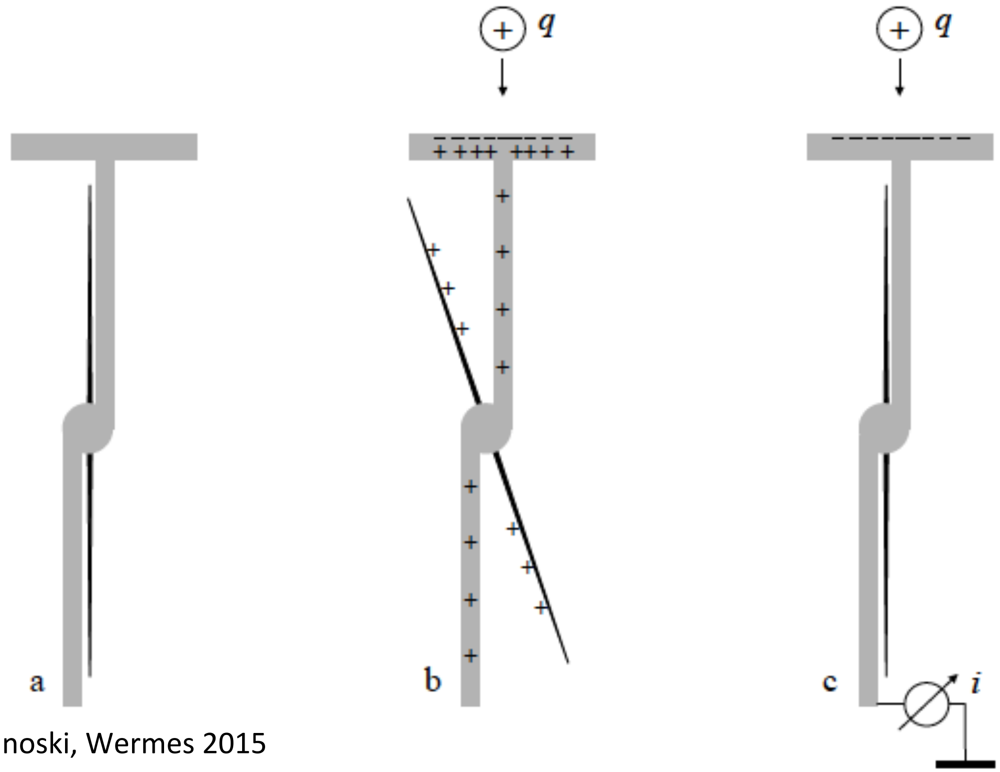

Kolanoski, Wermes 2015

a current is generated

Signal generation in an electrode configuration

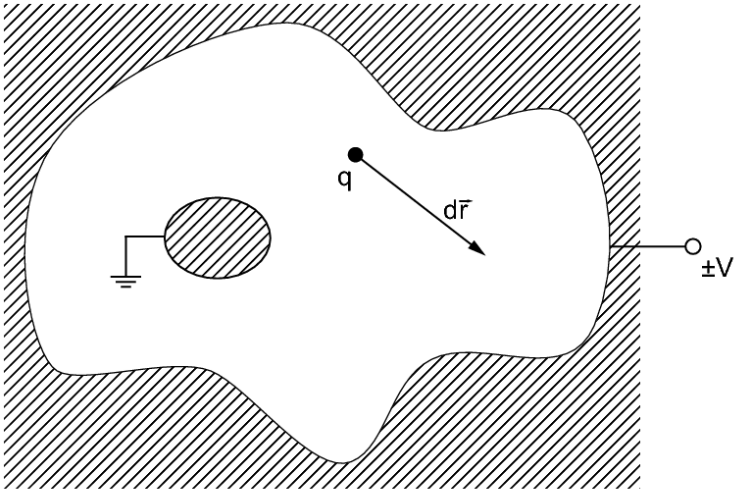

how does a moving charge couple to an electrode ?

- respect Gauss' law and find

Shockley- Ramo theorem
(Shockley J Appl.Phys 1938, Ramo 1939)

weighting field
determines how charge movement couples to a specific electrode

$$i_S = -\frac{dQ}{dt} = q\,\vec{E}_w\,\vec{v}$$

$$dQ = q\vec{\nabla}\Phi_W\,d\vec{r}$$

induction (weighting) potential
determines how charge movement couples to a specific electrode

Ramo Theorem in a many electrode configuration

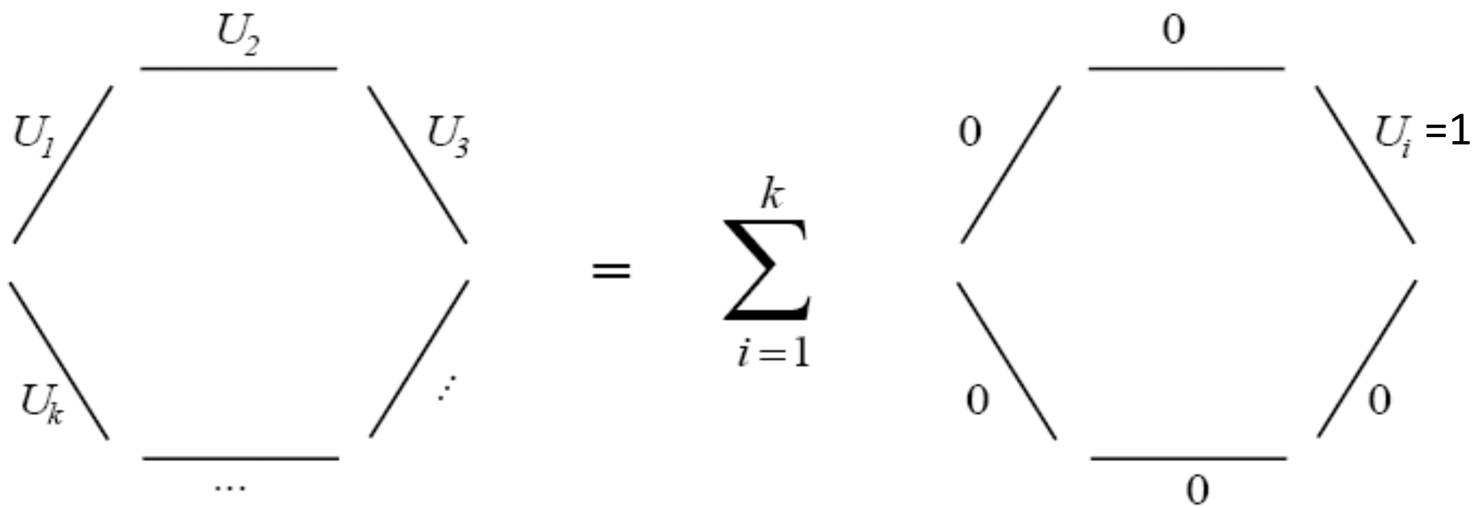

$$dQ_i = -q\,\vec{E}_{w,i}\,d\vec{r}$$

Recipe: To compute the weighting field of a readout electrode i, set voltage of electrode i to 1 and all other electrodes to 0.

Normal Field and Weighting Field

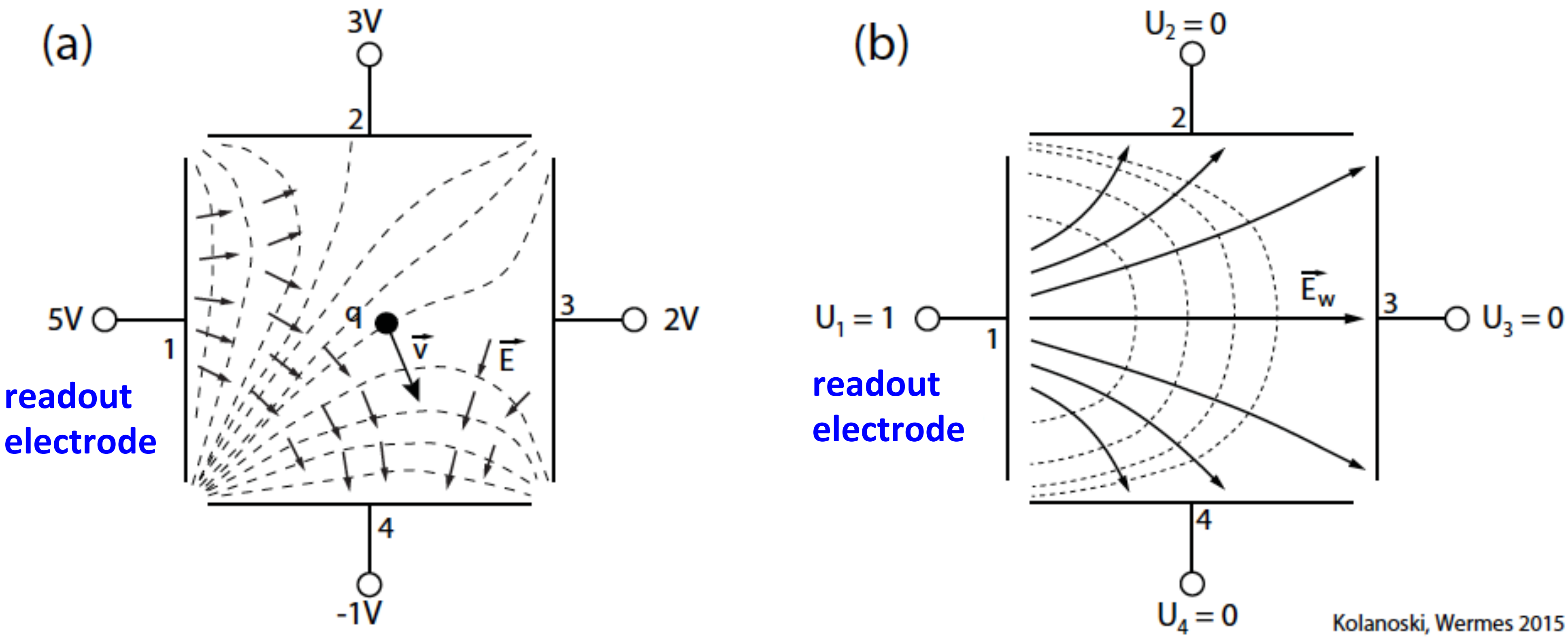

Kolanoski, Wermes 2015

$$i_S = -\frac{dQ}{dt} = q\,\vec{E}_w\,\vec{v}$$

A detector is a **current source**

delivers a current pulse
independent of the load

one can convert current into
charge (integral) or voltage (via R or C)

A parallel plate detector (capacitor)

universitätbonn

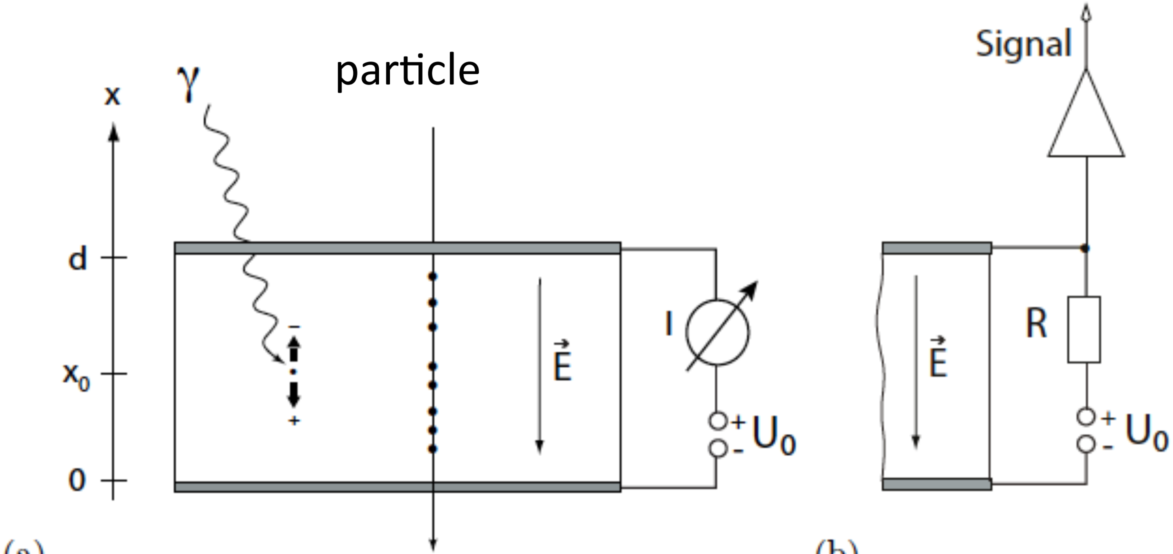

Kolanoski, Wermes 2015

$$\vec{E} = -\frac{U_0}{d}\vec{e}_x \;; \qquad C = \frac{\epsilon\epsilon_0 A}{d}$$

- constant E-field
- almost constant velocity (v=μE)
- weighting field simple

$$dQ = -q\,\frac{\vec{E}_0}{U}\,d\vec{r}. \qquad \vec{E}_w = -\frac{1}{d}\vec{e}_x$$

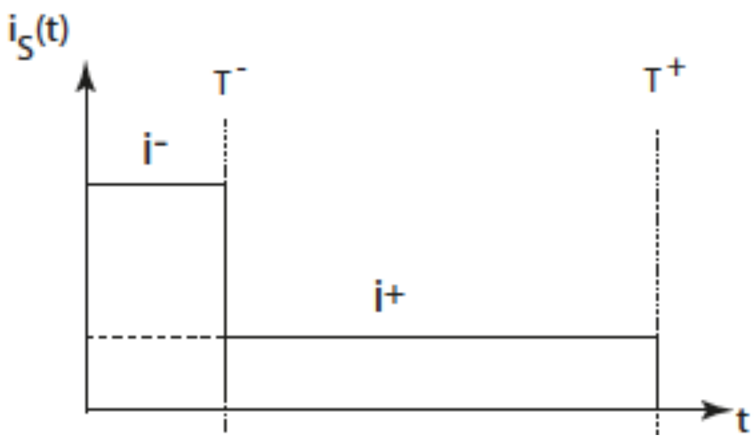

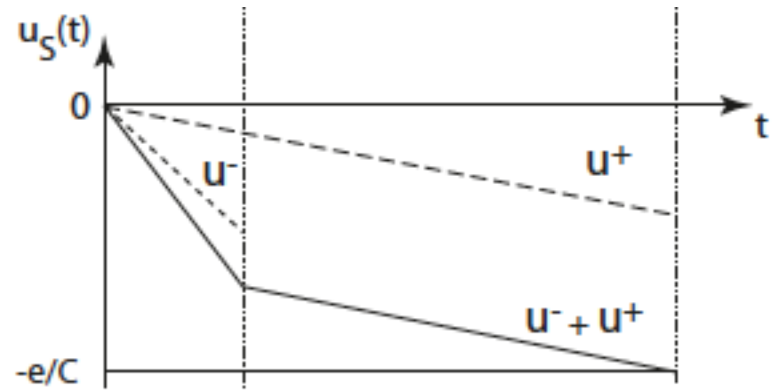

$$i_S^\pm = q^\pm \vec{E}_w\,\vec{v}^\pm = -\frac{q^\pm}{d}\,\vec{e}_x\,\vec{v}^\pm = \frac{e}{d}v^\pm$$

$$Q_S^{tot} = Q_S^- + Q_S^+ = -\frac{e}{d}\left(\int_0^{T^-} v^- dt + \int_0^{T^+} v^+ dt\right)$$

$$= -\frac{e}{d}v^-\left(\frac{d - x_0}{v^-}\right) - \frac{e}{d}v^+\left(\frac{x_0}{v^+}\right) = -e\,.$$

Signal in a Silicon detector (= parallel plate w/ space charge)

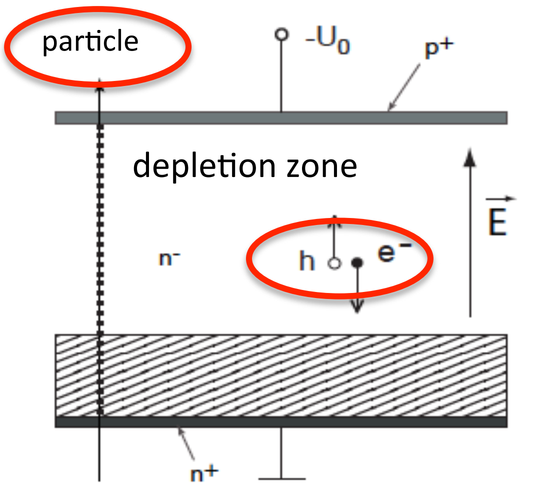

© Kolanoski, Wermes

see lecture 3

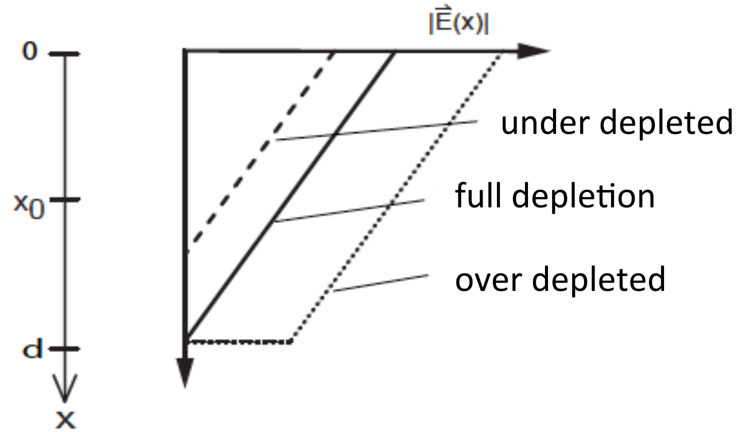

- E-field not constant
- velocity not constant
- weighting field still the same

$$\vec{E}_w = -\frac{1}{d}\vec{e}_x$$

$$E(x) = -\left[\frac{2U_{\rm dep}}{d^2}(d-x) + \frac{U-U_{dep}}{d}\right] = -\left[\frac{U+U_{dep}}{d} - \frac{2U_{dep}}{d^2}x\right] = -(a-bx)$$

$$v_e = -\mu_e E(x) = +\mu_e\,(a-bx) = \dot{x}_e$$
$$v_h = +\mu_h E(x) = -\mu_h\,(a-bx) = \dot{x}_h$$

$$i_S(t) = i_S^e(t) + i_S^h(t)$$
$$= -\frac{e}{d}\left(\frac{2U_{dep}}{d^2}\,x_0 - \frac{U+U_{dep}}{d}\right)$$
$$\times \left\{\mu_e \exp\left(-2\mu_e\frac{U_{dep}}{d^2}t\right)\Theta(T^- - t) - \mu_h \exp\left(+2\mu_h\frac{U_{dep}}{d^2}t\right)\Theta(T^+ - t)\right\}$$

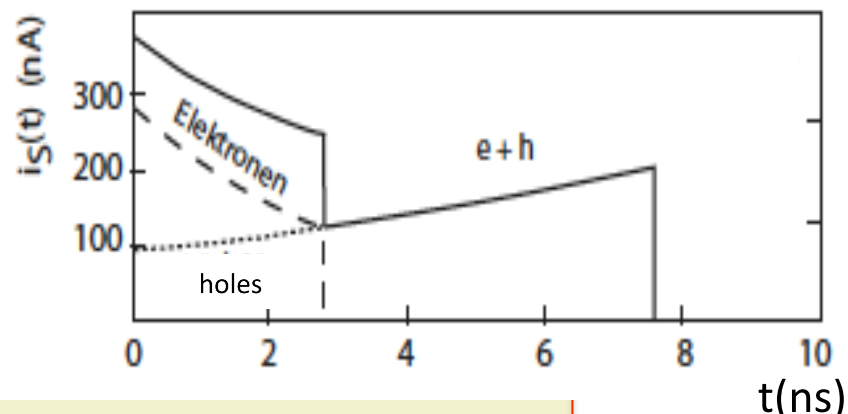

Current and charge signals

universitätbonn

point charge

charged particle track

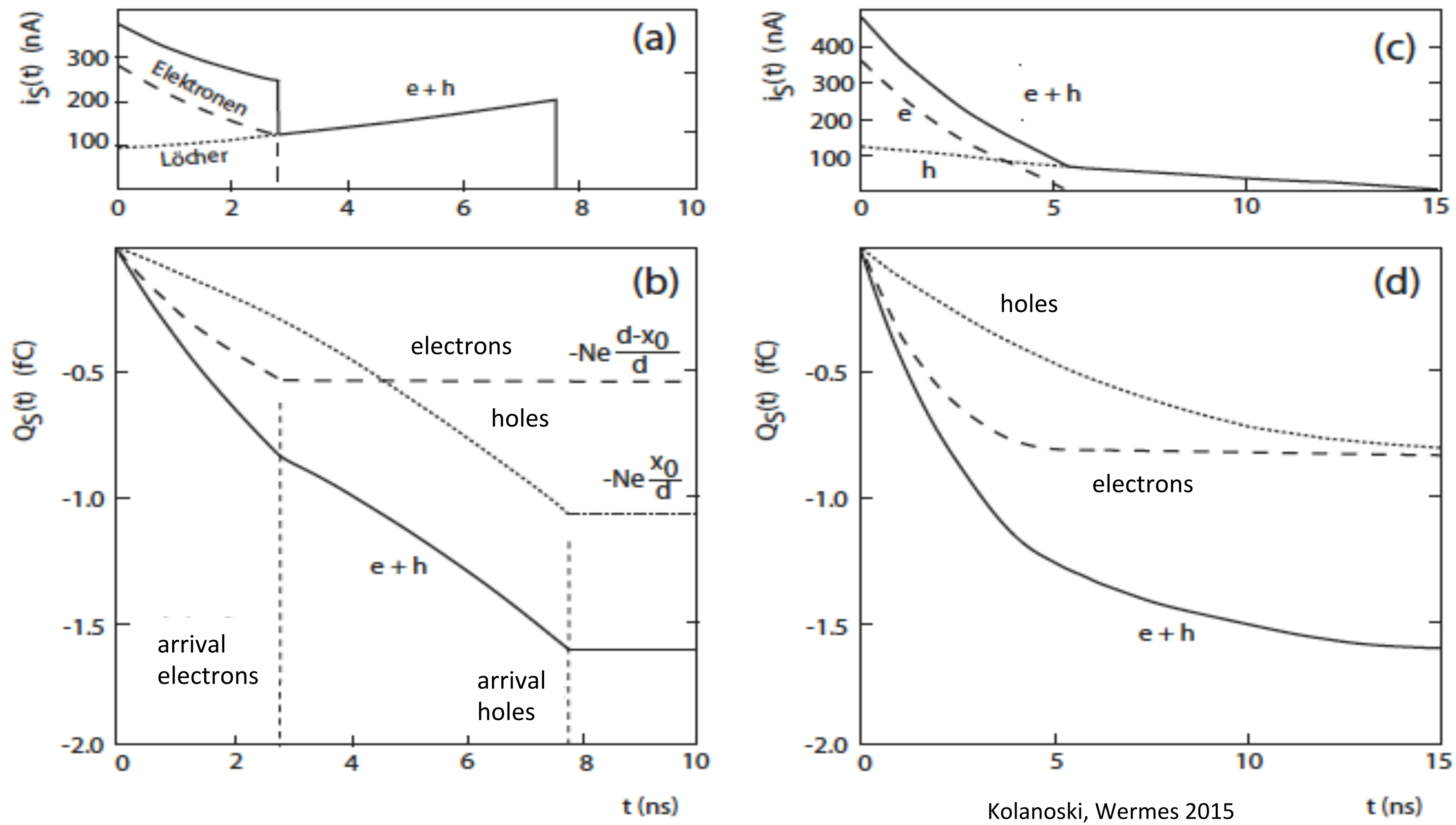

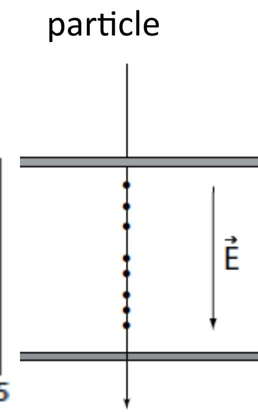

Current pulse measurements: TCT technique

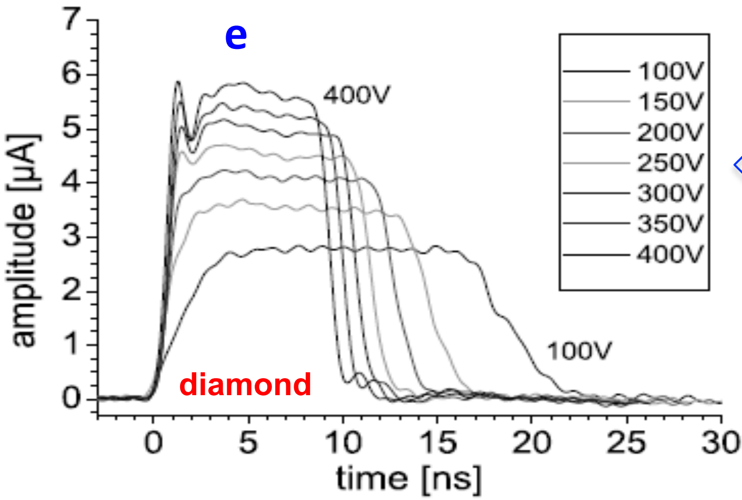

single crystal **diamond** is like a parallel plate detector filled with a dielectric w/o space charge

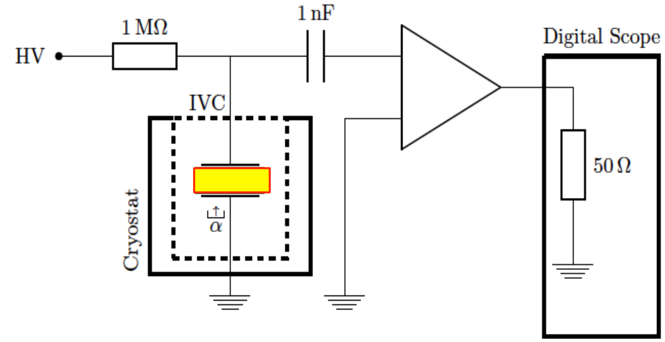

1mm pn – Diode **silicon**

- same weighting field
- different electric field

Si

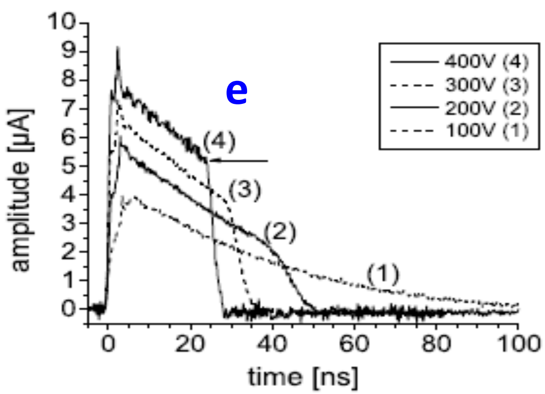

(a) Electron signals from α-particles impinging on the cathode.

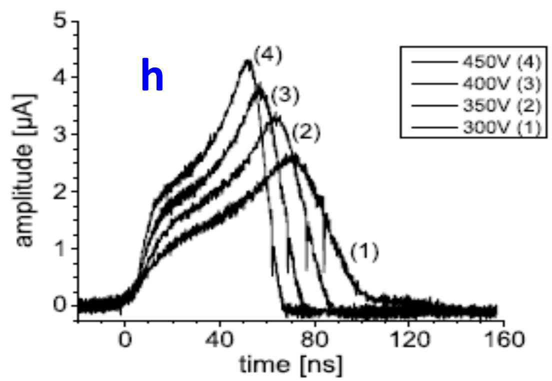

(b) Hole signals from α-particles impinging on the anode.

=>

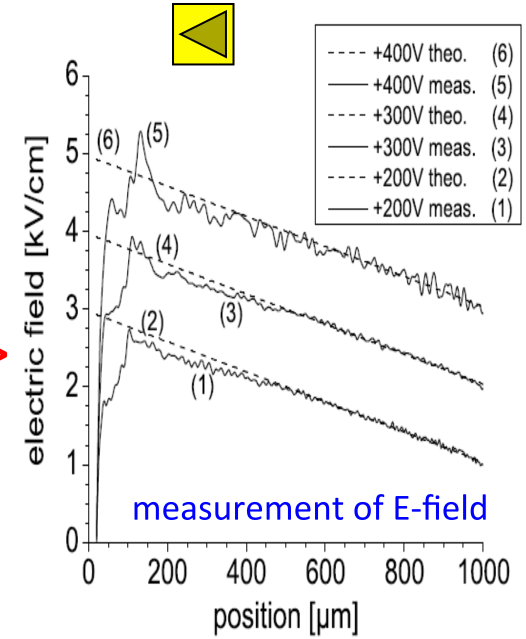

Note

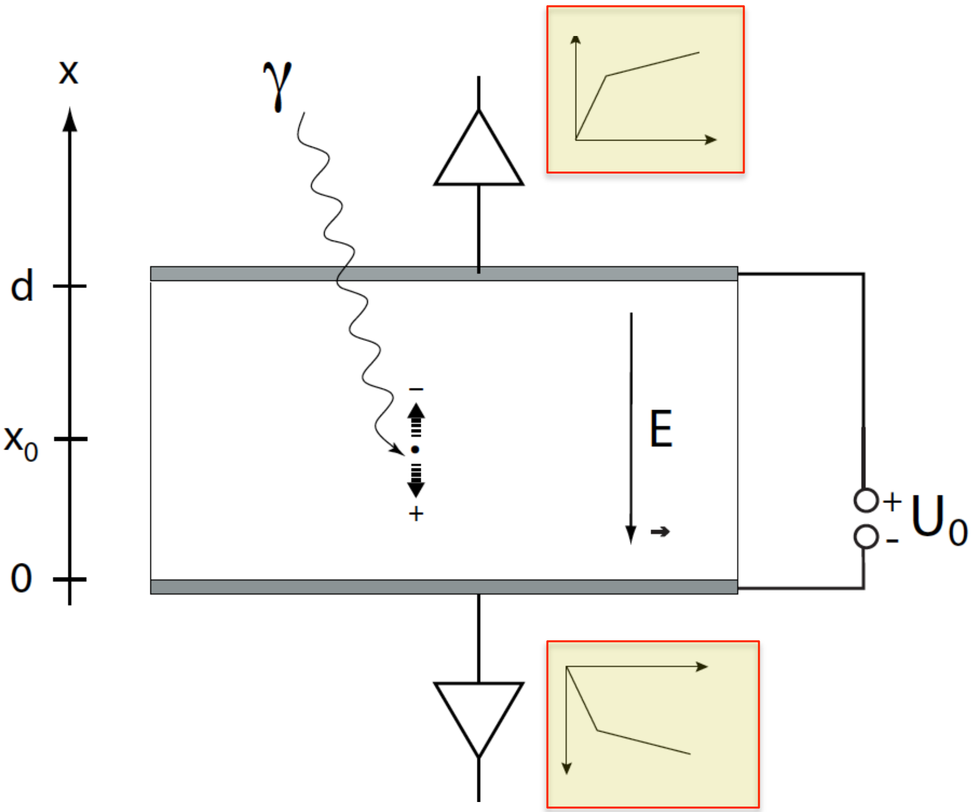

- movement of both charges create signals on both electrodes.
- on every electrode a total charge of

$$Q_S^{tot} = Q_S^- + Q_S^+ = -Ne$$

is induced.

- if a material the produced charges have very different mobilities (like CdTe) e.g. with $\mu_h \approx 0$, then part of the signal is lost and the signal becomes dependent on where the charge was deposited.

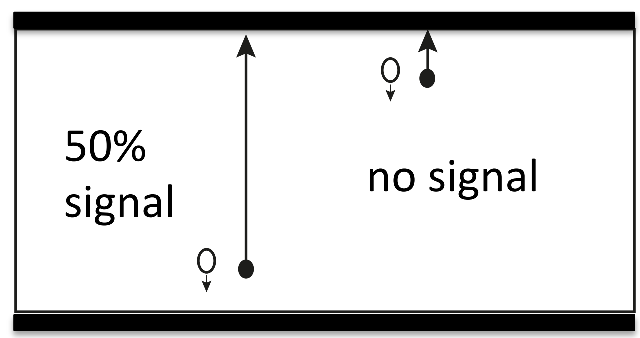

Signal development in a wire chamber

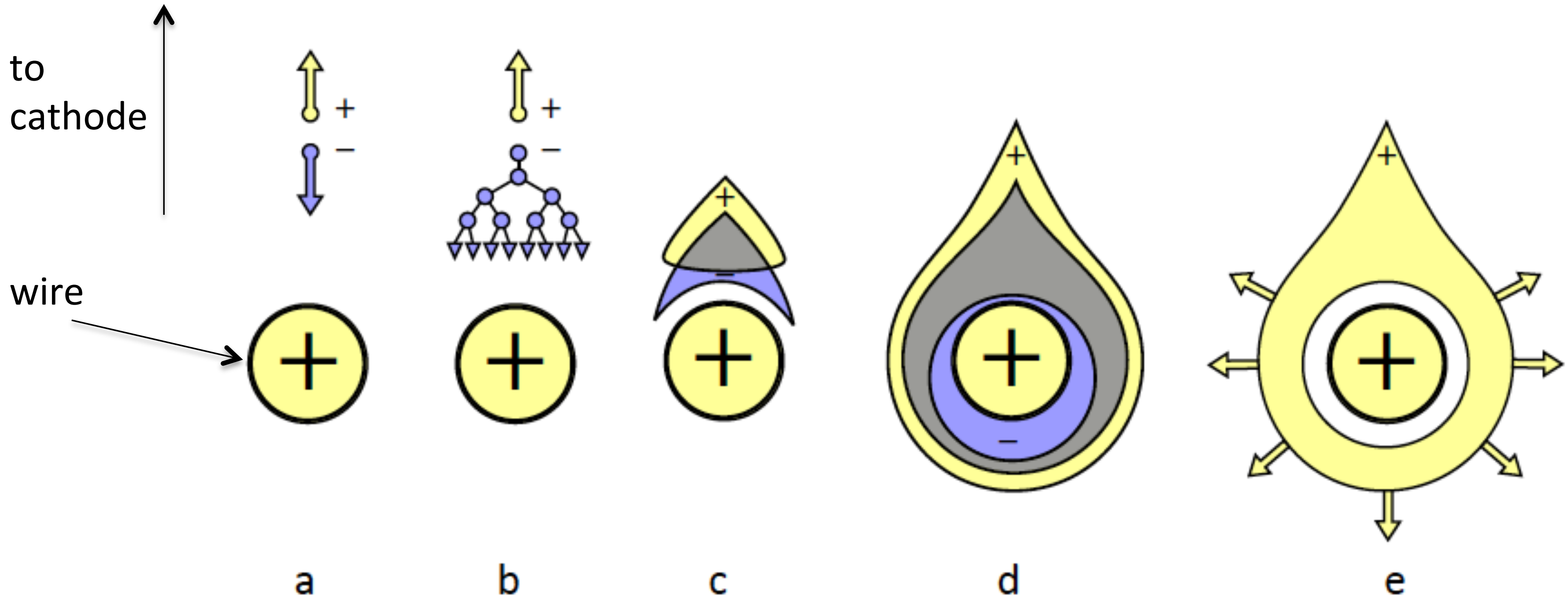

big difference:

- electrode (wire) does not “see” (too small) the charge before gas amplification
- signal (on wire) shape is governed by the (large) ion cloud moving away from the wire to cathode

Avalanche process:

$$dN = \alpha(E)\, N\, ds \quad \text{with} \quad \alpha = \sigma_{ion}\, n = \frac{1}{\lambda_{ion}}$$

$$N(x) = N_0 e^{\alpha x}$$

gas gain

$$\frac{N}{N_0} = G = e^{\alpha x}$$

1st Townsend coefficient

Signal development in a wire configuration (1)

universitätbonn

configuration

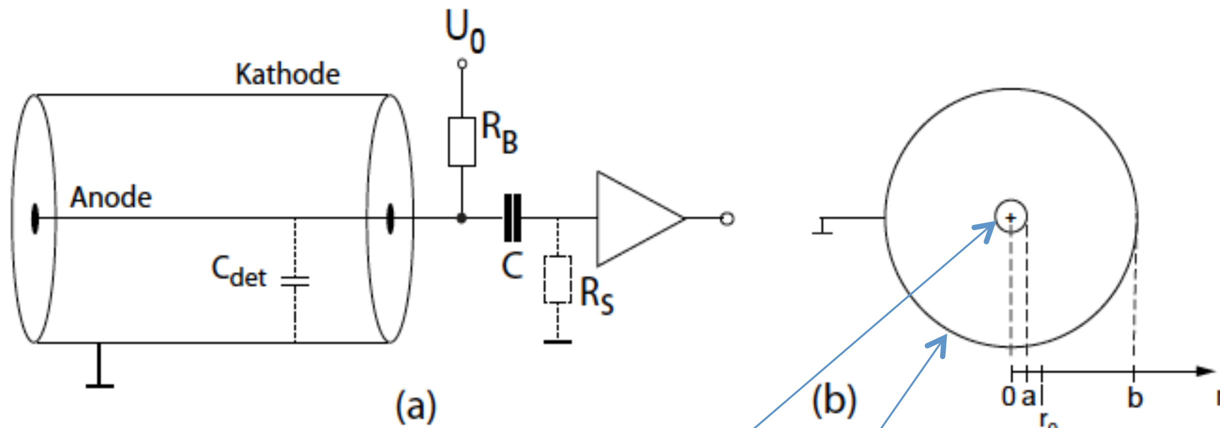

$$\vec{E}(r) = \frac{1}{r}\frac{U_0}{\ln b/a}\frac{\vec{r}}{r}, \qquad \phi(r) = -U_0\frac{\ln r/b}{\ln b/a}, \qquad C_l = \frac{2\pi\epsilon_0}{\ln b/a}.$$

- we follow our Shockley-Ramo-recipe: find the weighting field E_W or the weighting potential Φ_W by setting

$$\phi_w(a) = 1, \quad \phi_w(b) = 0 \qquad (*)$$

- we know already the shape of $\Phi_W \sim \ln r$, since $E(r) \sim 1/r$
- hence

$$\vec{E}_w(r) = \frac{1}{r}\frac{1}{\ln b/a}\frac{\vec{r}}{r}, \qquad \phi_w(r) = -\frac{\ln r/b}{\ln b/a}$$

which fulfils (*)

Signal development in a wire configuration (2)

universitätbonn

- now use Shockley-Ramo $dQ_S = -q\vec{E}_w d\vec{r}$

- we assume that N e/ion-pairs are produced at r = r_0. Note that, if there is avalanche amplification (starting only in the high field region) the vast majority of charges is produced very close to the wire (r_0 < 10 μm, see previous page)

- then we get immediately

$$Q_S^- = -(-Ne)\frac{1}{\ln b/a}\int_{r_0}^{a}\frac{1}{r}dr = -Ne\frac{\ln\ r_0/a}{\ln\ b/a}$$

$$Q_S^+ = -(+Ne)\frac{1}{\ln b/a}\int_{r_0}^{b}\frac{1}{r}dr = -Ne\frac{\ln b/r_0}{\ln b/a}$$

(**)

- and the total charge is $Q_S^{tot} = Q_S^- + Q_S^+ = -Ne$ ✔
however, due to the 1/r dependence of the weighting field the situation is much different from that of a parallel plate detector: the contribution from electrons and ions is not necessarily the same but depends on r_0 (i.e where the avalanche is created, because only there N becomes large enough that the signal is "felt" by the electrode (wire).

Signal development in a wire configuration (3)

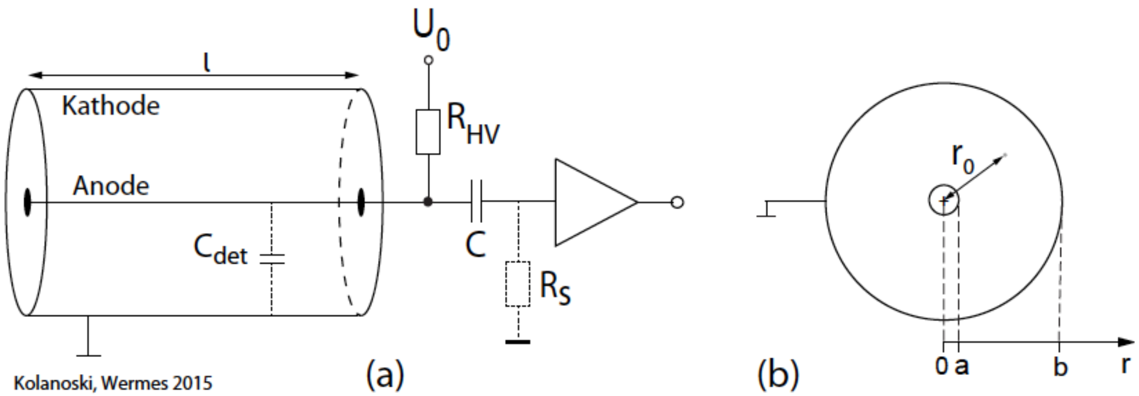

ratio depends on r_0

$$\left(\frac{Q_S^-}{Q_S^+}\right)_{r_0} = \frac{\ln r_0/a}{\ln b/r_0}$$

for a typical (a=10 µm, b=10 mm)

far away from wire

near wire

$$\left(\frac{Q_S^-}{Q_S^+}\right)_{r_0=b/2} \approx 9$$

$$\left(\frac{Q_S^-}{Q_S^+}\right)_{r_0=a+\epsilon} \approx 0.01 - 0.02$$

in wire chambers the (integrated) signal is dominated by the ion contribution. Reason: specific form of the weighting field

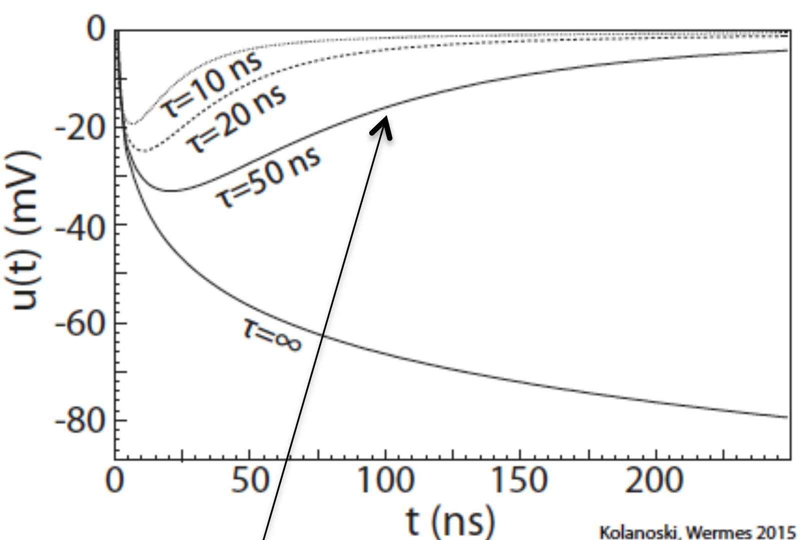

with RC filter

using Ramo and r(t) from the 1/r - E-field, we get …

$$i_S^+(t) = \frac{Ne}{2\ln b/a}\frac{1}{t+t_0^+}$$

ions only

$$u_s(t) = \frac{Q_S(t)}{C_l\, l} = -\frac{N\,e}{2\pi\epsilon_0\, l}\ln\left(1+\frac{t}{t_0^+}\right)$$

Summary: Signal formation characteristics in a wire chamber

universitätbonn

- electric field is large close to the wire @ $r \approx r_{wire}$
  => secondary ionisation has a much larger effect on signal
  than primary ionisation
  => avalanche near wire: $q \rightarrow q \times 10^{4\text{-}7}$
- from there (µm's away from wire) the electrons reach the wire fast
  => very small and fast e^- component of Q_{tot}
- ions move slowly away from wire => main component of $Q_{tot}(t)$
- signal only relevant after avalanche ionization ≅ quasi only $Q^+(t)$
- the term 'charge collection' is more justified in wire chambers than in other ionisation detectors (e.g. parallel plate detectors) since most of the signal is created only very close to the wire

Cathode readout

signals are induced on BOTH (ALL) electrodes => exploit for second coordinate readout

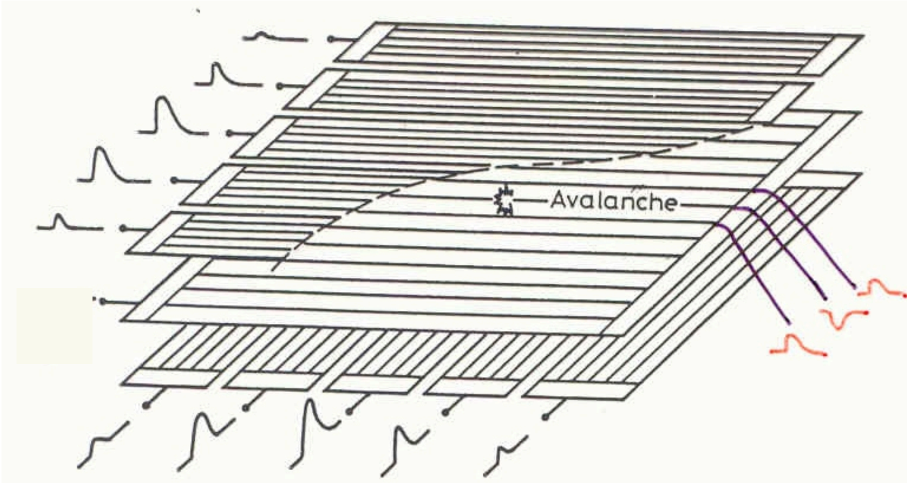

wire chamber
with cathode readout

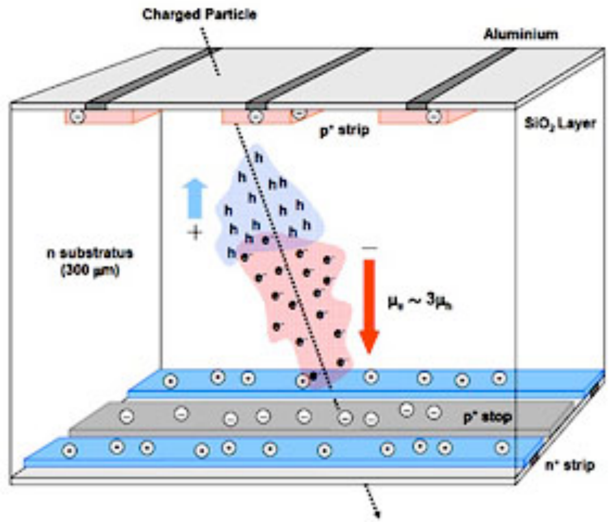

double sided
silicon strip detector

Signal generation in a pixellated detector (1-dim)

Φ_W for a strip/pixel geometry

$$\Phi(x,y) = \frac{1}{\pi}\arctan\frac{\sin(\pi y)\cdot\sinh(\pi\frac{a}{2})}{\cosh(\pi x) - \cos(\pi y)\cosh(\pi\frac{a}{2})}$$

(can be calculated e.g. by using "conformal mapping")

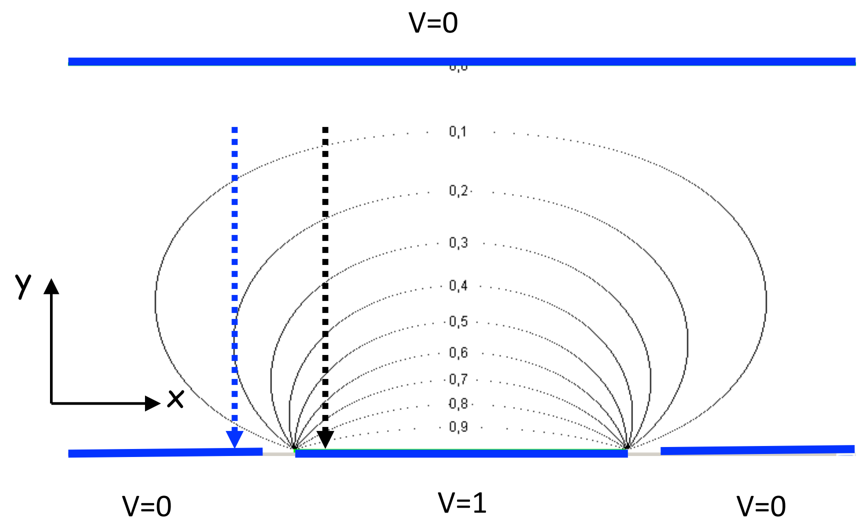

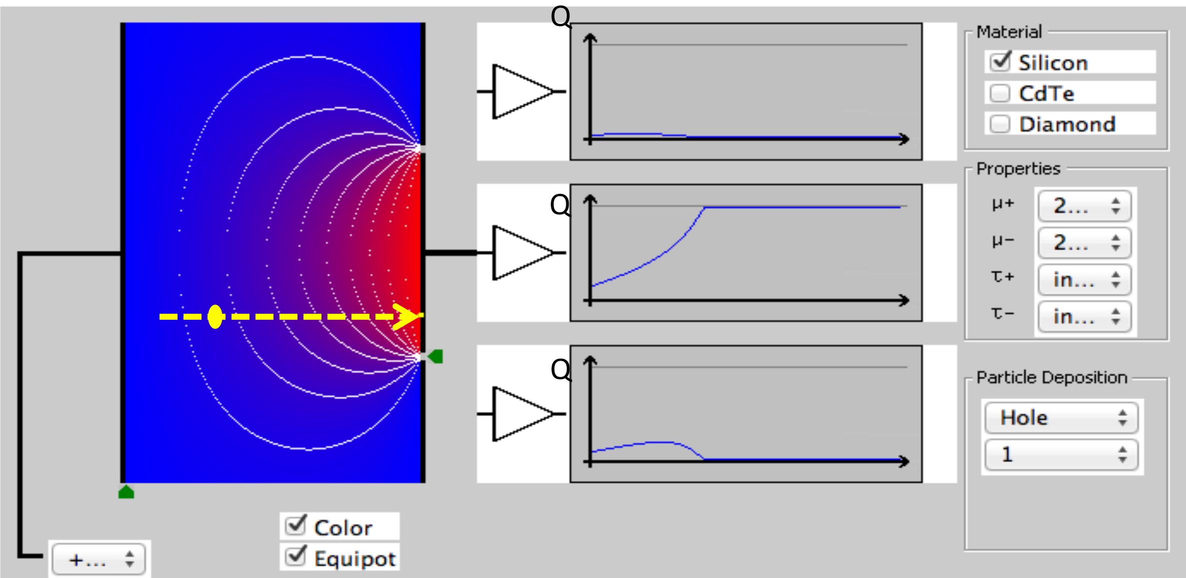

"small pixel effect" !

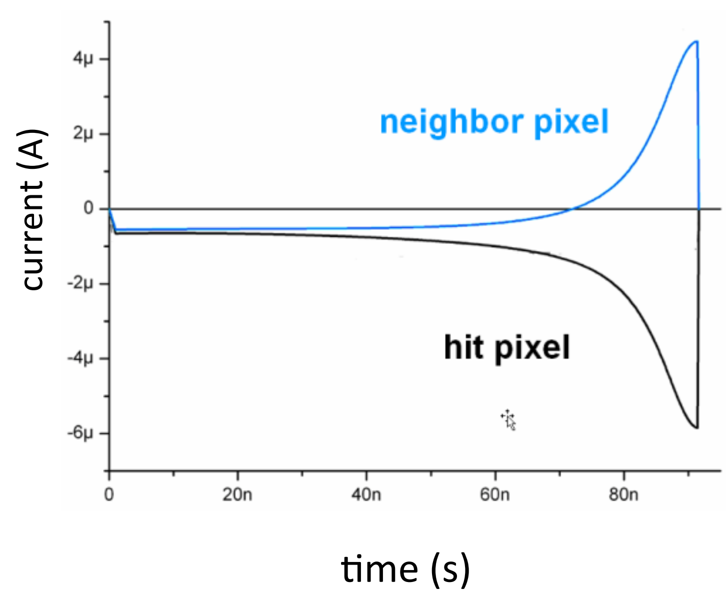

Concluding … consequences …

- The weighting field reaches also into regions of neighbor pixels → induced signals there as well
- At the beginning of the charge movement, neighbor pixels "see" almost as much signal as the "hit" pixel → no difference when electronics is (too) fast
- consequences for small electrodes is, that most of the charge is induced, when q is <u>near</u> the hit pixel → small pixel effect
- when charges drift only a short distance due to
  - $\mu_h << \mu_e$ (e.g. for CdTe)
  - trapping (e.g. for pCVD diamond)

  peculiar signal patterns may arise (worst case: holes do not move and electrons are trapped after 50 µm ➔ several pixels "fire")

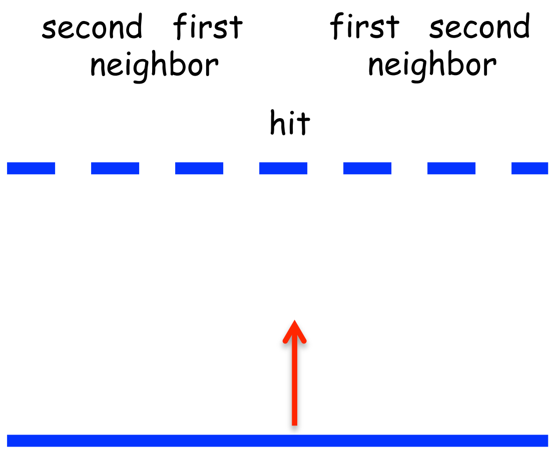

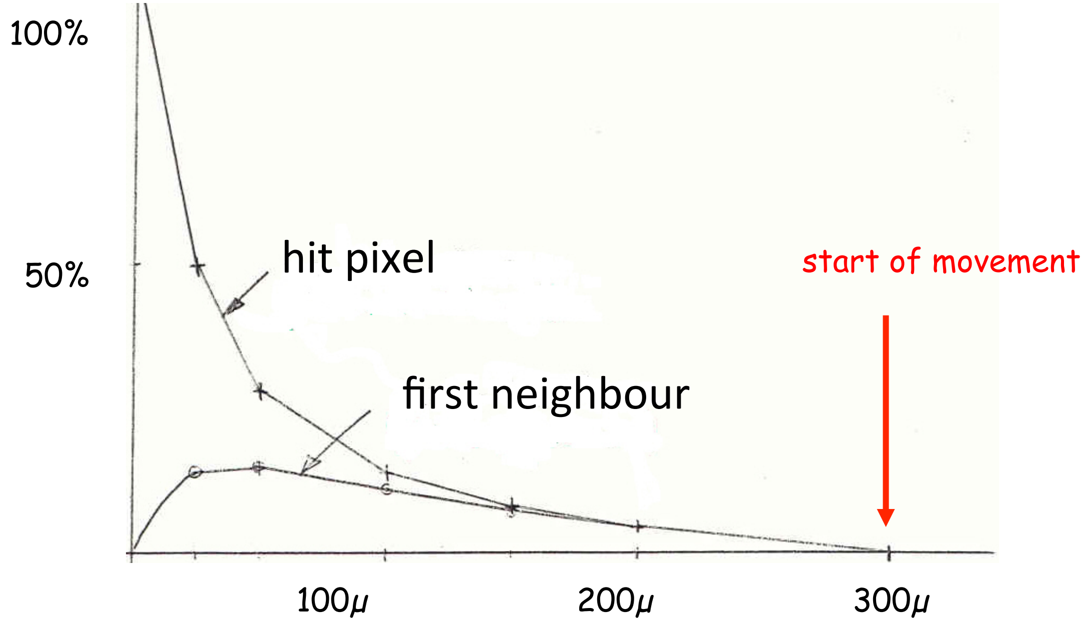

Transport of charges to the R/O electrode

generally described by the Boltzmann Transport Equation

$$\frac{df}{dt} = \frac{\partial f}{\partial t} + \frac{d\vec{r}}{dt}\vec{\nabla}_{\vec{r}} f + \frac{d\vec{v}}{dt}\vec{\nabla}_{\vec{v}} f = \frac{\partial f}{\partial t}_{|coll}$$

with f(r, v, t) describing the probability distribution in phase space

$$dp(\vec{r}, \vec{v}, t) = f(\vec{r}, \vec{v}, t)\, d^3\vec{r}\, d^3\vec{v}$$

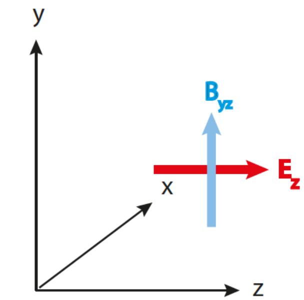

Which can treat arbitrary E and B-fields … (E in z-direction, B in z-y-direction)

$$v^B_{D,1} = -\frac{4\pi}{3}\frac{qE}{m}\int_0^\infty \tau \frac{\omega_2 \tau}{1+\omega^2\tau^2}\left(\frac{2\epsilon}{m}\right)^{3/2}\frac{\partial f_0}{\partial \epsilon} d\epsilon = \frac{qE}{m}\left\langle \tau \frac{\omega_2 \tau}{1+\omega^2\tau^2}\right\rangle_\epsilon$$

$$v^B_{D,2} = \frac{4\pi}{3}\frac{qE}{m}\int_0^\infty \tau \frac{\omega_2 \omega_3 \tau^2}{1+\omega^2\tau^2}\left(\frac{2\epsilon}{m}\right)^{3/2}\frac{\partial f_0}{\partial \epsilon} d\epsilon = \frac{qE}{m}\left\langle \tau \frac{\omega_2 \omega_3 \tau^2}{1+\omega^2\tau^2}\right\rangle_\epsilon$$

$$v^B_{D,3} = \frac{4\pi}{3}\frac{qE}{m}\int_0^\infty \tau \frac{1+\omega_3^2 \tau^2}{1+\omega^2\tau^2}\left(\frac{2\epsilon}{m}\right)^{3/2}\frac{\partial f_0}{\partial \epsilon} d\epsilon = \frac{qE}{m}\left\langle \tau \frac{1+\omega_3^2 \tau^2}{1+\omega^2\tau^2}\right\rangle_\epsilon$$

with

$\omega_i = qB_i/m$ = cyclotron frequencies

τ = mean collision time
ε = kin. energy

In detectors: usually either $\vec{E} \perp \vec{B}$ or $\vec{E} \parallel \vec{B}$

Diffusion and drift of charge cloud on way to electrode

E = 0, T > 0: diffusion

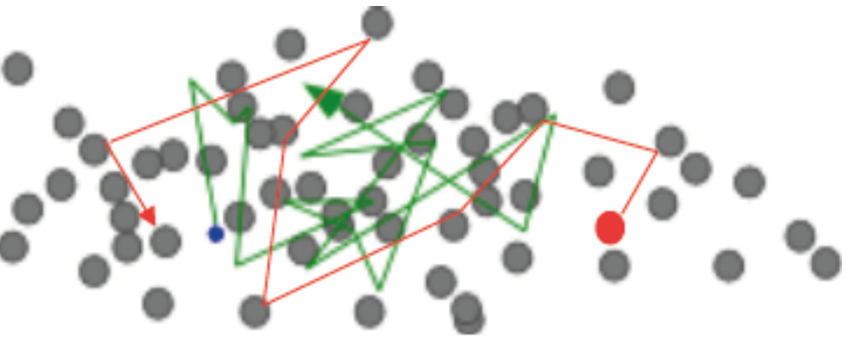

$$D = \frac{\langle \lambda v \rangle}{3} = \frac{1}{3\sigma p}\sqrt{\frac{8(kT)^3}{\pi m}}$$

E > 0, T > 0: diffusion + drift

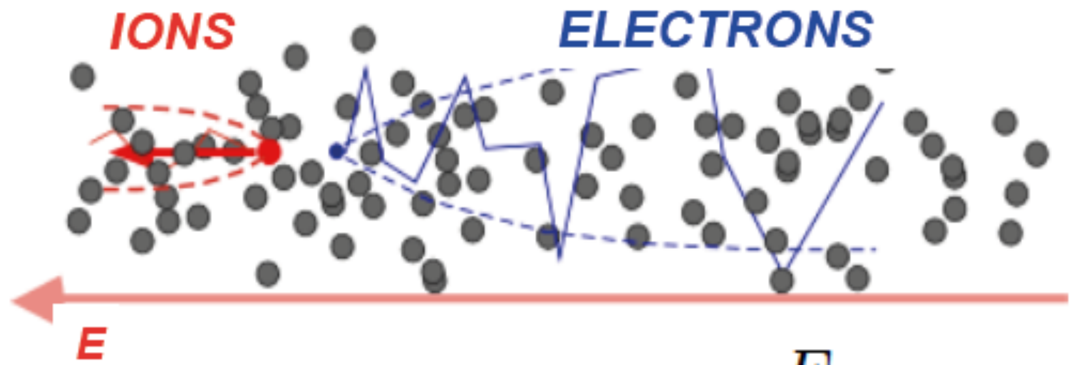

$$v_D = \mu(E)\,E = \frac{\mu_0 E}{\left[1 + \left(\frac{\mu_0 E}{v_{\text{sat}}}\right)^{\beta}\right]^{1/\beta}}$$

Drude Ansatz (emp.)
(especially semicond.)

β~1-2

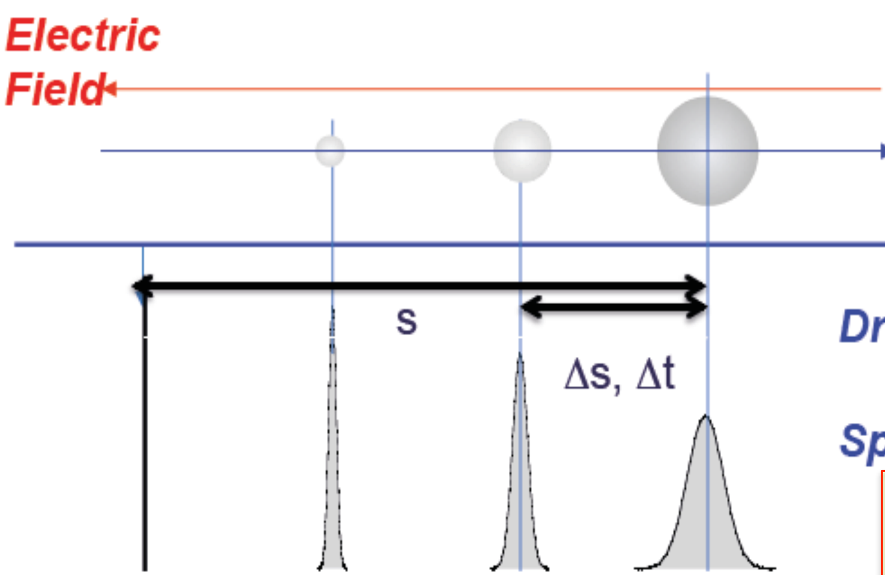

Drift velocity: $v_D = \frac{\Delta s}{\Delta t}$

Space diffusion rms:

$$\sigma_x = \sqrt{2Dt} = \sqrt{2D\frac{s}{v_D}}$$

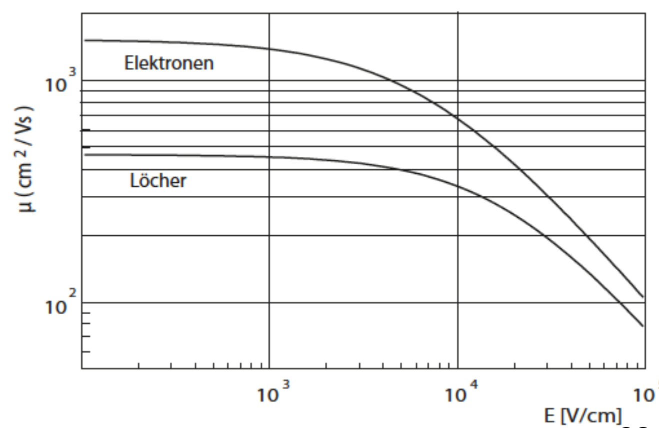

Movement in the presence of a magnetic field

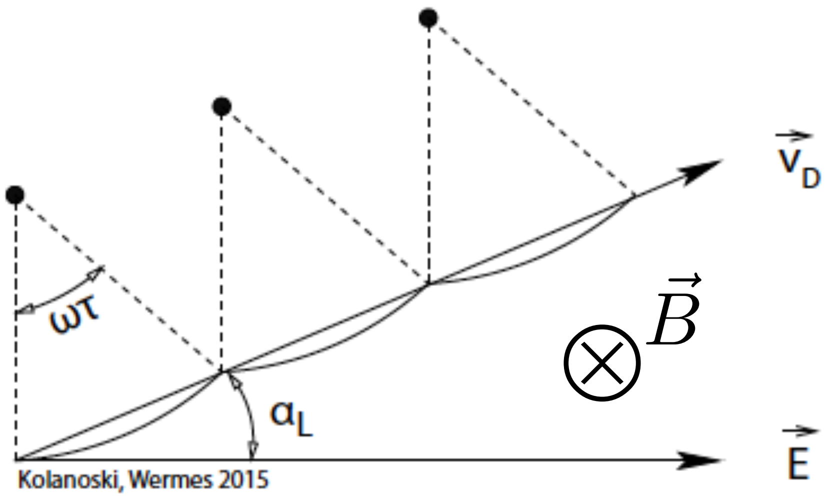

- if the electric field E is perpendicular to a magnetic field B then the charges drift on circle segments until they stop in a collision
- on average this results in a deflection of the drift path by an angle called

Lorentz angle

perp. to E

$$\tan \alpha_L = \frac{v_{D,\perp}}{v_{D,\parallel}} = \omega\tau$$

parallel to E

with

ω = qB/m = cyclotron frequency

τ = mean collision time

Spatial Resolution in segmented electrode configurations

remember Gluckstern formula

$$\left(\frac{\sigma_{p_T}}{p_T}\right)_{\rm mess} = \frac{p_T}{0.3|z|}\frac{\sigma_{\rm mess}}{L^2 B}\sqrt{\frac{720}{N+4}}$$

$$[p_T] = {\rm GeV/c},\ [L] = {\rm m},\ [B] = {\rm T}$$

- binary readout (hit/no hit)
- analog readout (pulse height information)

- signal (charge) distributed on more than one electrode

binary R/O

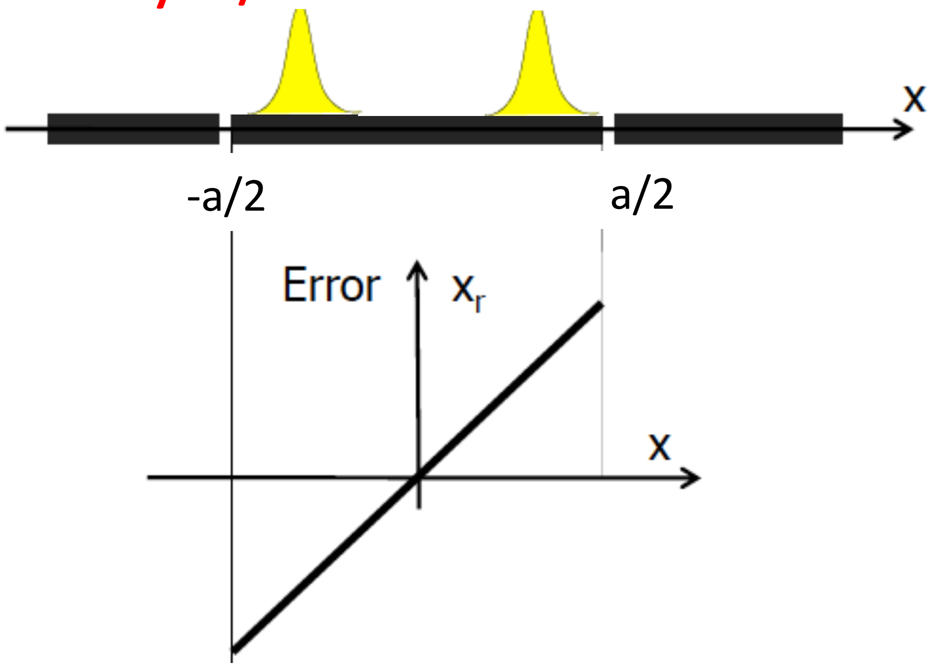

$$v = \int_{x_1}^{x_2} x^2 f(x)dx$$

$$\sigma_x^2 = \frac{1}{a}\int_{-a/2}^{a/2} \Delta_x^2\, d(\Delta_x) = \frac{a^2}{12}$$

$$\sigma_x = \frac{a}{\sqrt{12}}$$

Spatial Resolution in segmented electrode configurations

with analog information
and spread over more
than one electrode

center of gravity

$$x = x_c = \frac{\sum S_i\, x_i}{\sum S_i}$$

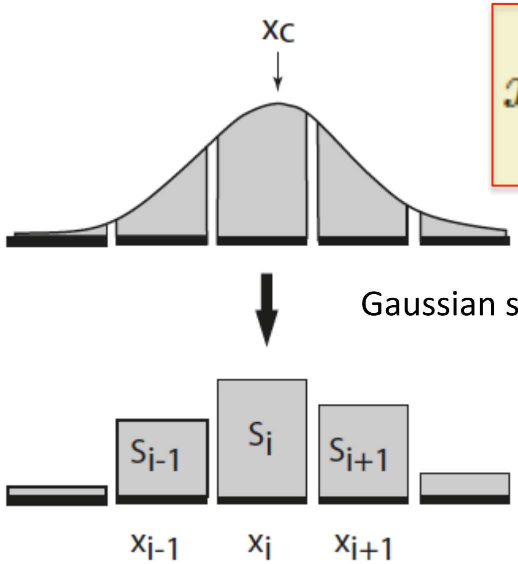

Gaussian signal

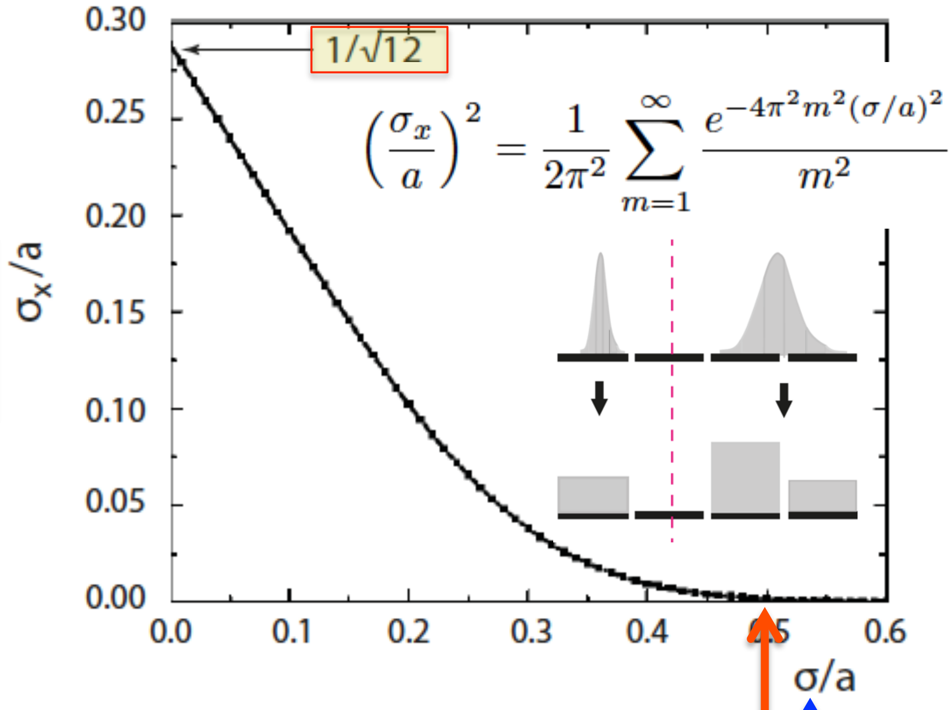

$$\left(\frac{\sigma_x}{a}\right)^2 = \frac{1}{2\pi^2}\sum_{m=1}^{\infty}\frac{e^{-4\pi^2 m^2(\sigma/a)^2}}{m^2}$$

perfect resolution
but only w/o noise

width of charge cloud

$$x_{rec} = \frac{\sum(S_i + n_i)\,x_i}{\sum(S_i + n_i)} = \frac{x + \sum n_i x_i}{1 + \sum n_i} = \left(x + \sum n_i x_i\right)\left(1 - \sum n_i + \mathcal{O}(n_i^2)\right)$$

with uncorrelated noise
(normalized to signal and with S=1) $\langle n_i^2 \rangle = \sigma_n^2,$

$$\Rightarrow \sigma_x^2 = \sigma_n^2\left[\left(\sum_{i=1}^{N} x_i^2\right) + N\langle x^2\rangle\right] + \mathcal{O}(\sigma_n^3)$$

P. Fischer
publ. in prep.
also in KW2016

Observations

universitätbonn

formalism can be extended accordingly **to 2D**

$$\sigma_x^2 = \sigma_n^2 \left[\left(\sum_{i=1}^{N} x_i^2 \right) + N\langle x^2 \rangle \right] + \mathcal{O}(\sigma_n^3)$$

small number of electrodes good (because of noise)

good, if charge confined in small area -> circle like

Geometry	factor for (a = A = 1)
strips	0.816
pixel (square)	1.155
pixel (hexagonal)	0.491

hexagons least sensitive to noise contributions on electrodes

Example:

- two strips at $x_1 = -a/2$ and $x_2 = +a/2$ (N = 2)
- Signals for a hit at x are

$$S_1(x) = (x_2 - x)/a \text{ and } S_2(x) = (x + x_2)/a$$

- $S_1 + S_2 = 1$; $x_1 S_1 + x_2 S_2 = x$; $x_1 + x_2 = 0$ ✓

$$\left(\frac{\sigma_x}{\sigma_n}\right)^2 \approx x_1^2 + x_2^2 + \frac{2}{a}\int_{x_1}^{x_2} x^2 dx = \frac{2}{3}a^2$$

$$\sigma_x = 0.816\, a\, \sigma_n$$

- Thus the resolution for S/N = 10 (σ_n= 0.1) is

$$\sigma_x = 0.08a$$

It is better than binary (a/√12) as long as S/N > 2.8.

Arbitrary detector response ("data driven method")

universitätbonn

typical for semiconductor detectors
and patterned gaseous detectors
channels have different gains

$N_{electrodes}$ = 2-3, S/N ~ 10

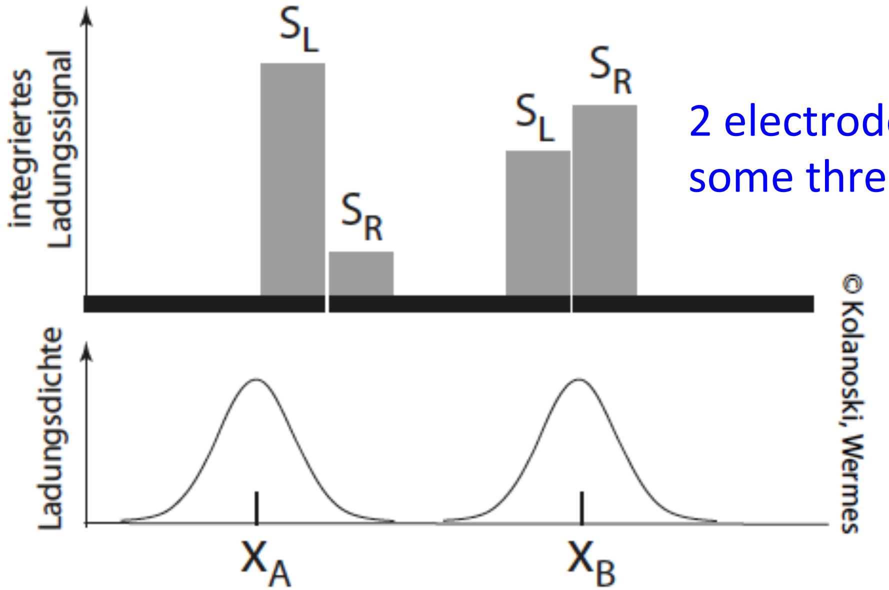

2 electrodes have signal over some threshold

$$S_L(x) = Q\,\eta(x)$$

$$S_R(x) = Q - S_L(x) = Q\,(1 - \eta(x))$$

η = response function, indep. of Q
can be determined from signals themselves

$$\eta = \frac{S_L}{S_L + S_R}$$

- assume a constant hit probability density
- => can build inverse of η-function (η -> x)
- pick best estimate of position from measured distribution
- algorithm can also be extended to three – electrode situations

$$x_{rec} = \eta^{-1}\left(\frac{S_L}{S_L + S_R}\right) = \frac{a}{N}\int_0^{\eta} \frac{dN}{d\eta'}d\eta'$$

Arbitrary detector response

universitätbonn

Belau, E. et al.: NIM 214 (1983) 253–260

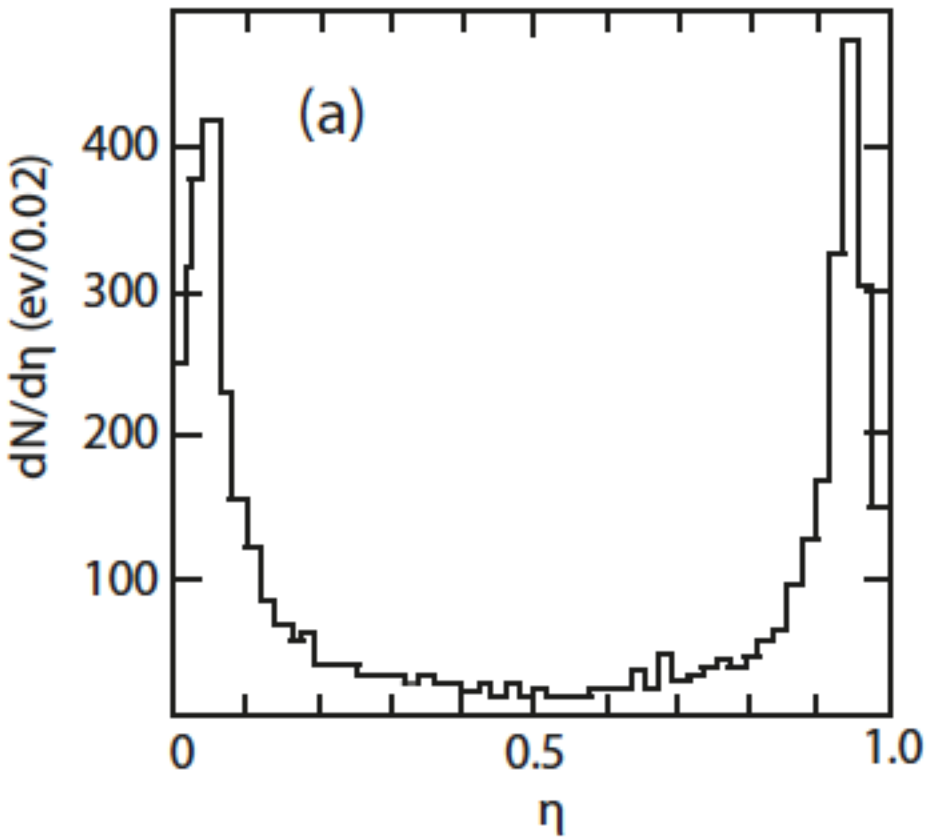

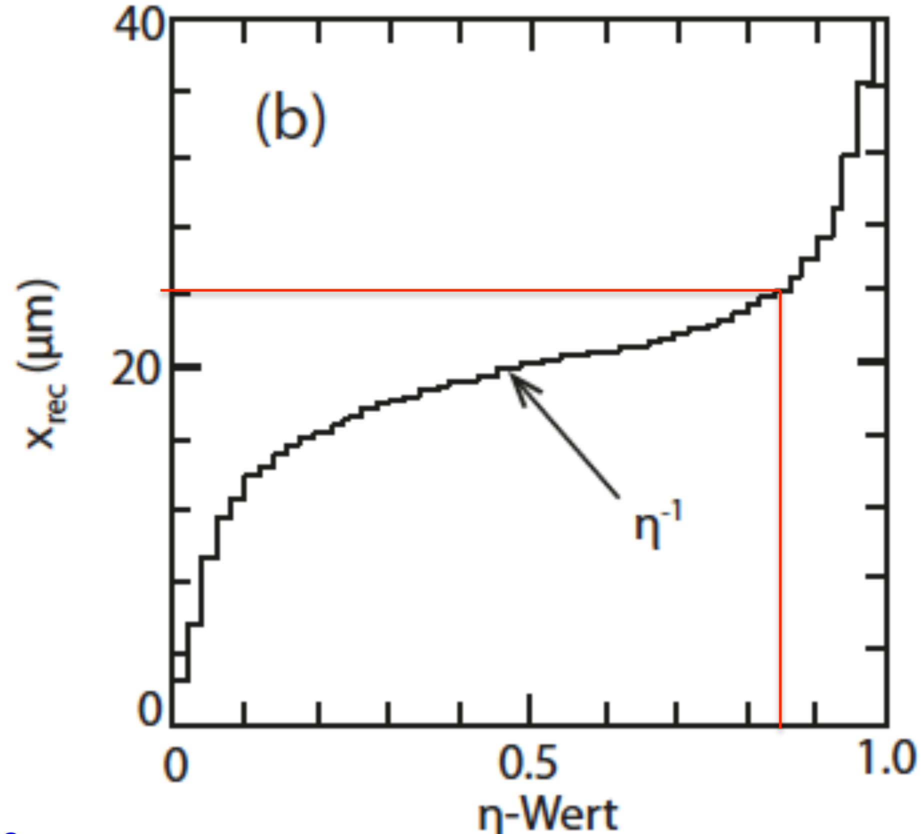

noise

reconstruction
with noise

$$x_{rec_{noise}} \approx x_{rec} = \frac{1}{\eta'}\left(n_L\,(1-\eta(x)) - n_R\eta(x)\right)$$

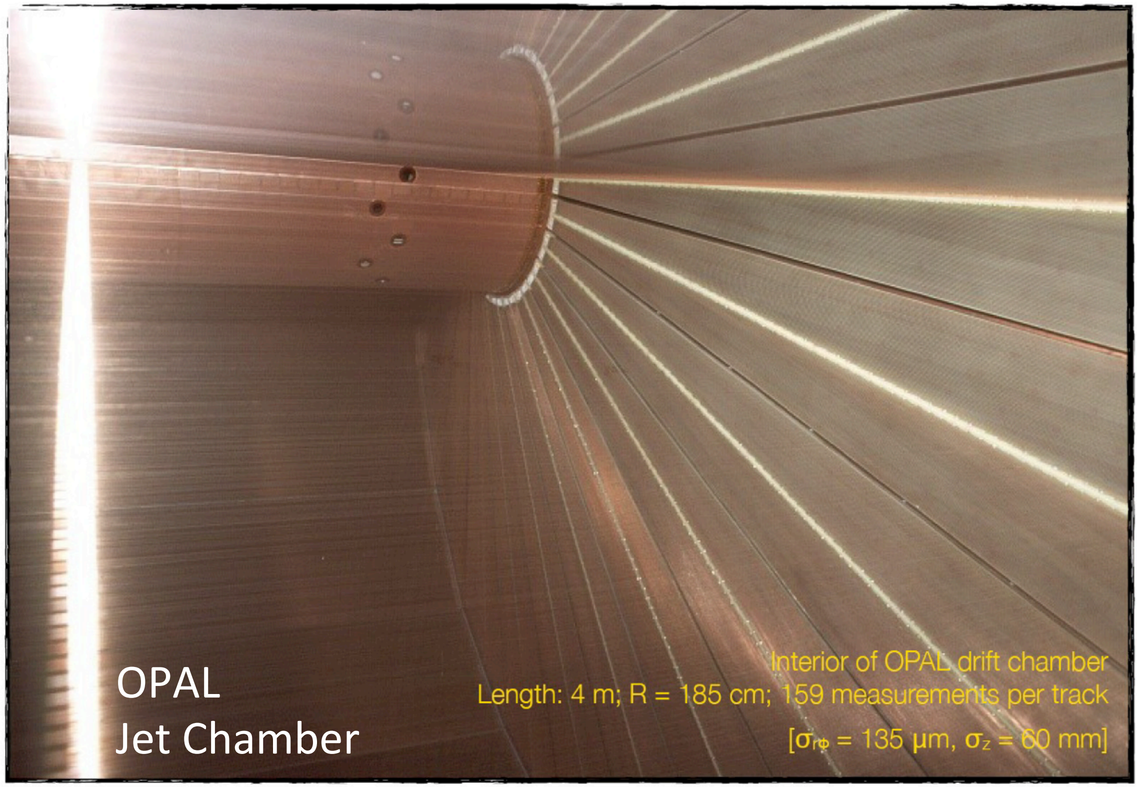

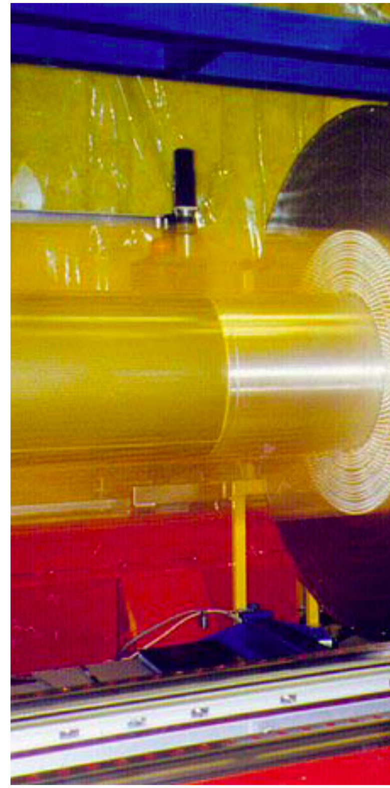

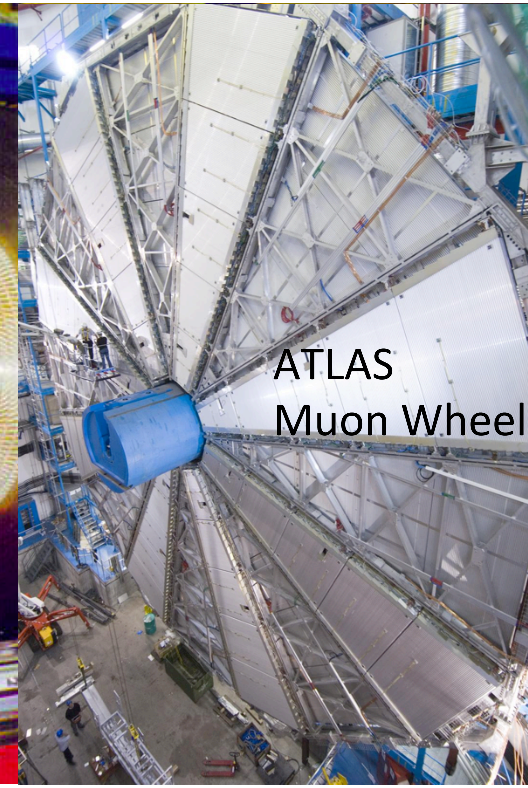

Gas-filled detectors

>40 min ?

Multi Wire Proportional Chamber

universitätbonn

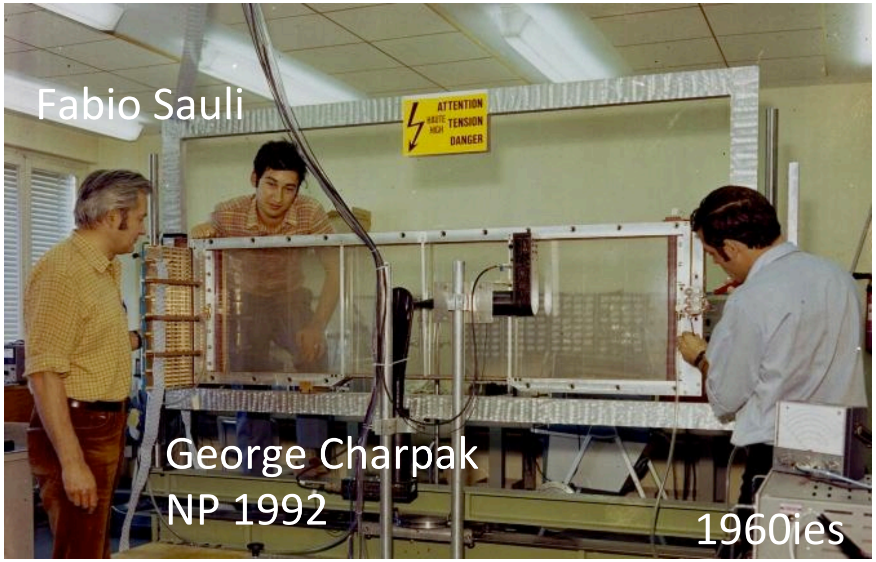

- mother of all wire chambers (1960ies)
- break through in tracking, because tracks became electronically recordable
- Nobel Prize 1992

cathodes often patterned for 2nd coordinate or more chambers

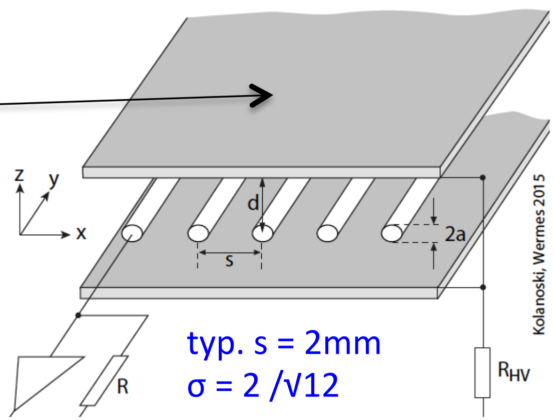

typ. s = 2mm
σ = 2 /√12

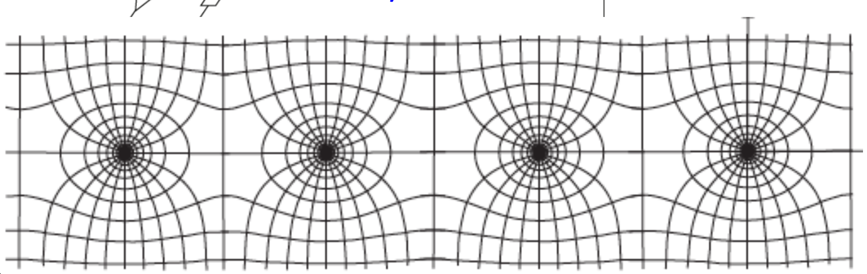

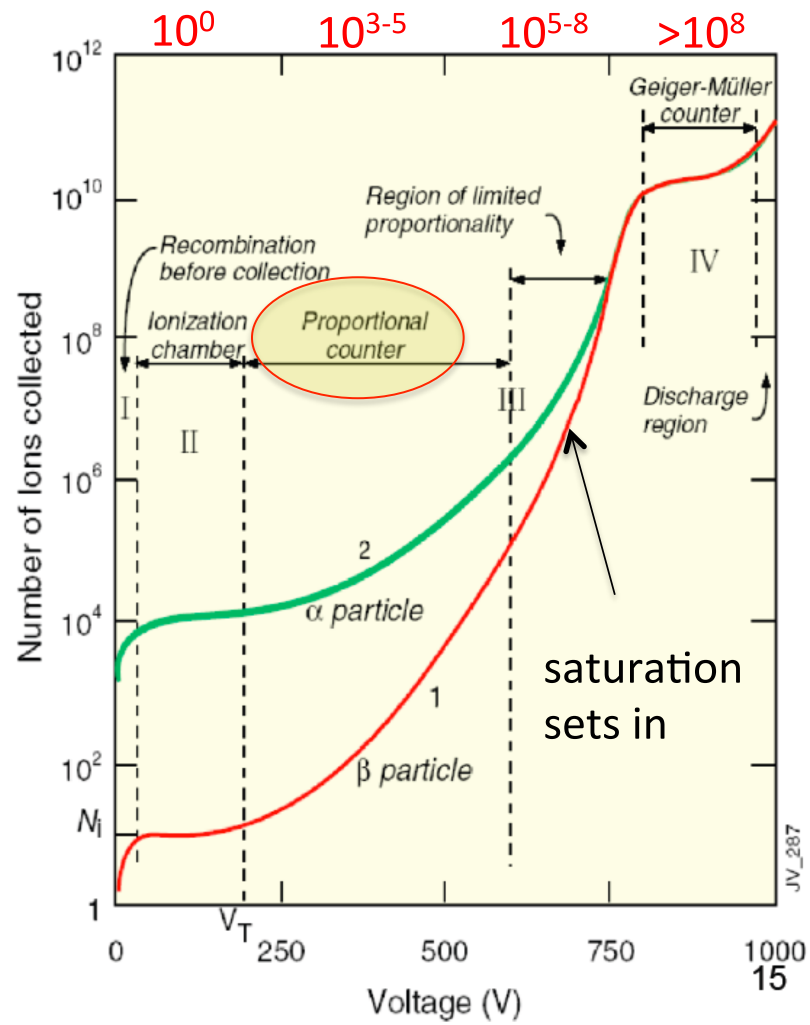

Operation modes of wire chambers

region of limited proportionality → multi wire chamber operation in saturation region (G ~10^5 - 10^7)

- operation point: gain > 10^6 → strong secondary ionization
- space charge effects (stationary ion cloud decreases the electric field at the anode) destroy 1/r shape near wire
- saturation of signal sets in

  this is sometimes wanted, when the number of particles is to be determined by the total signal height; e.g. when slow ($1/\beta^2$!) protons shall give the same signal height as m.i.p.s

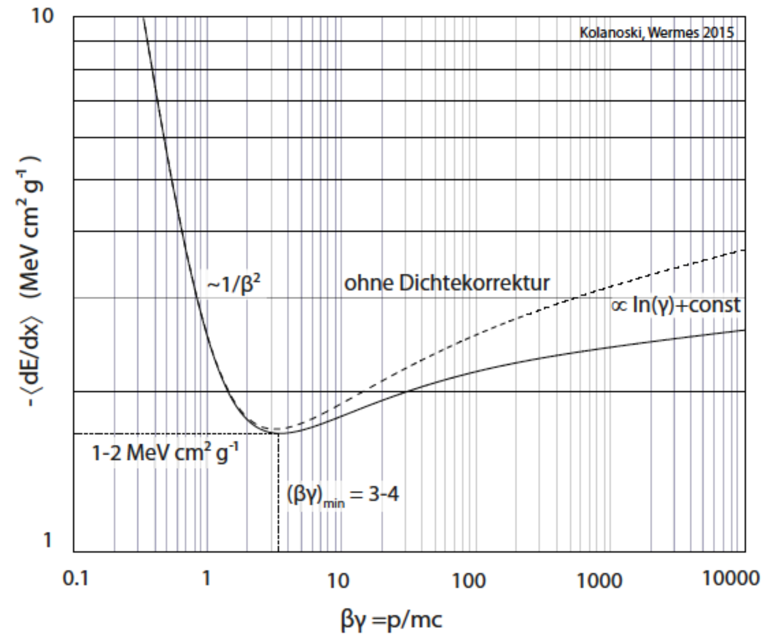

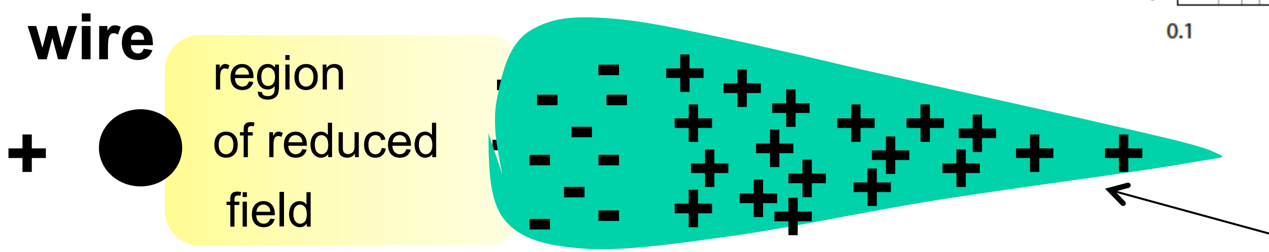

ion cloud is ~ stationary acts like a space chage

Saturation –> Avalanche -> Streamer -> Spark

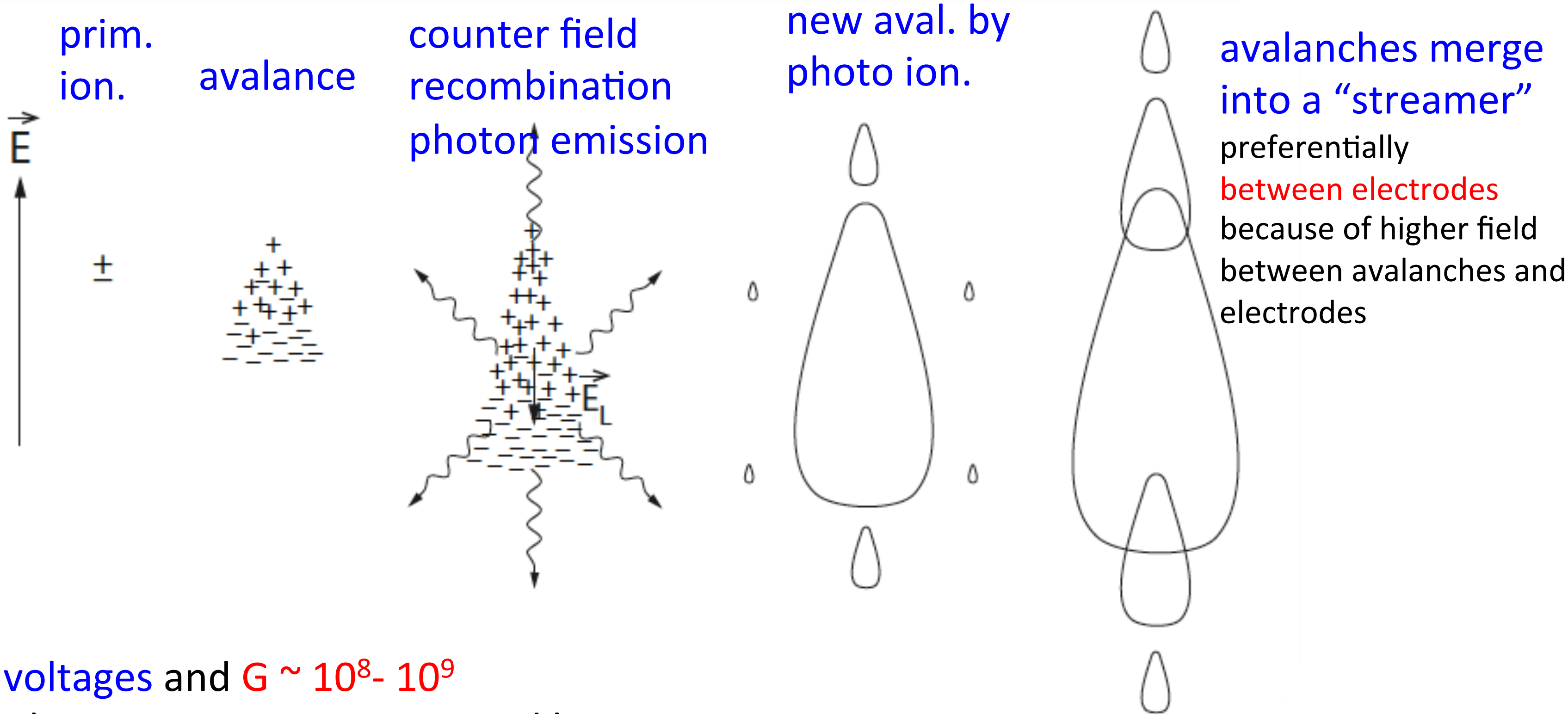

- at very high voltages and G ~ 10^8- 10^9
- discharges either spontaneous or initiated by ionisation
- => saturated avalanche -> streamer -> discharge (= glow –> corona –> spark) occur
- streamer/discharge accompanied by photon emission (can be visible) and need to be quenched (by space charge screening, HV-lowering, pulsed HV, etc.) when used as detectors rather than demonstration objects (spark ch.)
- very fast (10^6 m/s) governed by photon emission, 10x faster than avalanche dev. (governed by v_{drift})
- when streamer reaches electrode => spark/discharge => avoid in detectors (limited streamer mode)
- streamer operation in: straw tube geometries or RPCs

skip gas mixtures
and ageing?

The magic of the choice of the gas / gas-mixture

- high ionisation density => best are heavy nobel gases (Ar, Kr, Xe) or CO_2, C_xH_y, CF_4
- little charge loss => no O_2 or electronegative gases
- high gain at low voltage => nobel gases best => Ar (cheapest)
- proportionality between prim. ionisation and signal
- spark robustness => need photon quencher (Ar no good) => hydrocarbons or CO_2

examples:		
	Ar – C_2H_6	50:50
	Ar – CH_4	90:10
	Ar – C_4H_{10}	75:25
	Ar – CO_2 – CH_4	90:9:1

- small diffusion and constant v_{drift}
  => also provided by quench gas => tune mixture
- no polymerisation (ageing) => ions from organic gases tend to polymerize => add propanol, methylal

- rate tolerance w/o space charge
- radiation resistance
- non flammable

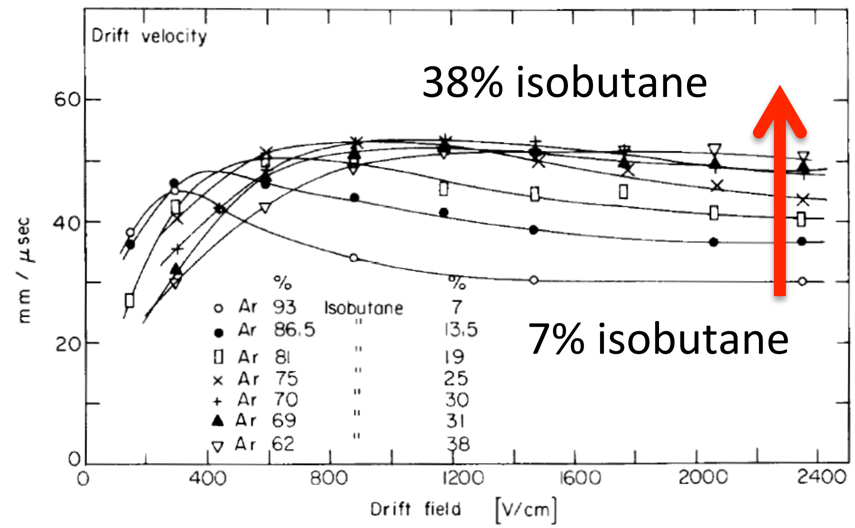

Drift velocity in several argon-isobutane (C_4H_{10}) mixtures

The ageing problem

- cause: avalanche process + radiation
- polymerisation on wires -> wisker growth
- result
  - gain reduction
  - dark currents
  - corrosion
  - mechanical damage

- chemical disintegration of complex gas molecules, i.e. by hydrocarbons (quencher) or by gas impurities

- long chains of molecules become attached to the electrodes

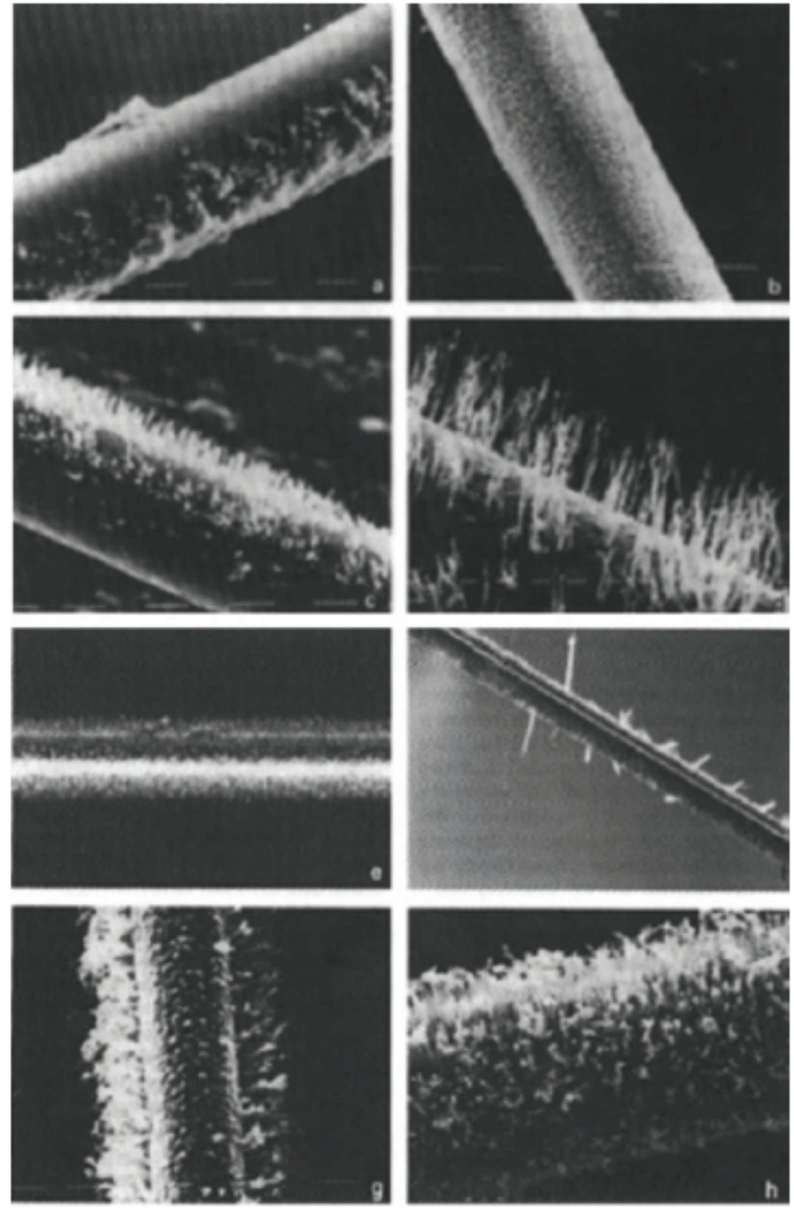

The second coordinate

universitätbonn

cathode readout (see page 24) or crossed wire planes

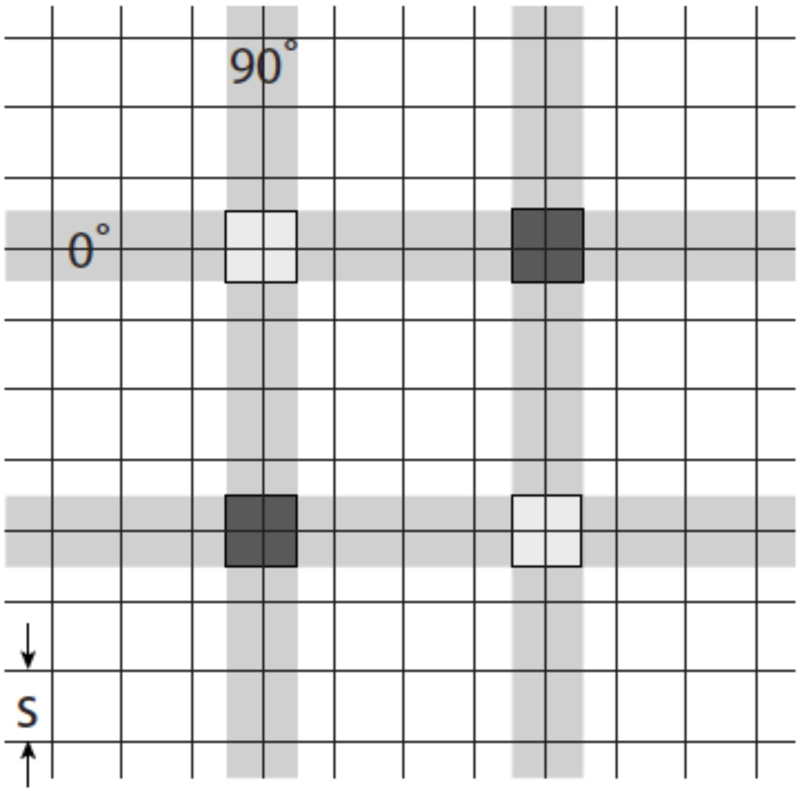

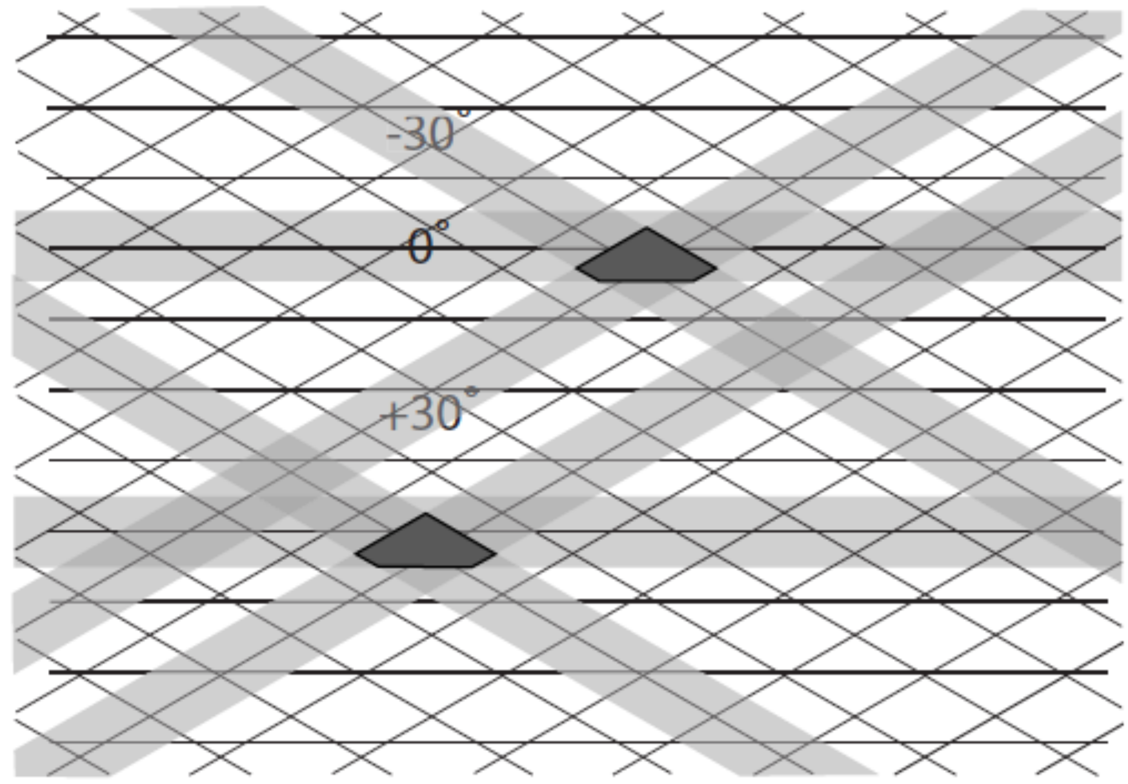

90° "stereo" arrangement
best for resolution
but n^2 "ghost" hits

±30° "stereo" arrangement
(3 layers)
small angles often easier due to wire fixations or R/O
no ghosts in this example

The Driftchamber

universitätbonn

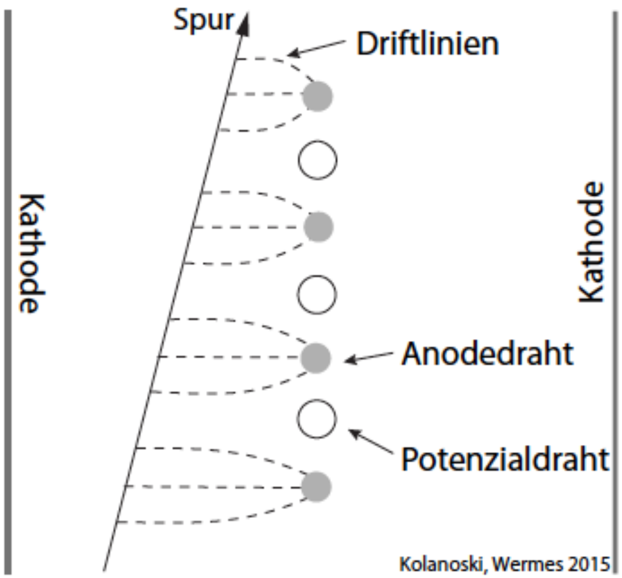

- MWPC limited for very narrow wire spacing due to electro-static repulsion: typ.: s > 1mm for ⌀ 10 µm, l = 25 cm
- better resolution obtained by measurement of arrival time of the electron cloud (measured by TDC or similar)
- need additional “potential wire” to avoid low field regions
- track space point to drift-time relation usually field dependent and thus non linear (-> calibration)

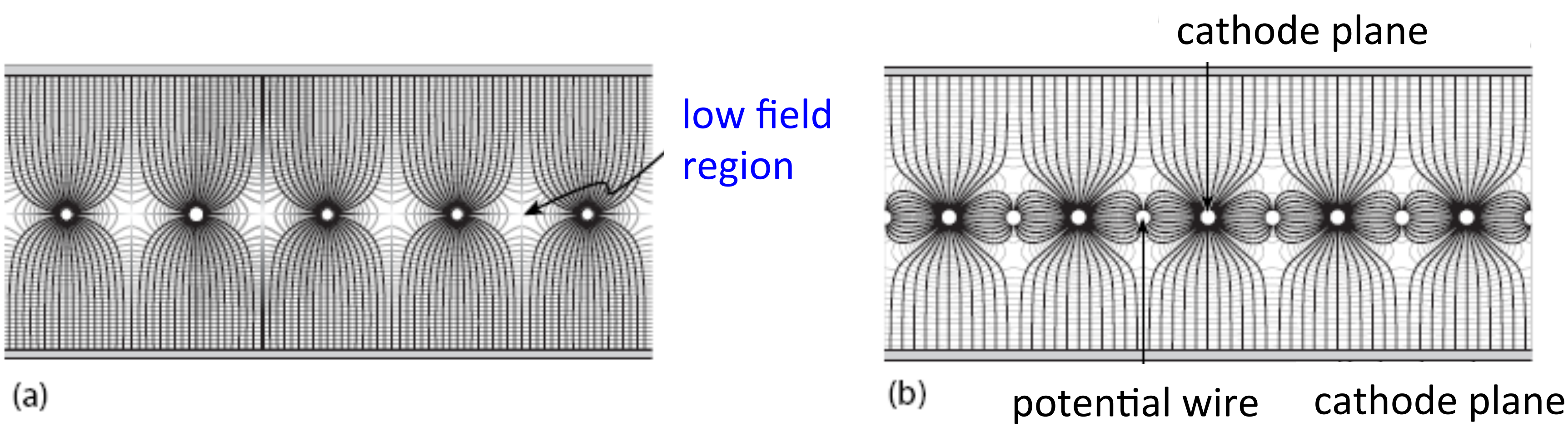

Driftchambers for tracking

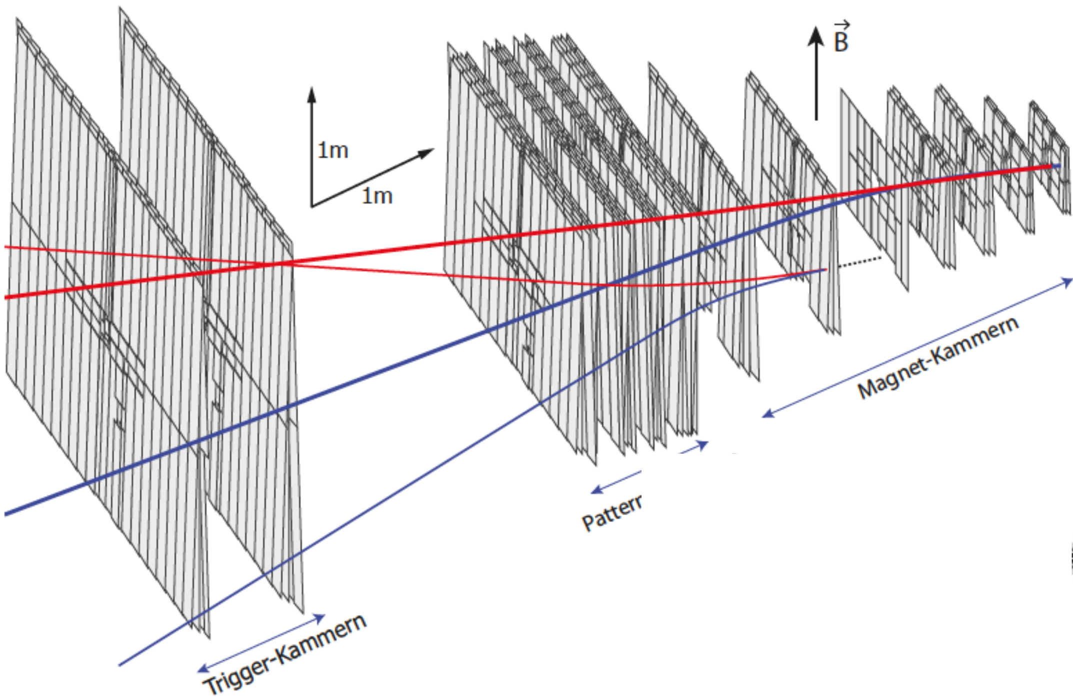

planar chambers
in fixed target experiments

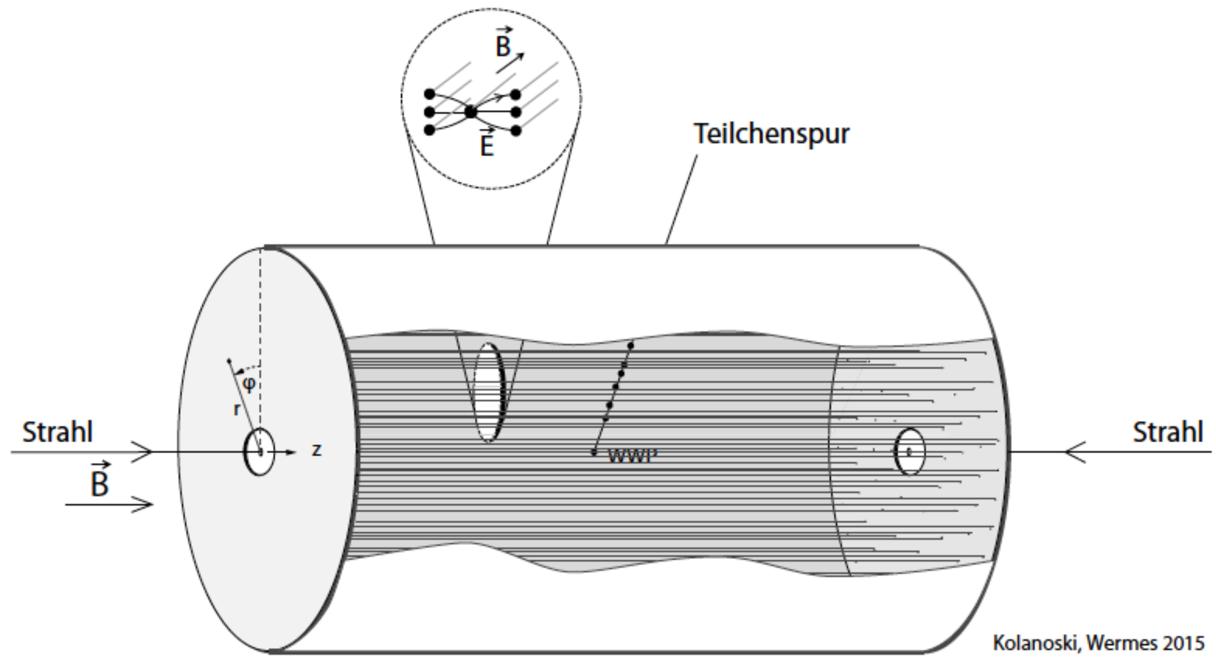

cylindrical chambers
in collider experiments

Drift cells

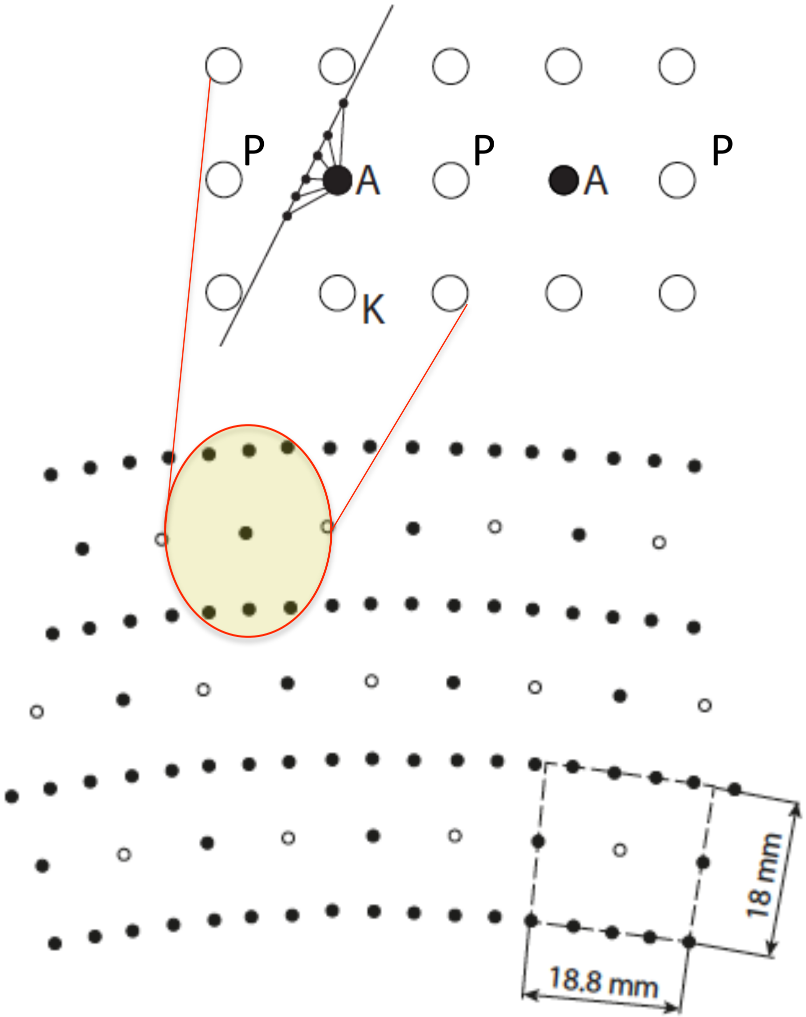

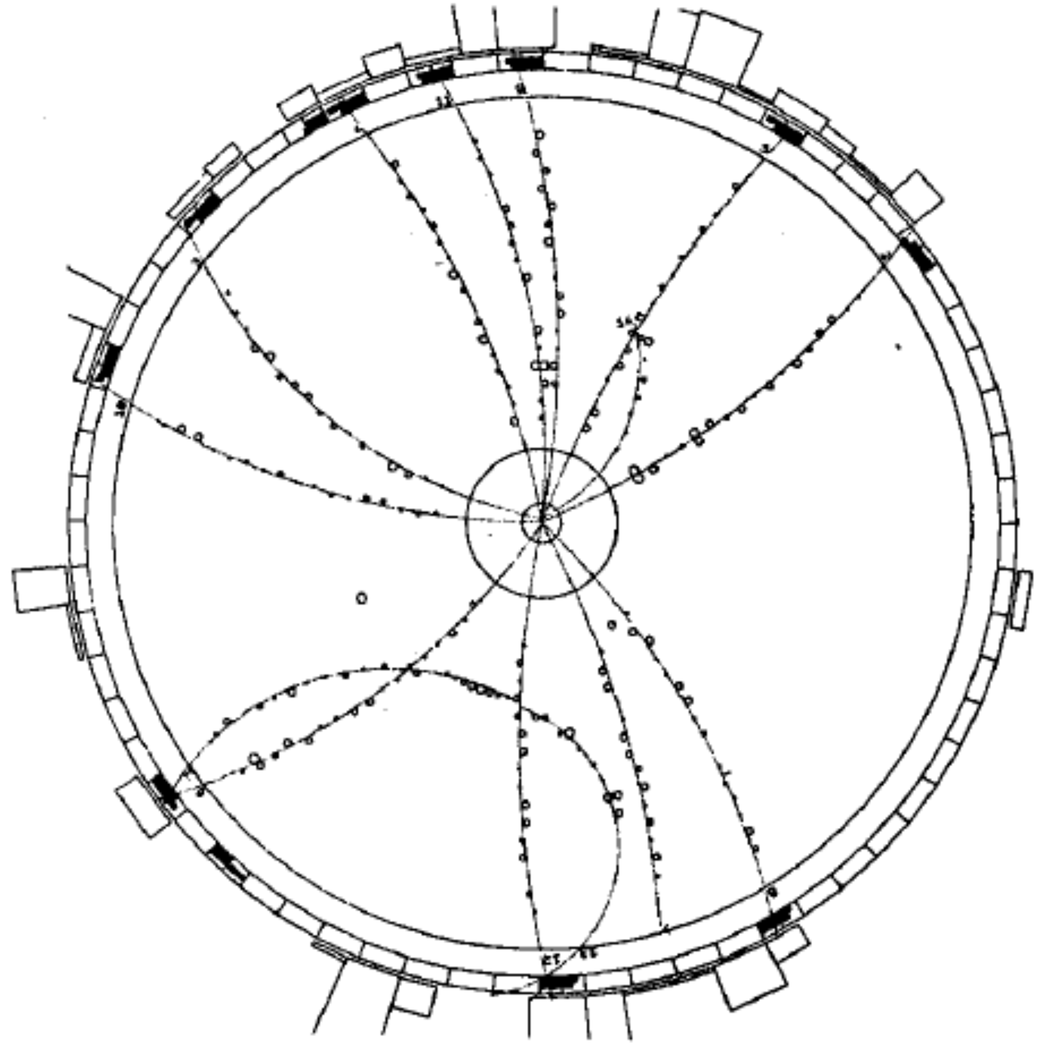

used for example in ARGUS and TASSO experiments at DESY in the 1980ies.

Drift cells: OPAL Jet Chamber

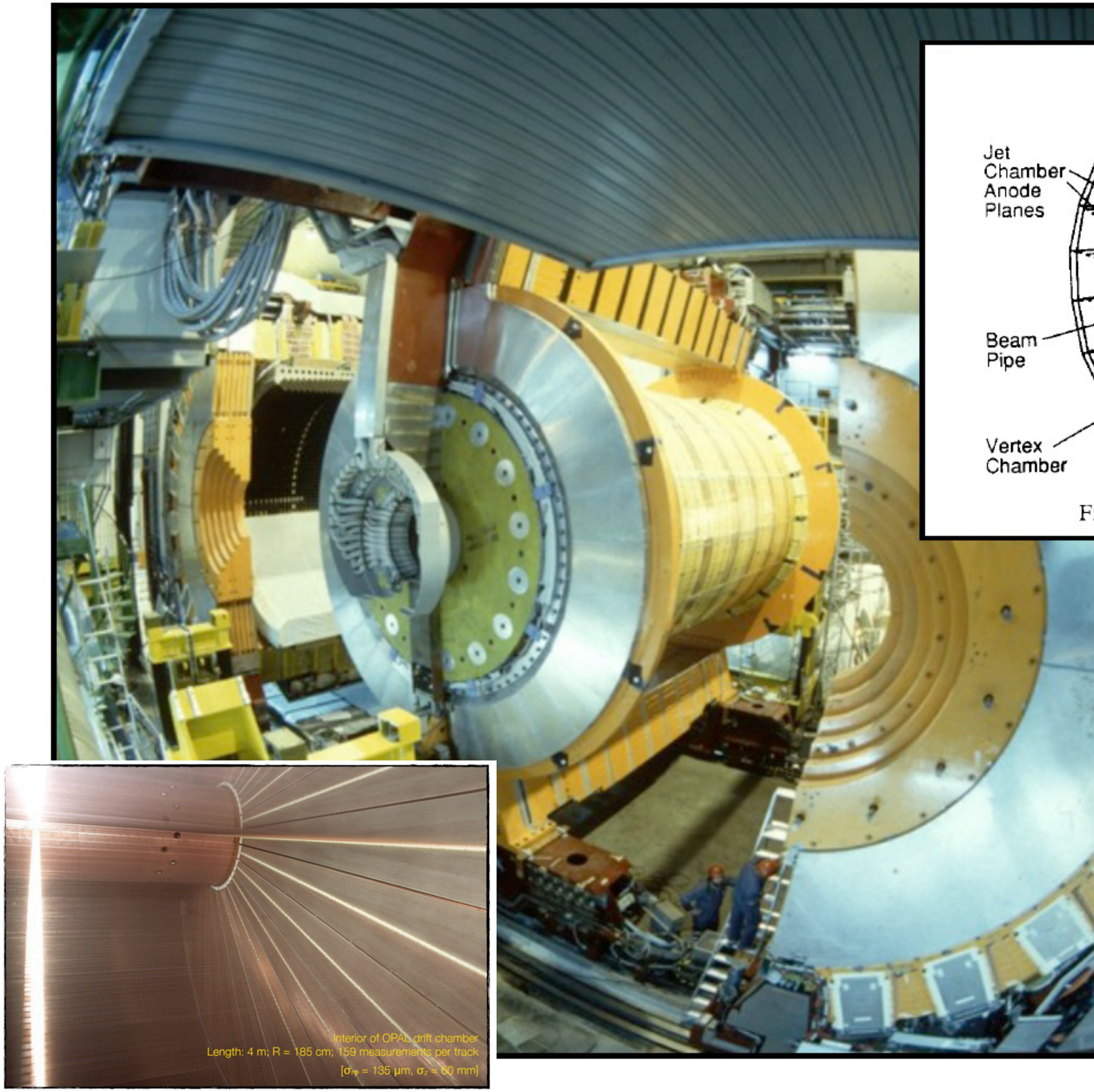

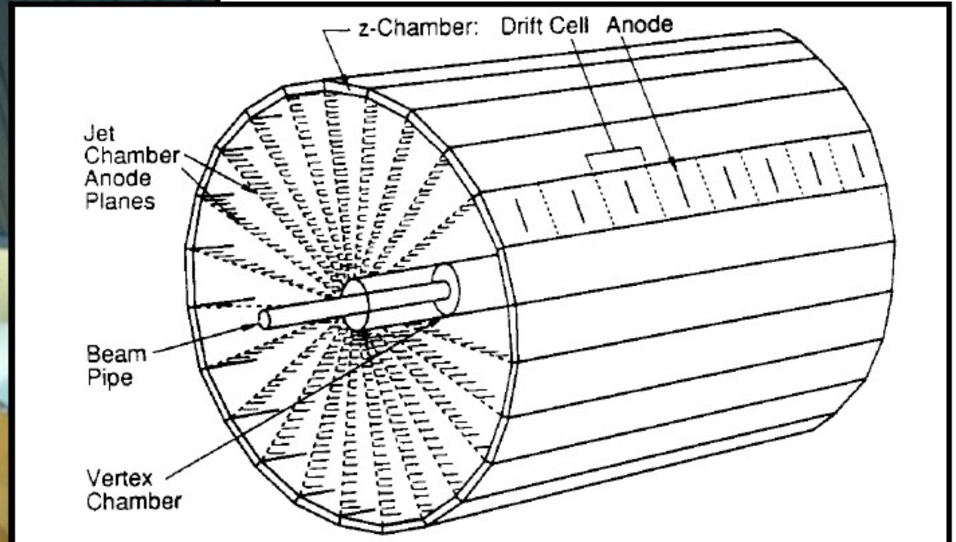

Fig. 1. Schematic view of the OPAL central detector.

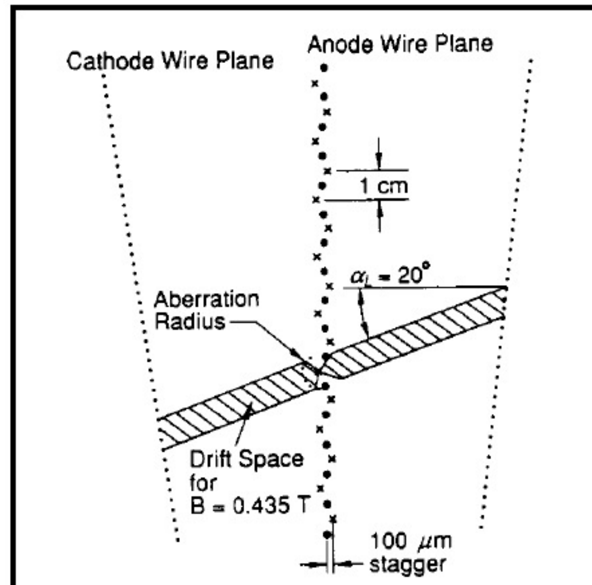

Drift cells: OPAL Jet Chamber

+ many hits per particle track
+ but still only modest number of wires needed in total
+ homogeous E-field → easy space point to drift-time relation

± large drift distances

- get 3D space point by charge division on wire
- multi-hit electronics → good 2-track resolution
- "staggering" of anode wires to resolve the left-right ambiguity

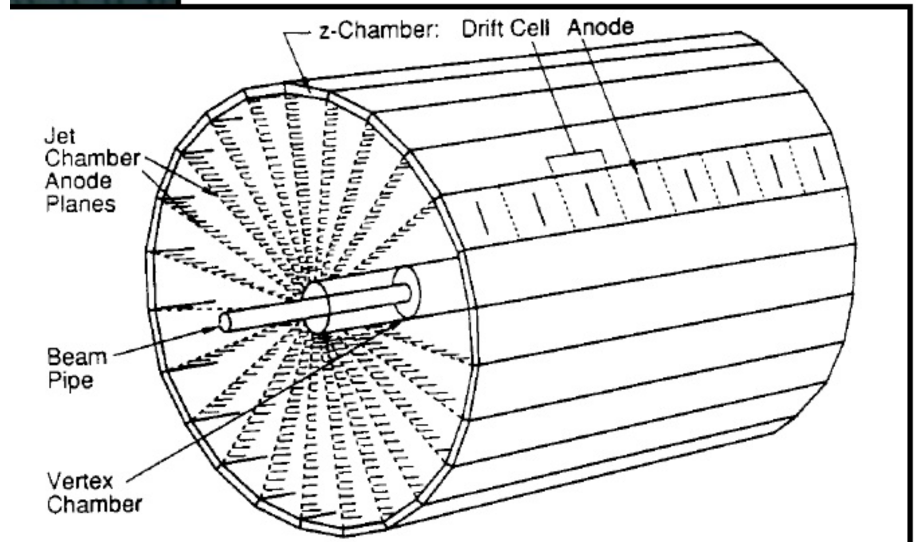

Fig. 1. Schematic view of the OPAL central detector.

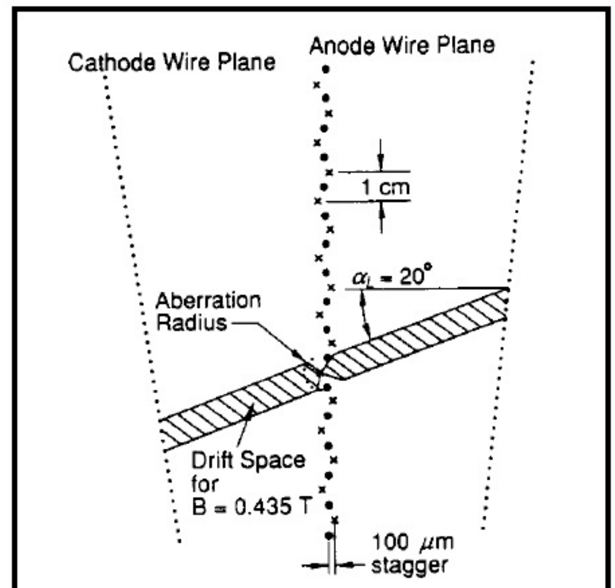

Drift cells: OPAL Jet Chamber

+ many hits per particle track
+ but still only modest number of wires needed in total
+ homogeous E-field → easy space point to drift-time relation

± large drift distances

- get 3D space point by charge division on wire
- multi-hit electronics → good 2-track resolution
- "staggering" of anode wires to resolve the left-right ambiguity

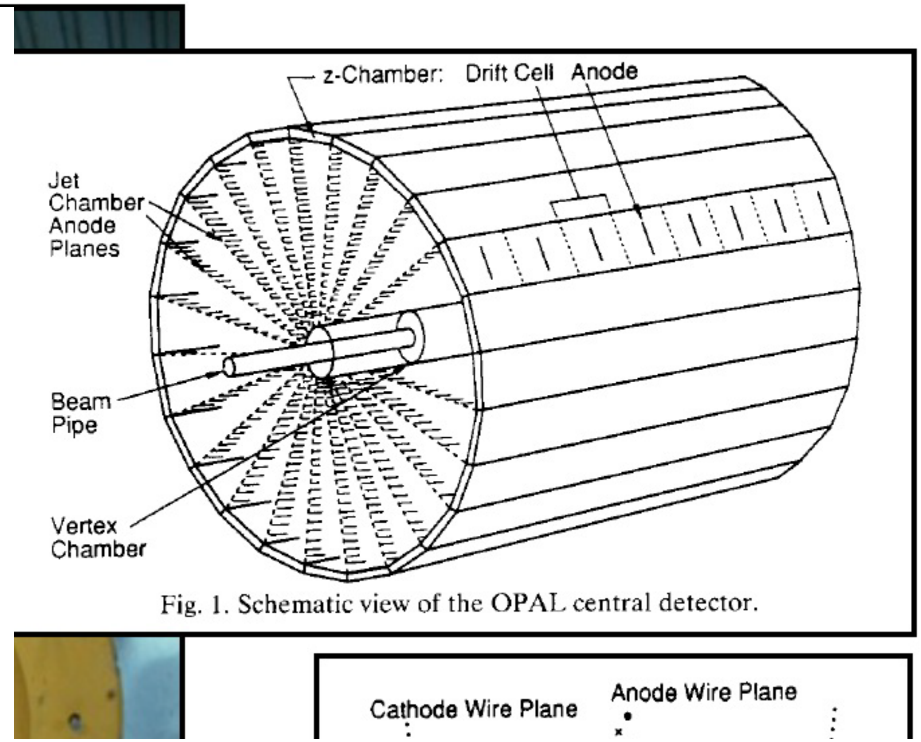

Fig. 1. Schematic view of the OPAL central detector.

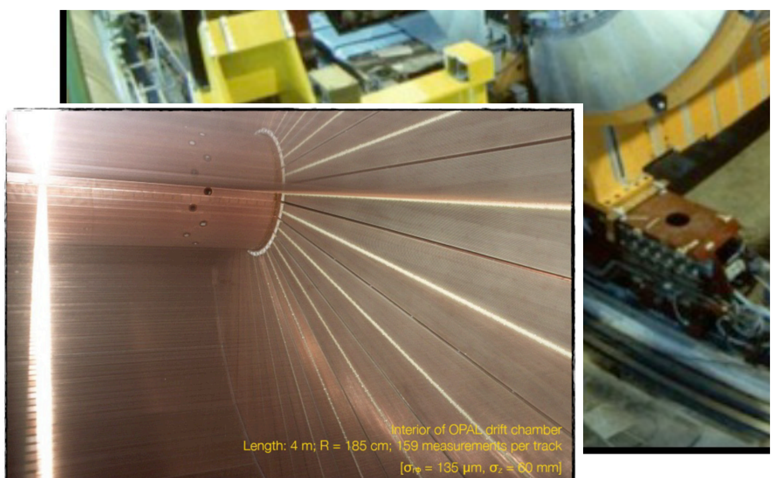

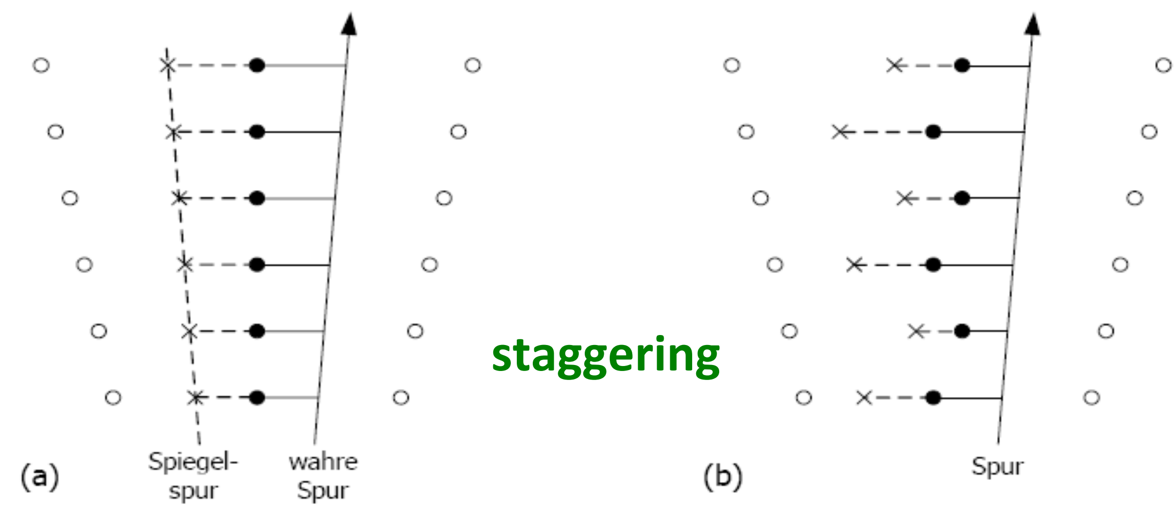

The jet chamber concept

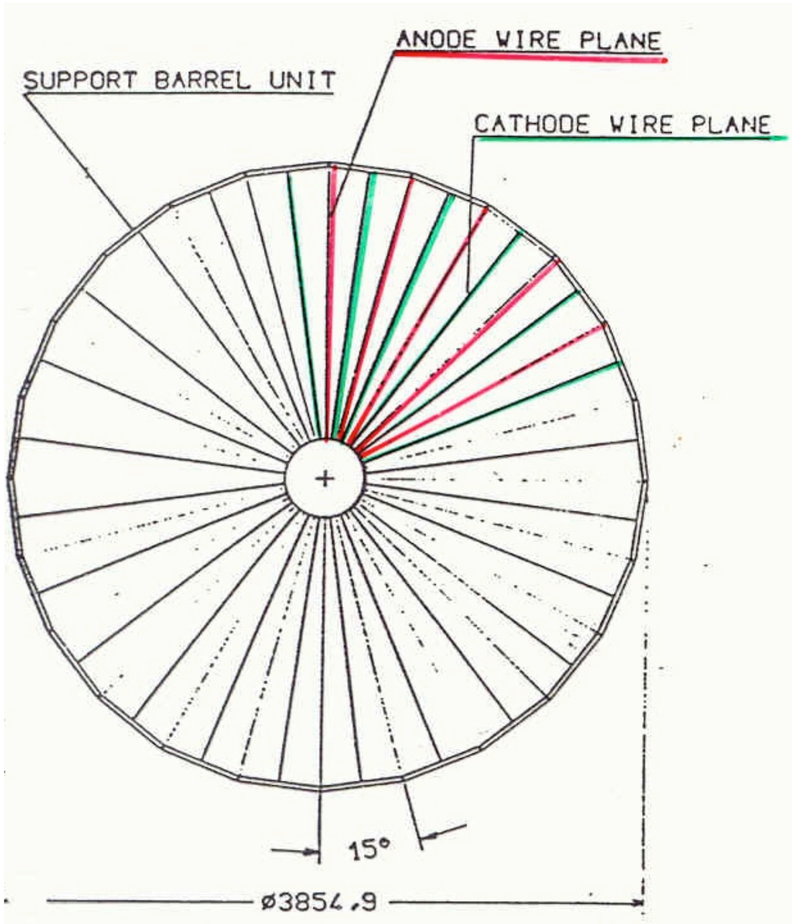

+ many hits per particle track
+ but still only modest number of wires needed in total
+ homogeous E-field → easy space point to drift-time relation

± large drift distances

- get 3D space point by charge division on wire
- multi-hit electronics → good 2-track resolution
- "staggering" of anode wires to resolve the left-right ambiguity

How to resolve left/right ambiguities

staggering

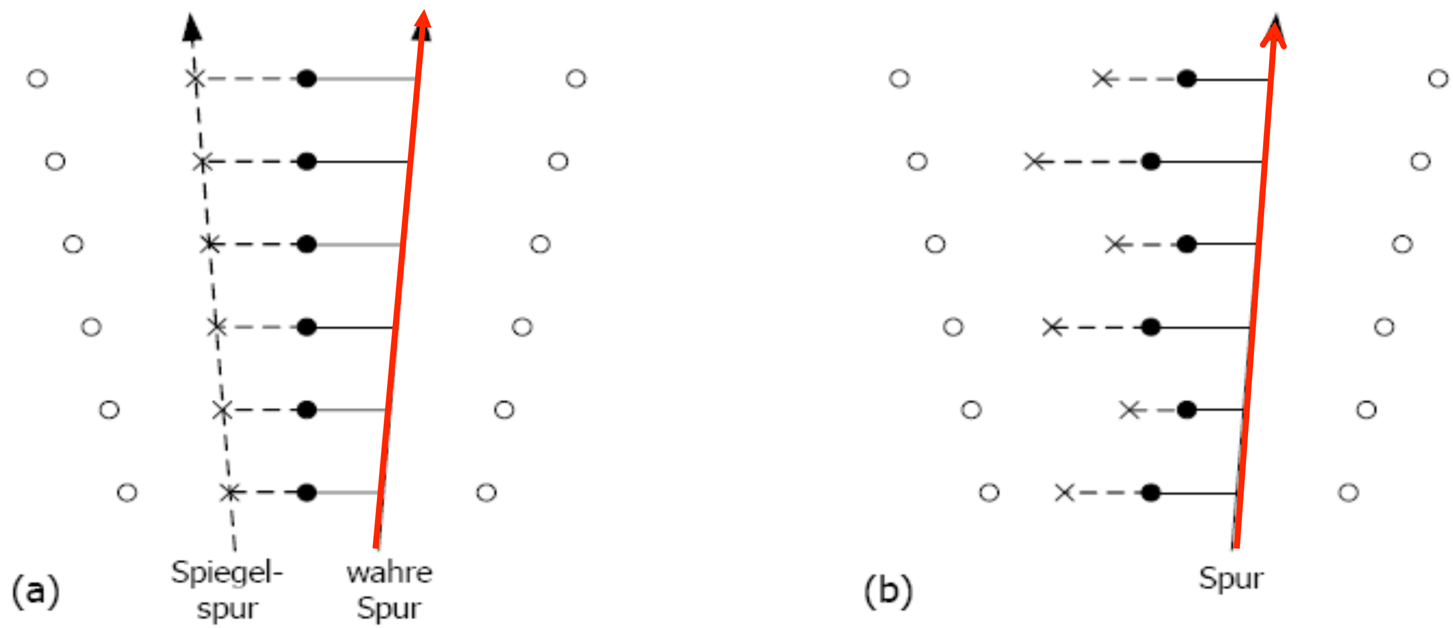

Effect of B-field

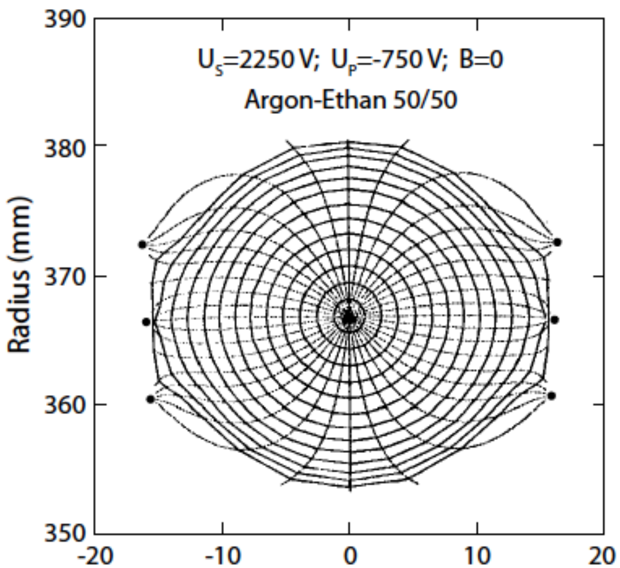

B = 0

isochrone-curves
with
same drift time to wire

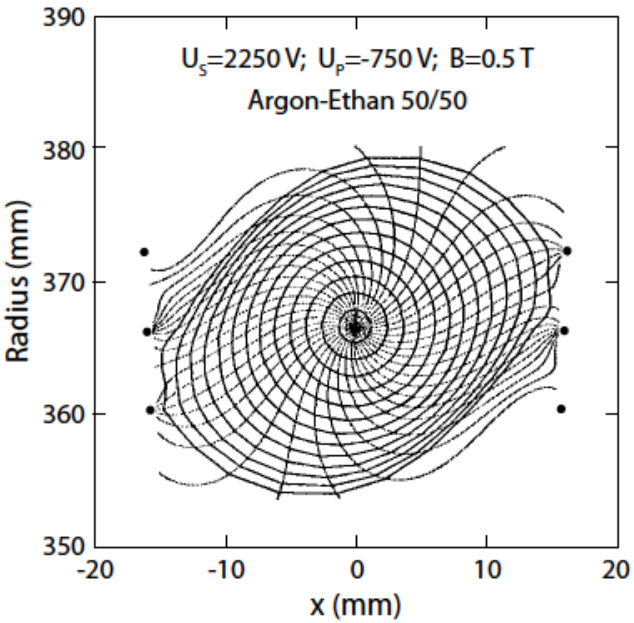

B = 0.5 T

B ⊥ E

$\vec{B} \neq 0$

equipotential lines

drift trajectories

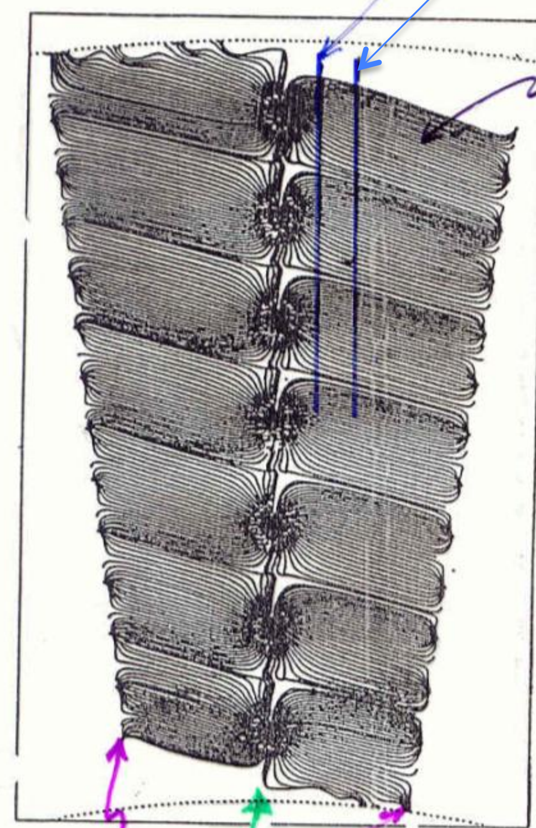

cathode wire planes

anode wire plane

z-coordinate measurement

"stereo" wires in a cylindrical geometry

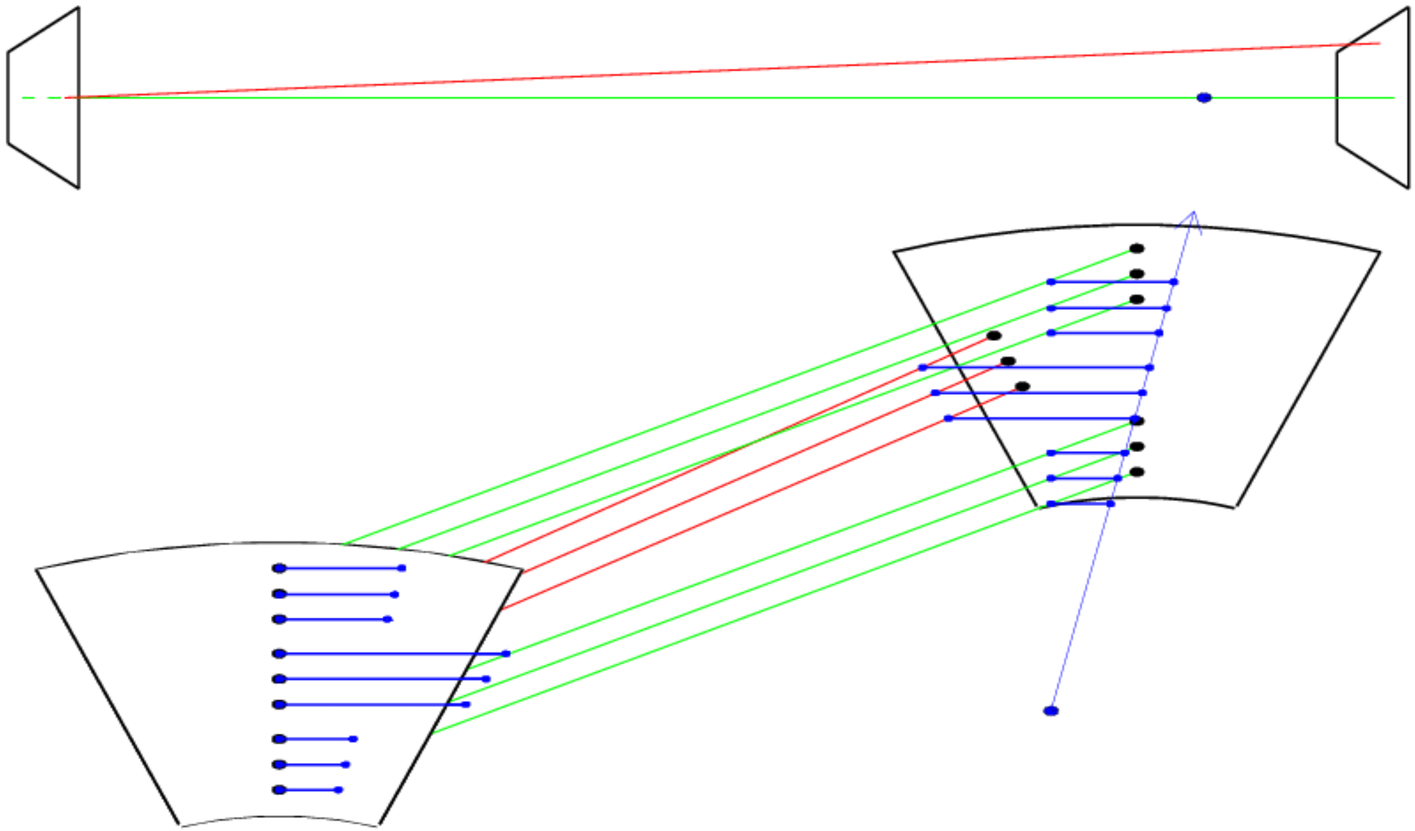

$$\sigma_z = \sigma_{r\phi} \cdot \frac{1}{\sin \alpha_{\mathrm{stereo}}}$$

+ (still) relatively good spatial resolution
- one looses wires for other tasks (rϕ)
- not practical in high track density

Resolution of a driftchamber

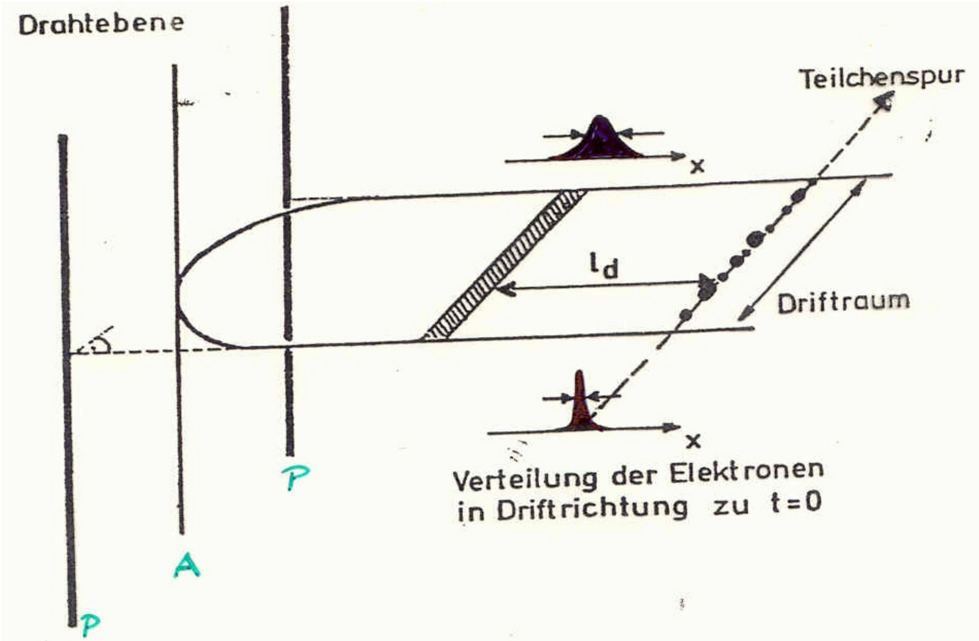

$$\sigma^2_{tot} = \sigma^2_{point} + \sigma^2_{multiple\ scattering} + \sigma^2_{sys}$$

σ_{point} →
- longitudinal diffusion (~ 1/pressure × √drift distance)
- ionisation statistics ~ (distance from wire)$^{-1}$
- time resolution for e-cloud → leading edge discrimination, Flash ADC timing

σ_{MS} →
- $\propto \frac{1}{p}\sqrt{\frac{L}{X_0}}$

σ_{sys} →
- wire sagging, electrostatic wire attraction, torsion of chamber flanges, electric cross-talk

Resolution of a Driftchamber

$L' = L \sin\theta$

$$\left(\frac{\sigma_{p_T}}{p_T}\right)_{\text{point}} = \frac{p_T}{0.3} \cdot \frac{\sigma_{point}}{L'^2 B}\sqrt{\frac{720}{N+4}} \qquad [p_T] = \text{GeV/c},\ [L'] = \text{m},\ [B] = \text{T}$$

$$\left(\frac{\sigma_{p_T}}{p_T}\right)_{\text{MS}} = \frac{0.054}{L'\,B\,\beta}\sqrt{\frac{L}{X_0}} \qquad [p_T] = \text{GeV/c},\ [L, L'] = \text{m},\ [B] = \text{T}$$

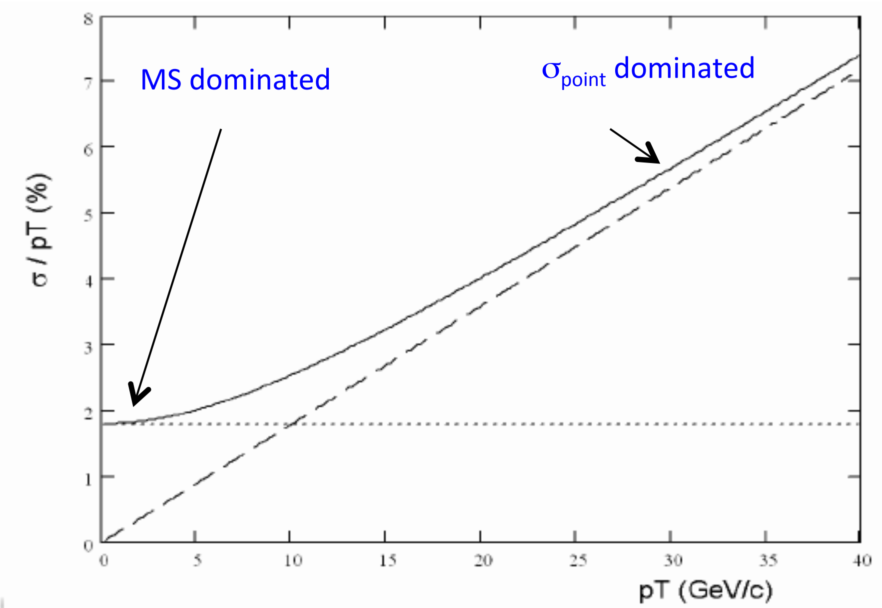

L = 2m, N = 159, σ_{point} = 120 µm

$$\frac{\sigma_{p_T}}{p_T} = \sqrt{(0.15\,\%\,p_T)^2 + (2\%)^2}$$

$$= \begin{cases} \textbf{2\% @ 1 GeV} \\ \textbf{7.5\% @ 50 GeV} \end{cases}$$

Time Projection Chamber

invented by D. Nygren (1976)

universitätbonn

large wire-less volume

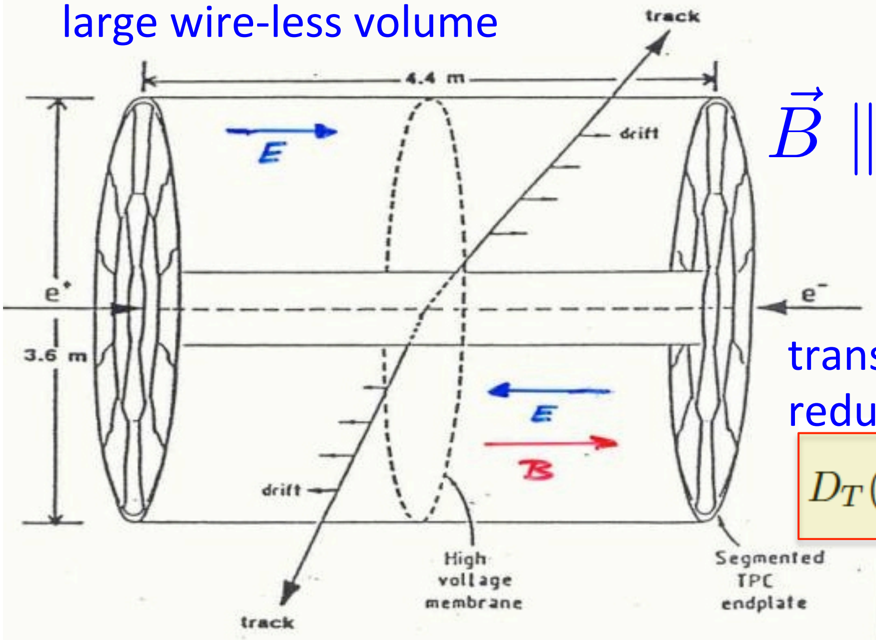

$\vec{B} \parallel \vec{E}$

transverse diffusion reduced

$$D_T(B) = \frac{D_T(0)}{1+\omega^2\tau^2}$$

long drift along , amplification at end of long drift

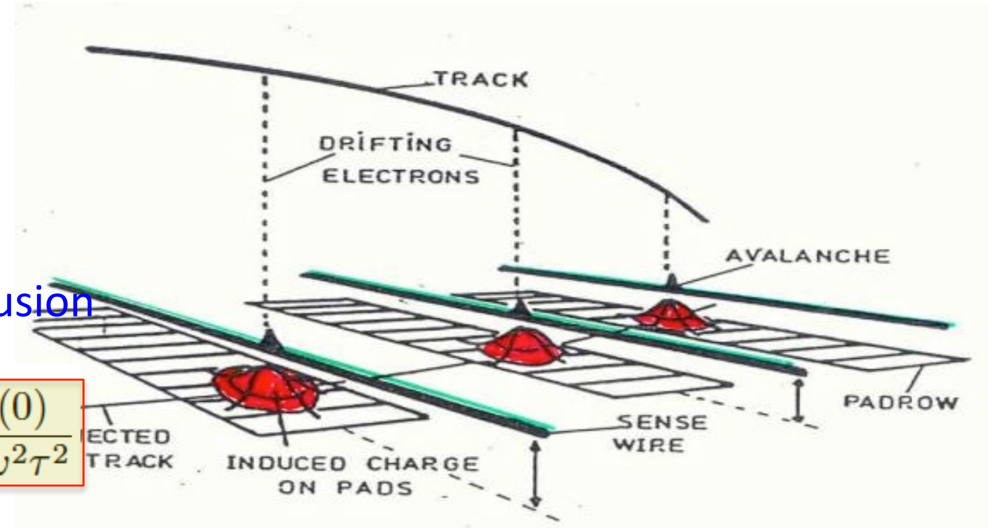

prevent ion-feedback by gating grid

- full 3-D reconstruction (voxels): xy from wire/pad geometry at the end flanges; z from drift time
- 3D track information recorded -> good momentum resolution
- also dE/dx measurement easy -> particle ID (not topic of this lecture)
- large field cage necessary
- typical resolutions: in z and y ≈ mm, in x = 150-300 µm
- challenges
  - long drift time -> limited rate capability
  - large volume -> geometrical precision
  - large voltages (discharges)

Time Projection Chamber

invented by D. Nygren (1976)

universitätbonn

large wire-less volume

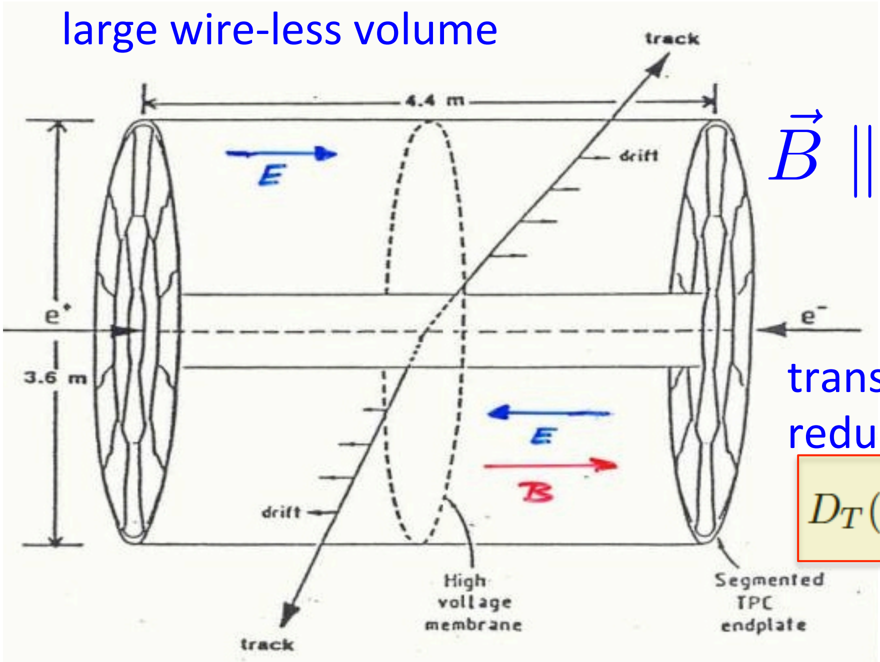

$\vec{B} \parallel \vec{E}$

transverse diffusion reduced

$$D_T(B) = \frac{D_T(0)}{1+\omega^2\tau^2}$$

long drift along , amplification at end of long drift

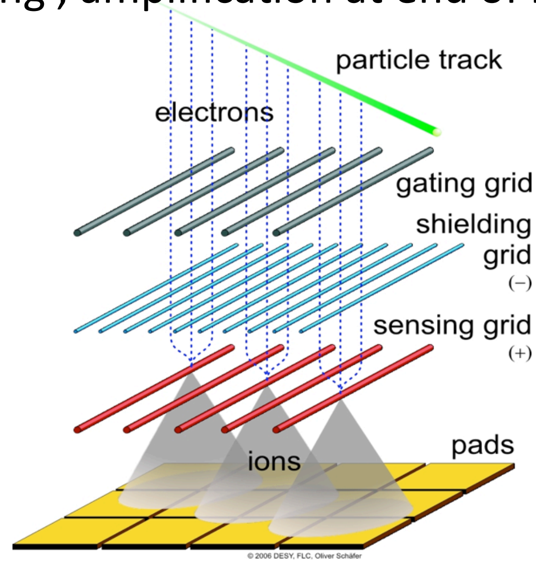

pulsed

prevent ion-feedback by gating grid

- full 3-D reconstruction (voxels): xy from wire/pad geometry at the end flanges; z from drift time
- 3D track information recorded -> good momentum resolution
- also dE/dx measurement easy -> particle ID (not topic of this lecture)
- large field cage necessary
- typical resolutions: in z and y ≈ mm, in x = 150-300 µm
- challenges
  - long drift time -> limited rate capability
  - large volume -> geometrical precision
  - large voltages -> potential discharges

Big TPCs in experiments

universitätbonn

Parameter/Experiment	PEP4 [612]	ALEPH [100]	ALICE [72]
Volume (m^3)	5	20	26
$\sigma_{r\phi}$ (µm)	130–200	170–450	800–1100
σ_z (µm)	160–260	500–1700	1100–1250
Zweispurtrennung (mm), T/L	20	15	13/30
σ_p/p^2 (GeV^{-1}) (p groß)	0.0065	0.0012	0.022

ALICE TPC

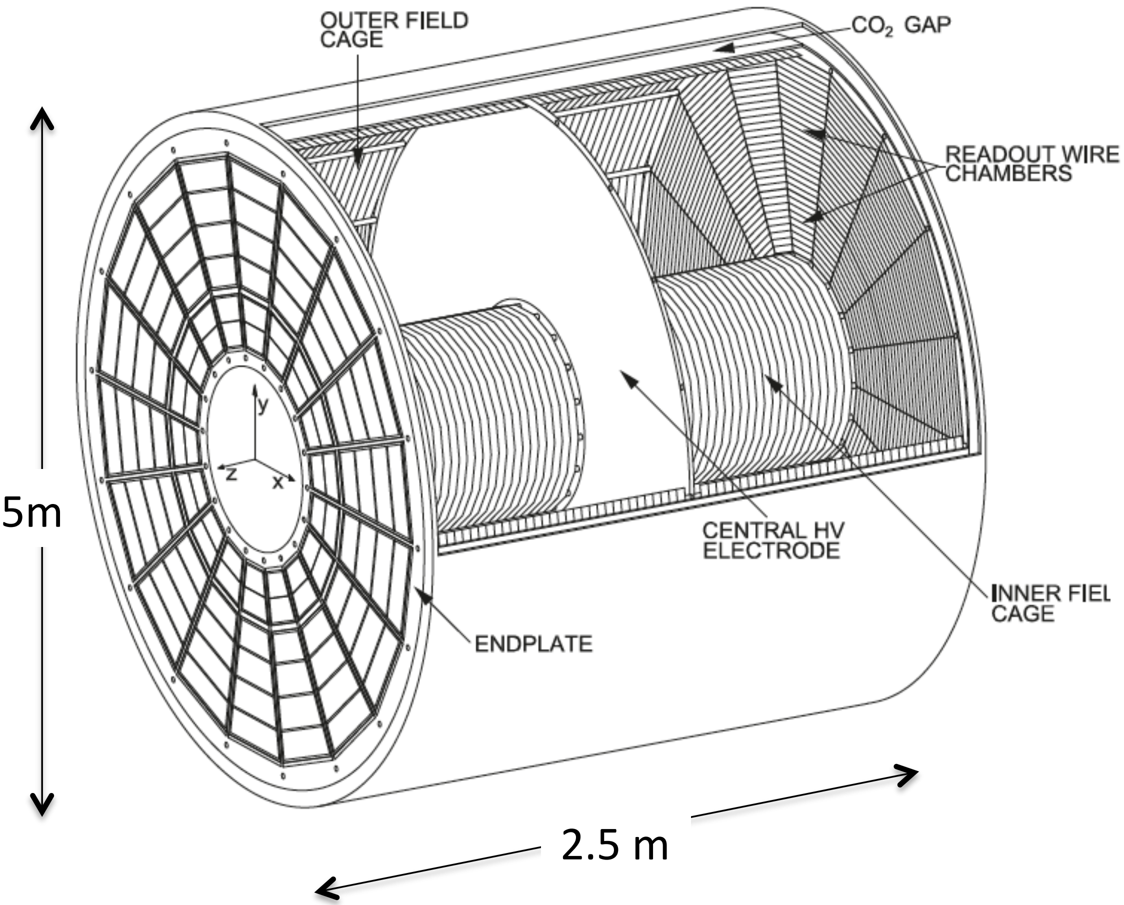
OUTER FIELD CAGE
CO_2 GAP
READOUT WIRE CHAMBERS
CENTRAL HV ELECTRODE
INNER FIEL CAGE
ENDPLATE
y
z
x
5m
2.5 m

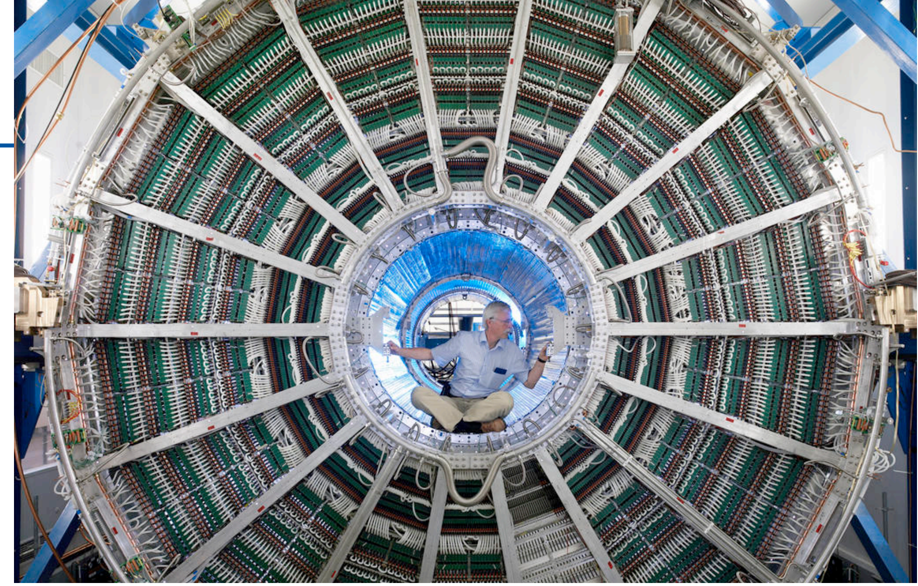

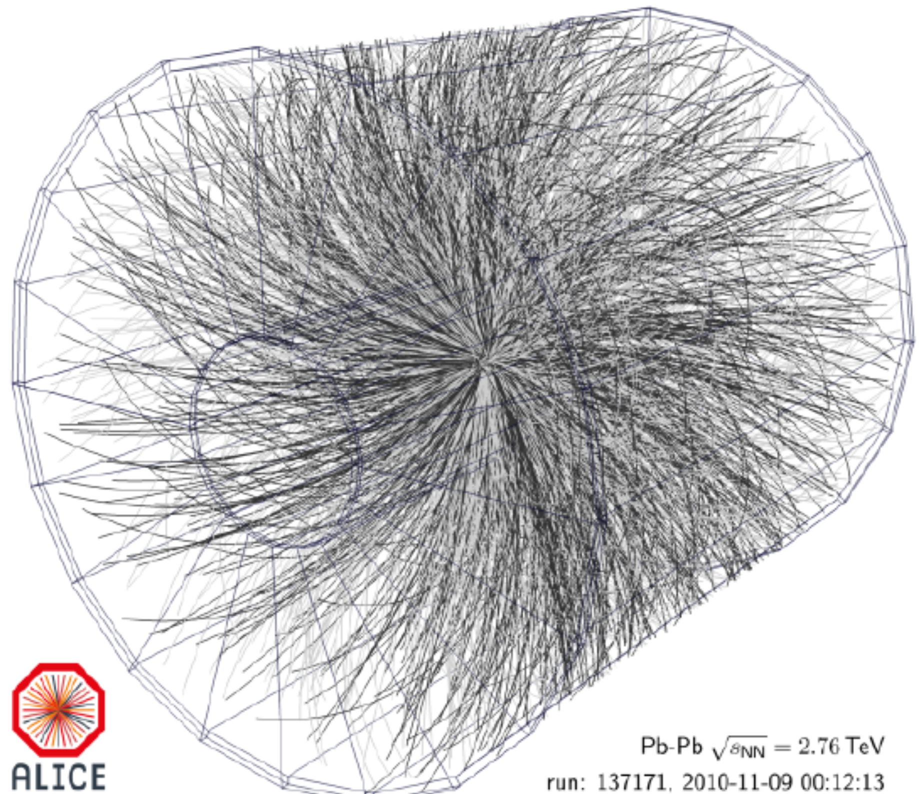
ALICE
Pb-Pb $\sqrt{s_{NN}} = 2.76$ TeV
run: 137171, 2010-11-09 00:12:13

ALICE TPC

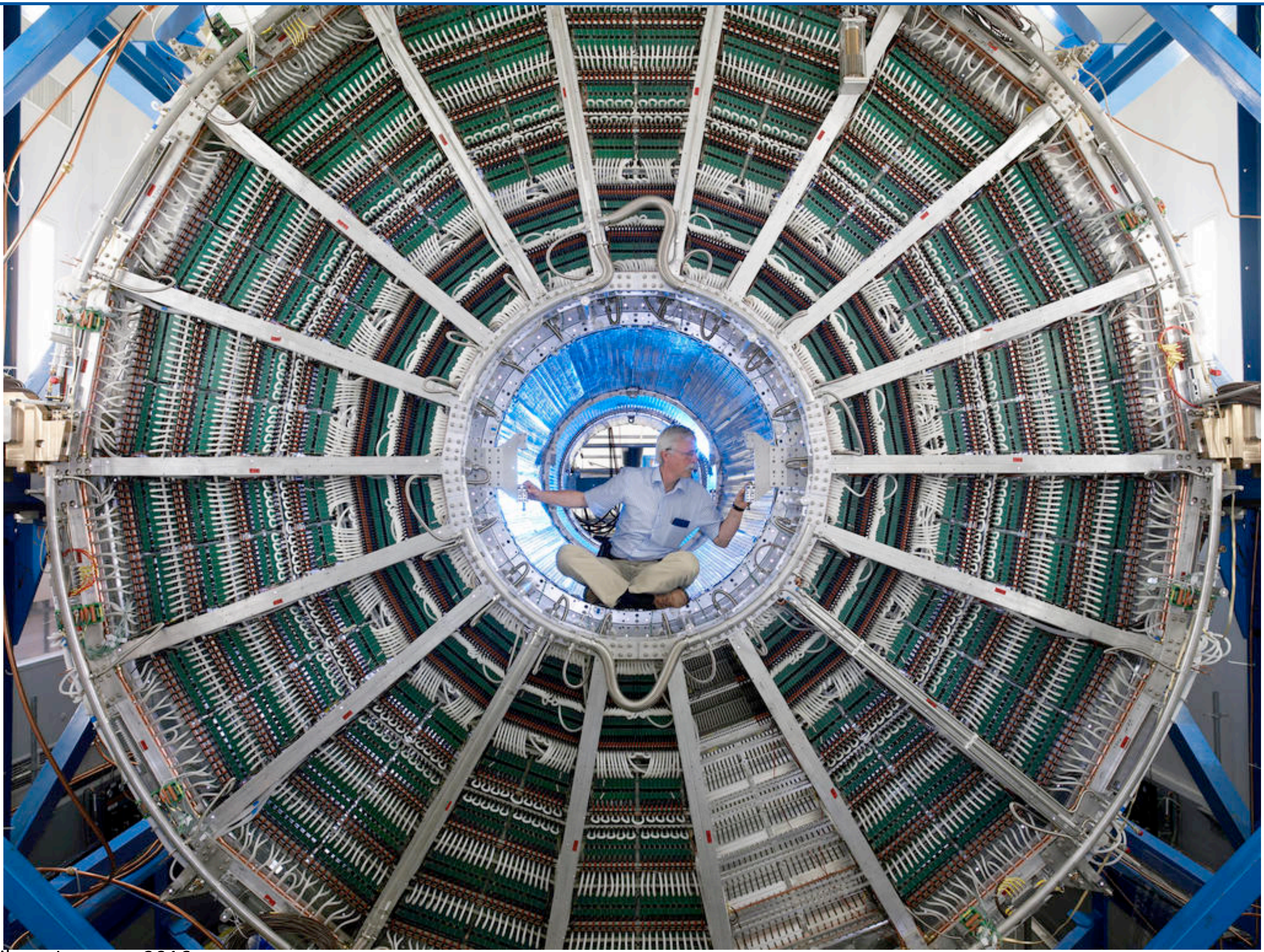

New developments in the context of high rate applications (i.e. LHC)

What is different at the LHC (pp experiments)?

universitätbonn

- particle rates ($\mathcal{L} = 10^{34}$ cm^{-2} s^{-1}) note: heavy ions: $\mathcal{L} = 10^{27}$ cm^{-2} s^{-1}
  - bunch crossing every 25 ns
  - $N_{trk} = \sigma\, \mathcal{L} = 100$ mb $\times$ 10^{34} cm^{-2}s^{-1} $\times$ 120 $\approx 10^{11}$ tracks/s in 4π
    this is 10^6 times the track rate at LEP
  - @ r = 5cm => 9.5 tracks/cm^2/25 ns but only 10^{-4} per pixel (100x100 μm^2)
- radiation level (@ r = 5cm, per detector lifetime)
  - ionizing dose = energy/mass (J/kg) = 100 Mrad
  - non ionizing fluence (breaks the lattice) = 10^{15} particles per cm^2
  - affects ageing on wires, electronics, …
- way out
  - high granularity, small cells
  - high timing precision << 25 ns
  - solid state detectors (-> lecture 3)
    - micro structuring => highest granularity
    - but: sensitive to radiation (different to gaseous detectors at moderate gas gains)

Straw tubes

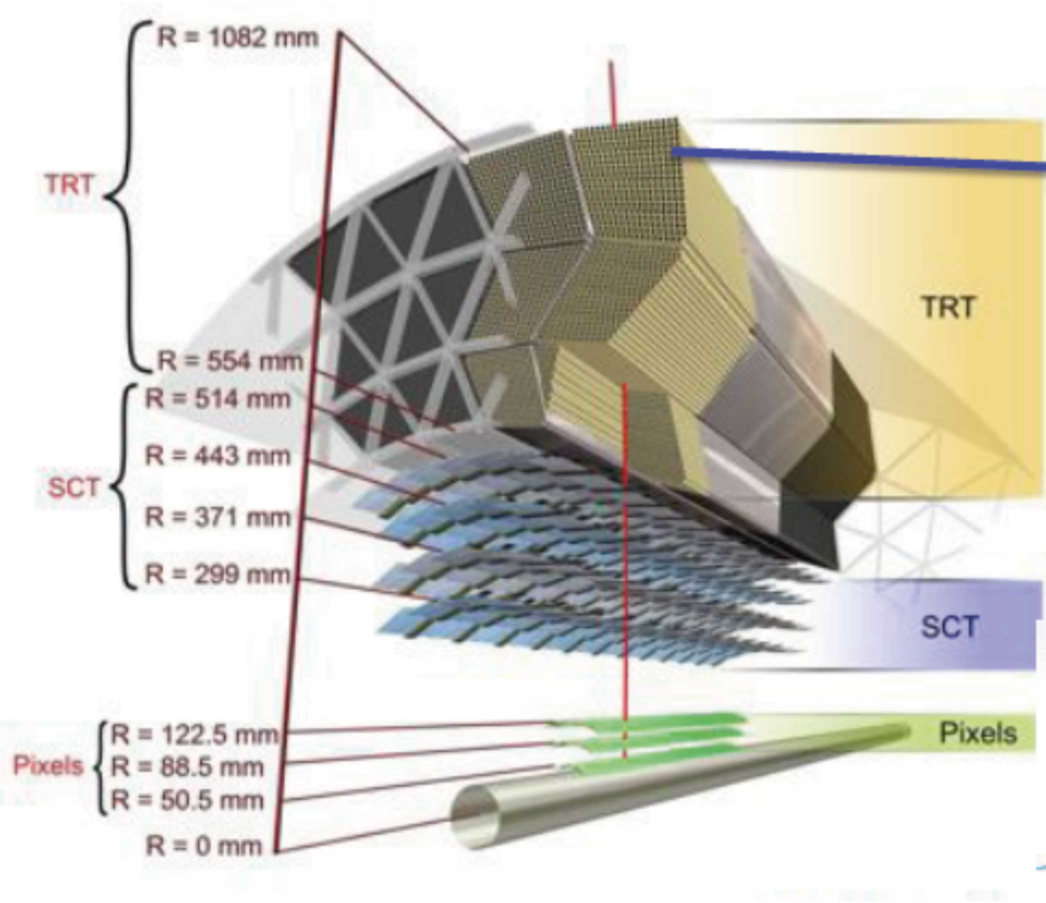

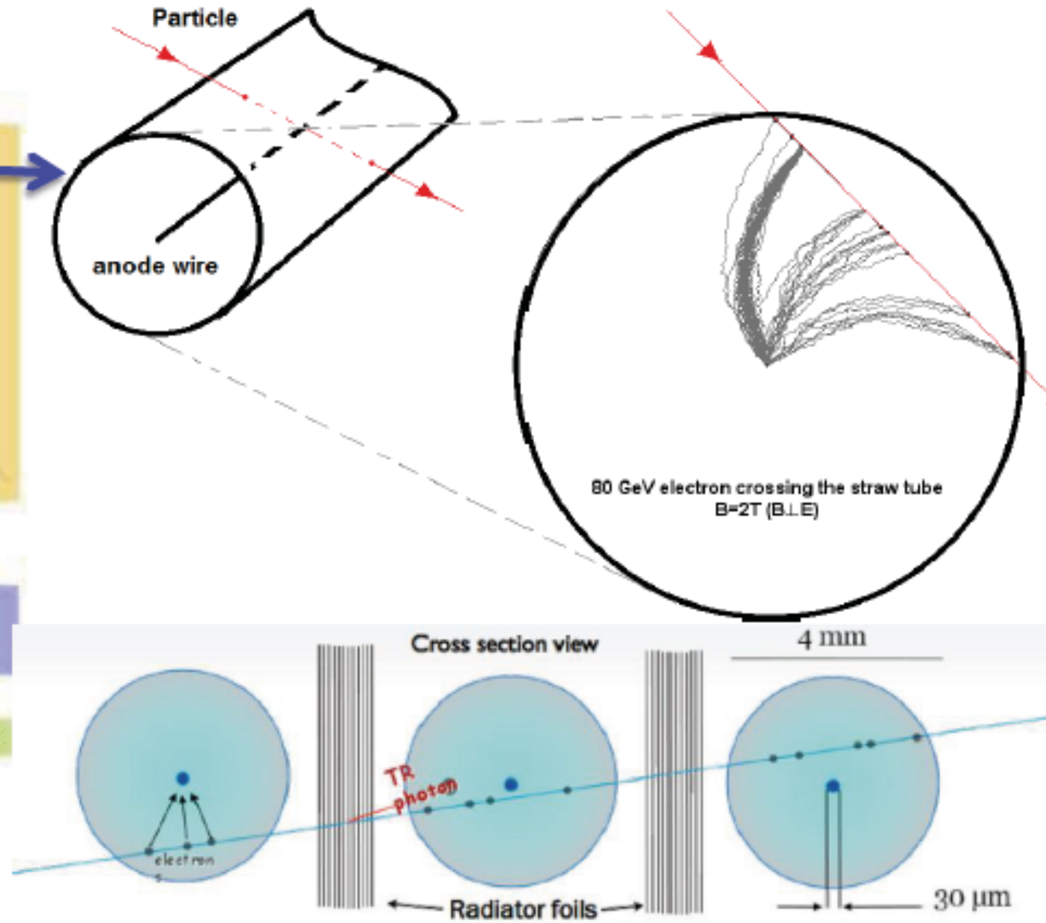

ATLAS ID Barrel

- diameter = 4 mm
- ~36 hits along a barrel track
- gas: Xe - CO_2 - O_2 (70%:27%:3%)
- serves as tracker and e- ID at the same time
- can better cope with high rates due to individual units and short drift distances

MPGCs (Micro Pattern Gas Detectors)

- advances in micro structuring also entered clever chamber designs
- goals:
  - thin gap
  - high rate capability (100 x MWPC)
  - high resolution

GEM (Sauli et al.)

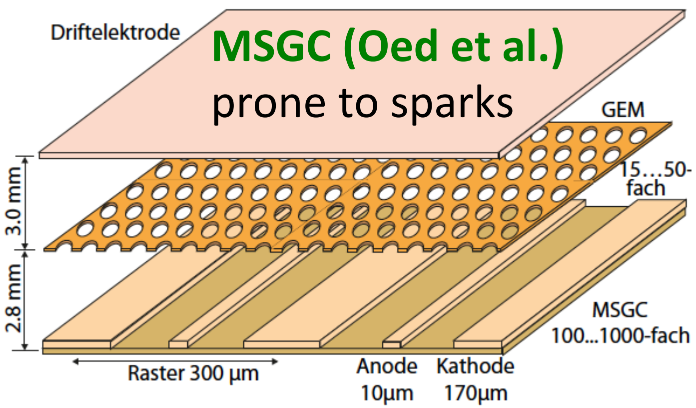

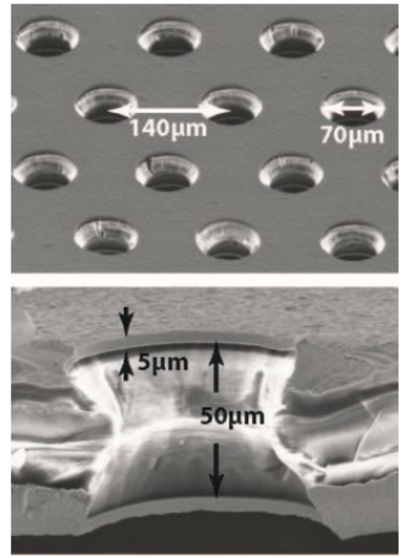

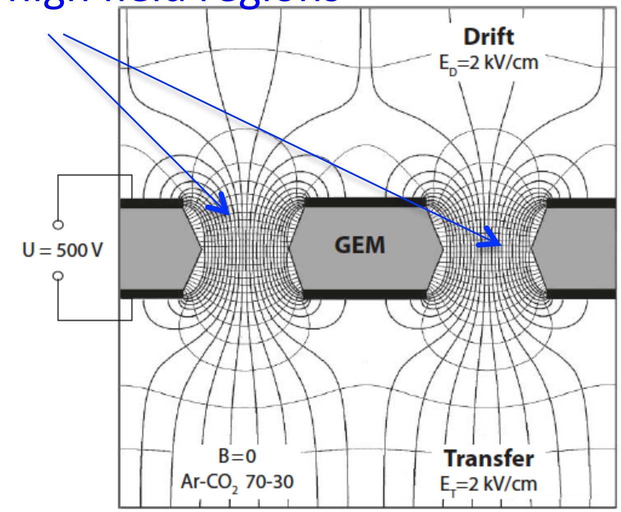

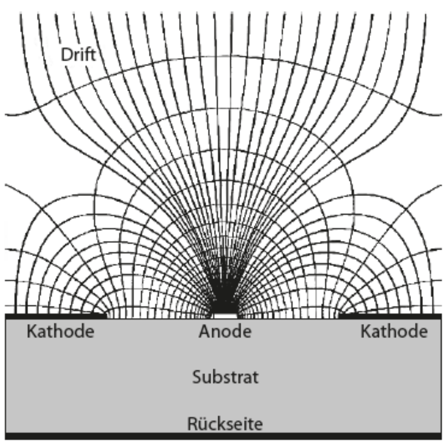

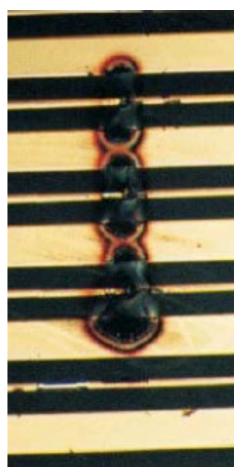

today's standard: Triple GEMs (stand alone detectors)

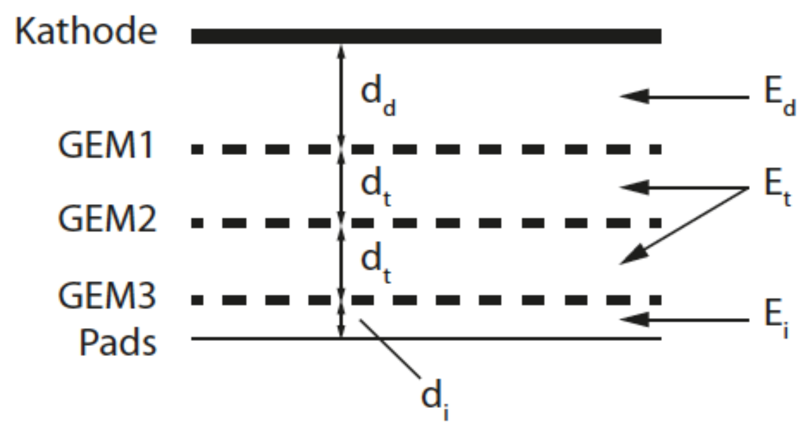

Example: GEM tracker in COMPASS

COMPASS Magnetic Spectrometer
22 TRIPLE GEMs

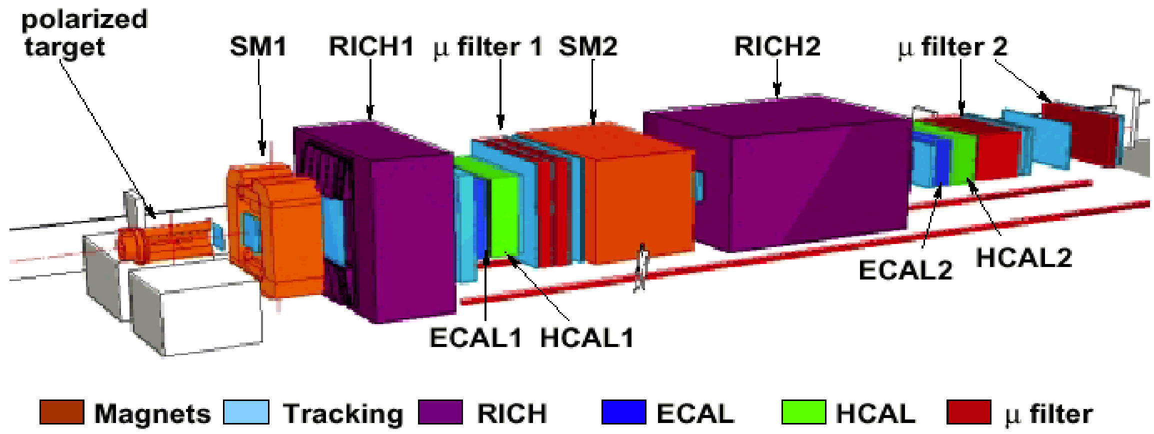

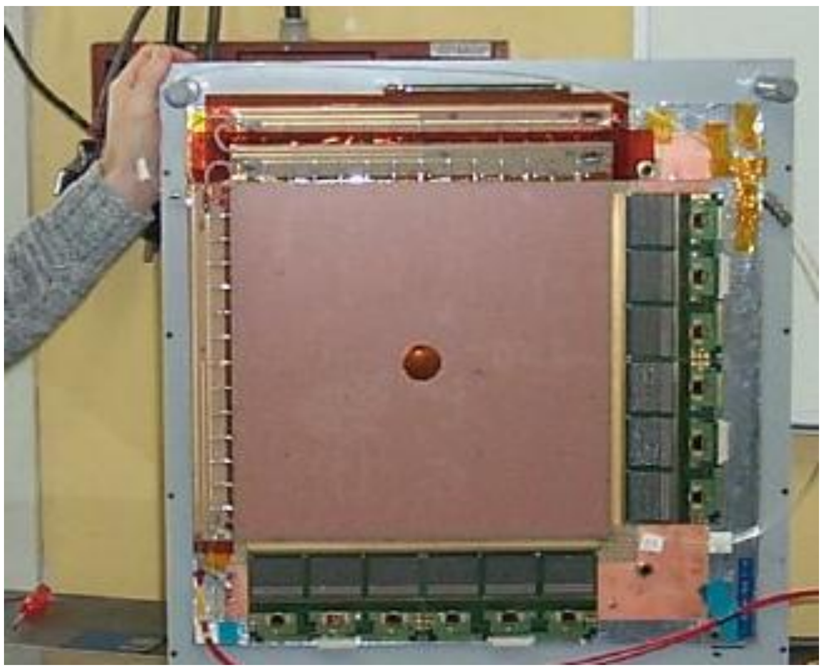

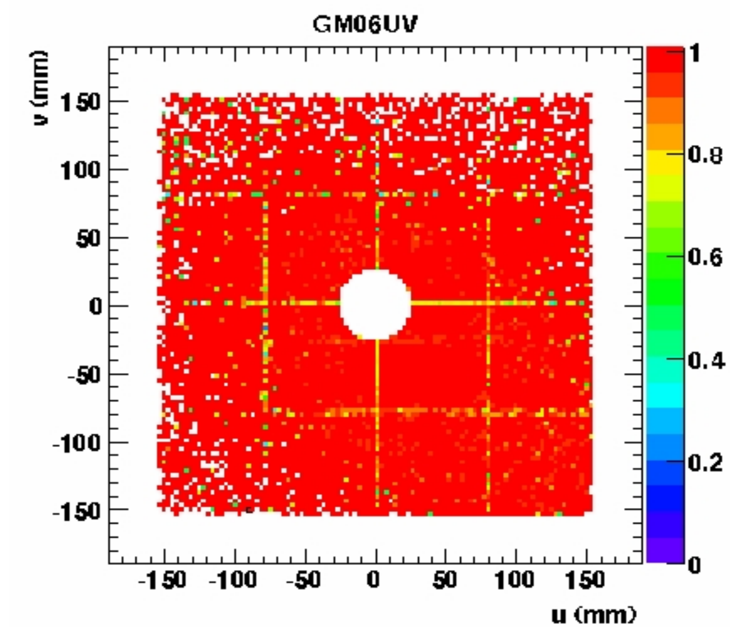

UNIFORMITY OF TRACKING EFFICIENCY

MICROMEGAS (MICRO MEsch GASeous Structure)

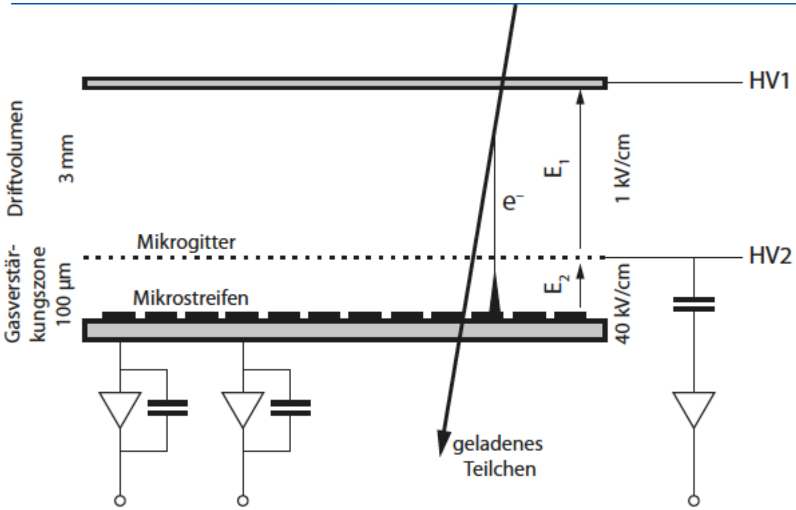

- ❑ separation of drift region and (short) amplification region by a micro grid
- ❑ R/O of induced charges by patterned electrode
- ❑ fast induced signals
- ❑ need precise grid alignment
- ❑ new development: INGRID structure obtained by "post processing" of grid directly on R/O chip

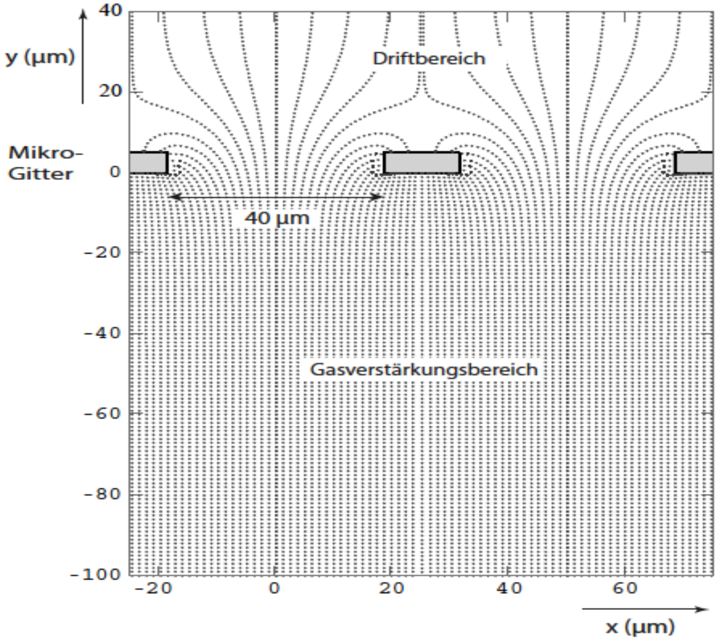

INGRID structure

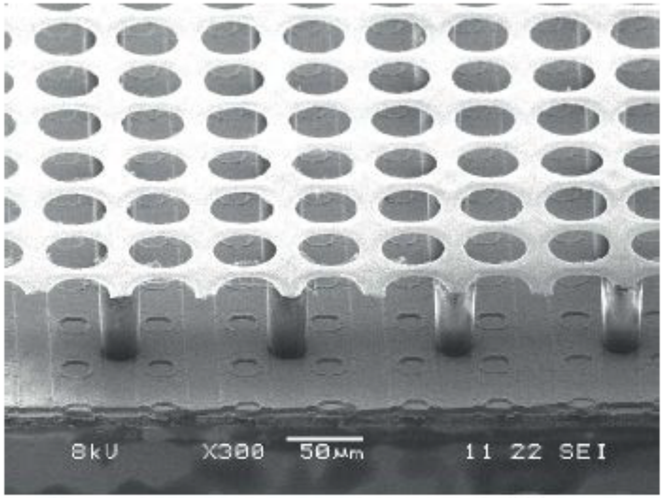

RPCs (resistive plate chambers)

universitätbonn

- target **high timing precision** (trigger and timing chambers, e.g. ATLAS Muon Spectrometer)

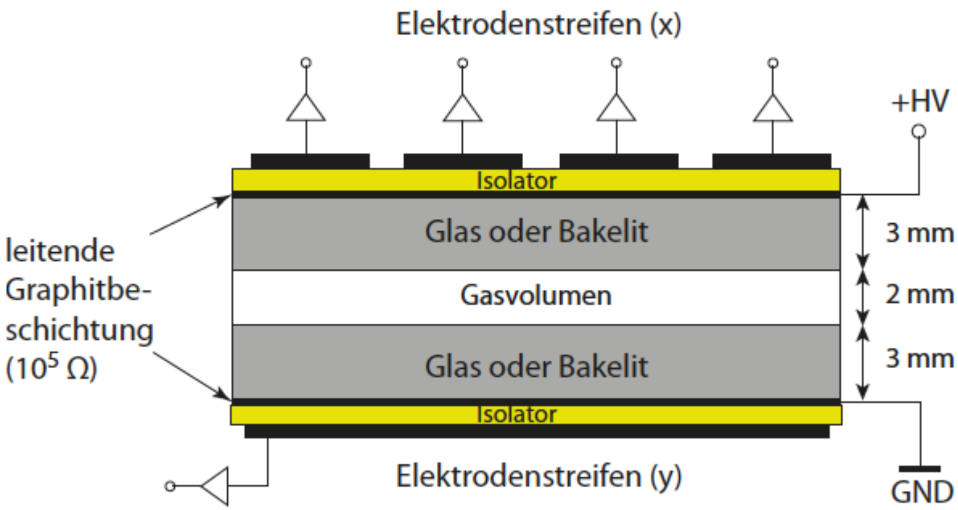

- use high ohmic (10^8-10^{12} Ω cm) plates (glass, bakelit) with small gap (2mm)
- operation (~10 kV) in avalanche (shorter quench times) or streamer mode (larger and faster signals)
- induced signals reach through to patterned electrodes
- large signals: <100pC streamer, <10pC avalanche
- gas with high ionisation density and high quenching efficiency needed:
  e.g. 94.7% $C_2H_2F_4$, 5% i – C_4H_{10}, 0.3% SF_6

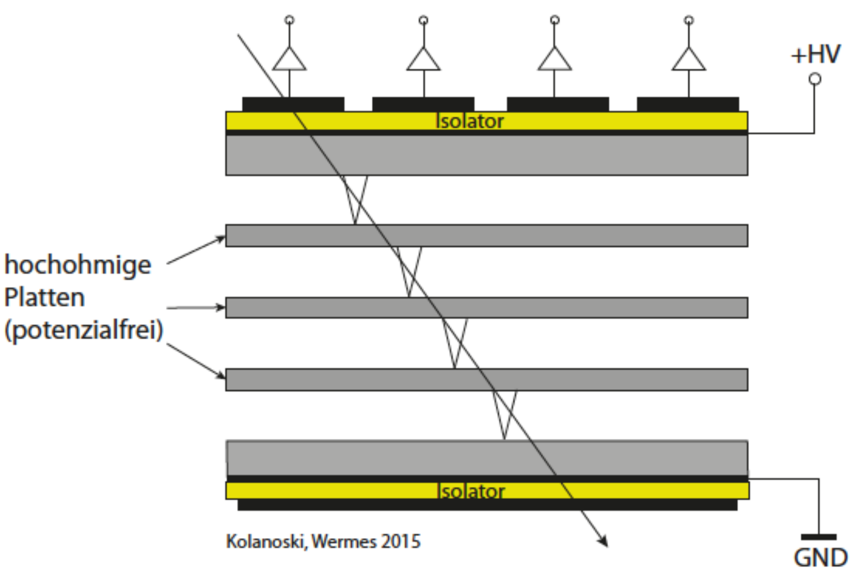

Kolanoski, Wermes 2015

Trigger-RPC avalanche mode		Timing-RPC streamer mode	
$E = 50$ kV/cm		$E = 100$ kV/cm	
$\alpha = 13.3$/mm	$\eta = 3.5$/mm	$\alpha = 123$/mm	$\eta = 10.5$/mm
$v_D = 140$ μm/ns	d = 2 mm	$v_D = 210$ μm/ns	d = 0.3 mm
$\sigma_t = 1$ ns		$\sigma_t = 50$ ps	
$\epsilon = 98\%$		$\epsilon = 75\%$	

End of Lecture 2